HexPly 8552
MATERIAL PROPERTIES DATABASE
for use with COMPRO CCA
and Raven

Created for

by

David Van Ee & Anoush Poursartip
Convergent Manufacturing Technologies, Inc.
November 15th, 2009

TABLE OF CONTENTS

Overview

History

This materials database for HexPly 8552 was created by Convergent Manufacturing Technologies Inc. (CMT). CMT received samples of the material from Hexcel on October 18, 2006.

The materials database was specifically developed for the use with the finite-element based processing codes COMPRO 3-D/CCA and Raven.

Data Gathering Issues

The DSC tests were performed by Dr. Ali Shahkarami and the viscosity tests were performed at McGill University by Dr. Jonathan Laliberte. Analysis of the data was performed by Convergent Manufacturing Technologies Inc.

Analysis Issues

Not Applicable.

Code Versions

The nomenclature follows that of COMPRO CCA build 1495.

COMPRO Modules

COMPRO is divided into three main modules: thermochemical, flow, and stress. All three modules directly use the materials database.

- The *thermochemical* module predicts the internal temperature in the part and tooling as well as the degree of cure in composite structural components.
- The *flow* module predicts the resin flow and fibre bed compaction in composite materials.
- The *stress* module models the development of residual strains and deformation in the structure and tooling.

OVERVIEW OF INPUT PROPERTIES

COMPRO INPUT PROPERTY	IMPORTANCE for DEFORMATION*	TESTS/ANALYSIS REQUIRED	TEST PERFORMED	DATA REC'D by CMT	STATUS OF ANALYSIS
Fibre Volume Fraction	low-medium	Not Applicable.	N/A	N/A	N/A
Density	low	Measurement of mass and volume during cure.	NO	N/A	N/A
Specific Heat	low	DSC to measure amount of energy required to increase temp of specimen by delta T.	YES	N/A	COMPLETE
Thermal Conductivity	medium	Conductivity tests - through thickness, longitudinal on uncured and fully cured neat resin	NO	N/A	N/A
Thermal Expansion	high	Bi-material 3 Pt Bend Test or TMA test	NO	N/A	N/A
Resin Cure Shrinkage	high	Bi-material 3 Pt Bend Test or TMA test	NO	N/A	N/A
Resin Modulus Development	high	Bi-material 3 Pt Bend Test	NO	N/A	N/A
Resin Poisson's Ratio	low-medium	No standard test exists.	NO	N/A	N/A
Resin Cure Kinetics	high	DSC - Isothermal Runs DSC - Dynamic Runs	YES	N/A	COMPLETE
Fibre Bed Properties	low	Compaction Tests	N/A	N/A	N/A
Resin Viscosity	low	Parallel Plate Test on Neat Resin	YES	N/A	COMPLETE
Fibre Bed Permeability	low	No standard test exists.	N/A	N/A	N/A

*The relative importance of different COMPRO material input properties depends on the geometry, lay-up, and thickness of the part. This list refers to warpage and spring-back of solid parts.

Theory

For a detailed description of the theoretical foundations of COMPRO, see Johnston (1997)[1] and Hubert (1996)[2].

[1] A. Johnston, "An Integrated Model of the Development of Process-Induced Deformation in Autoclave Processing of Composite Structures", *Ph.D. Thesis,* The University of British Columbia, Vancouver, B.C., February 1997.
[2] P. Hubert, "Aspects of Flow and Compaction of Laminated Composite Shapes During Cure", *Ph.D. Thesis*, The University of British Columbia, Vancouver, B.C., May, 1996.

Thermochemical Module

In this section, the following material properties are determined:

- Cure Kinetics
- Fibre Volume Fraction and Density
- Thermal Conductivity
- Specific Heat

All the relevant model equations and a summary table with all the determined thermochemical COMPRO inputs are presented at the beginning of the section. A detailed description of how the inputs were determined follows.

MODEL EQUATIONS - THERMOCHEMICAL MODULE

Resin Cure Kinetics

COMPRO model 15 is used to calculate the resin cure kinetics. The mathematical form of this model is:

$$\dot{x} = \left(\frac{1}{\dot{x}_k} + \frac{1}{\dot{x}_d} \right)^{-1}$$

$\dot{x}_k$ is the kinetic component of the reaction, defined as:

$$\dot{x}_k = \left(\frac{1}{\dot{x}_{c_1}} + \frac{1}{\dot{x}_{i_2} + \dot{x}_{c_2}} \right)^{-1} + \dot{x}_e$$

where for each reaction $\dot{x}_{c_1}, \dot{x}_{i_2}, \dot{x}_{c_2}, \dot{x}_e$,

$$\dot{x}_i = K_{0_i} e^{-\frac{E_{a_i}}{RT}} (1-x)^{l_i} \left(\frac{1}{r} - x \right)^{m_i} \left(x^{n_{2_i}} + b_i \right)^{n_i}$$

$\dot{x}_d$ represents the diffusion effects and is defined as:

$$\dot{x}_d = k_{d_0} e^{-\frac{B}{f}}$$

where

$$f = a_f (T - T_g) + b_f$$

and a_f and b_f are defined as:

$$a_f = \begin{cases} a_1 & T_g < T_{g_{a1}} \\ S_a T_g + C_a & T_{g_{a1}} < T_g < T_{g_{a2}} \\ a_2 & T_{g_{a2}} < T_g \end{cases} \quad \text{where} \quad \begin{cases} S_a = \dfrac{a_2 - a_1}{T_{g_{a2}} - T_{g_{a1}}} \\ C_a = a_2 - S_a T_{g_{a2}} \end{cases}$$

$$b_f = \begin{cases} b_1 & T_g < T_{g_{b1}} \\ S_b T_g + C_b & T_{g_{b1}} < T_g < T_{g_{b2}} \\ b_2 & T_{g_{b2}} < T_g \end{cases} \quad \text{where} \quad \begin{cases} S_b = \dfrac{b_2 - b_1}{T_{g_{b2}} - T_{g_{b1}}} \\ C_b = b_2 - S_b T_{g_{b2}} \end{cases}$$

The DeBenedetto equation is used to determine the glass transition temperature, T_g:

$$T_g = T_{g0} + \frac{\lambda x (T_{g\infty} - T_{g0})}{1 - (1 - \lambda) x}$$

Fibre Volume Fraction and Density

The equations used to find fibre volume fraction are:

$$V_f = (1 - m_r)\frac{\rho_c}{\rho_f}$$

$$\rho_c = V_f \rho_f + (1 - V_f)\rho_r$$

The COMPRO density model equations are:

$$\rho_r = \rho_{r(0)} + a_{\rho r}(T - T_0) + b_{\rho r}(x - x_0)$$
$$\rho_f = \rho_{f(0)} + a_{\rho f}(T - T_0)$$

Specific Heat Capacity

The specific heat capacity model equation implemented in COMPRO is:

$$C_p = C_{p_r} + \frac{C_{p_g} - C_{p_r}}{1 + e^{k\left[(T - T_g) - \Delta T_c\right]}}$$

where

$$C_{p_i} = (1 - x)C_{p_{i0}} + xC_{p_{i\infty}} \quad (i = r, g)$$

and

$$C_{p_{ij}} = s_{ij}T + c_{ij} \quad (i = r, g \quad \text{and} \quad j = 0, \infty)$$

Thermal Conductivity

The thermal conductivity model equations are:

$$k_{11c} = k_{11c(0)} + a_{k11c}(T - T_0) + b_{k11c}(x - x_0)$$

$$k_{22c} = k_{33c} = k_{33c(0)} + a_{k33c}(T - T_0) + b_{k33c}(x - x_0)$$

where c can be the fibre or the resin in the general case.

SUMMARY TABLE - COMPRO THERMOCHEMICAL INPUTS

(IMPERIAL UNITS)

HexPly 8552

Resin Cure Kinetics - COMPRO Model 15

Constant	Value				Units
	$\dot{x}_{c_1}$	$\dot{x}_{i_2}$	$\dot{x}_{c_1}$	$\dot{x}_e$	
HR [1]	257.954				BTU/lb
k_0	153,900.5	1,000	1,000	3.963E+11	1/s
E_a	61.541	0.0	0.0	126.219	BTU/mol
l	2.347	0.0	0.0	1.029	
r	1.0	1.0	1.0	1.0	
m	0.0	0.0	0.0	0.0	
n_2	1.0	0.0	0.0	1.0	
b	0.1594	1.0	1.0	0.0	
n	1.413	0.0	0.0	5.586	
$k_{d\,0}$	4.0				1/s
B	0.21				
a_1	2.67E-04				1/°F
a_2	2.67E-04				1/°F
$T_{g\,a1}$	32.0				°F
$T_{g\,a2}$	212.0				°F
b_1	0.021				
b_2	0.031				
$T_{g\,b1}$	248.0				°F
$T_{g\,b2}$	383.0				°F
T_{g0}	19.4				°F
$T_{g\infty}$	482.0				°F
λ	0.78				

[1] HR is the heat of reaction.

Fibre Volume Fraction and Density

Constant	Value	Units
V_f	0.55	
$\rho_{r(0)}$	4.7E-02	lb/in^3
$a_{\rho r}$	0.0	lb/(in^3 °F)
T_0	68.0	°F
$b_{\rho r}$	0.0	lb/in^3
x_0	0.0	
$\rho_{f(0)}$	6.467E-02	lb/in^3
$a_{\rho f}$	0.0	lb/in^3

Specific Heat Capacity

Constant	Value	Units
s_{g0}	5.009E-04	BTU/(lb*F^2)
c_{g0}	0.17437	BTU/(lb*F)
$s_{g\infty}$	4.511E-04	BTU/(lb*F^2)
$c_{g\infty}$	0.19825	BTU/(lb*F)
s_{r0}	4.339E-04	BTU/(lb*F^2)
c_{r0}	0.25988	BTU/(lb*F)
$s_{r\infty}$	2.654E-04	BTU/(lb*F^2)
$c_{r\infty}$	0.32246	BTU/(lb*F)
k	0.154	1/°F
ΔT_c	-2.7	°F

Thermal Conductivity

Constant	Value	Units
$k_{11r(0)}$	0.0855	BTU/h*ft*F
$k_{33r(0)}$	0.0855	BTU/h*ft*F
a_{k11r}	1.10E-04	BTU/h*ft*F^2
b_{k11r}	0.0351	BTU/h*ft*F
a_{k33r}	1.10E-04	BTU/h*ft*F^2
b_{k33r}	0.0351	BTU/h*ft*F
T_{0_r}	32.0	°F
x_0	0.0	

The following page shows the same information in SI units.

SUMMARY TABLE - COMPRO THERMOCHEMICAL INPUTS

(SI UNITS)

HexPly 8552

Resin Cure Kinetics - COMPRO Model 15

Constant	Value				Units
	$\dot{x}_{c_1}$	$\dot{x}_{i_2}$	$\dot{x}_{c_1}$	$\dot{x}_e$	
HR [1]	600,000				J/kg
k_0	153,900.5	1,000	1,000	3.963E+11	1/s
E_a	64,929.5	0.0	0.0	133,168.3	J/mol
l	2.347	0.0	0.0	1.029	
r	1.0	1.0	1.0	1.0	
m	0.0	0.0	0.0	0.0	
n_2	1.0	0.0	0.0	1.0	
b	0.1594	1.0	1.0	0.0	
n	1.413	0.0	0.0	5.586	
$k_{d\,0}$	4.0				1/s
B	0.21				
a_1	4.8E-04				1/°C
a_2	4.8E-04				1/°C
$T_{g\,a1}$	0.0				°C
$T_{g\,a2}$	100.0				°C
b_1	0.021				
b_2	0.031				
$T_{g\,b1}$	120.0				°C
$T_{g\,b2}$	195.0				°C
T_{g0}	-7.0				°C
$T_{g\infty}$	250.0				°C
λ	0.78				

[1] HR is the heat of reaction.

Fibre Volume Fraction and Density

Constant	Value	Units
V_f	0.55	
$\rho_{r(0)}$	1.301E+03	kg/m^3
$a_{\rho r}$	0.0	kg/(m^3*°C)
T_0	20.0	°C
$b_{\rho r}$	0.0	kg/m^3
x_0	0.0	
$\rho_{f(0)}$	1.79E+03	kg/m^3
$a_{\rho f}$	0.0	kg/m^3

Specific Heat Capacity

Constant	Value	Units
s_{g0}	3.775	J/(kg K^2)
c_{g0}	730.0	J/(kg K)
$s_{g\infty}$	3.40	J/(kg K^2)
$c_{g\infty}$	830.0	J/(kg K)
s_{r0}	3.27	J/(kg K^2)
c_{r0}	1088.0	J/(kg K)
$s_{r\infty}$	2.0	J/(kg K^2)
$c_{r\infty}$	1350.0	J/(kg K)
k	0.278	1/°C
ΔT_c	-1.5	°C

Thermal Conductivity

Constant	Value	Units
$k_{11r(0)}$	0.148	W/m°C
$k_{33r(0)}$	0.148	W/m°C
a_{k11r}	3.43E-04	W/m°C^2
b_{k11r}	6.07E-02	W/m°C
a_{k33r}	3.43E-04	W/m°C^2
b_{k33r}	6.07E-02	W/m°C
T_{0r}	0.0	°C
x_0	0.0	

The following page shows the corresponding COMPRO material data file, for these material inputs.

COMPRO Data File for Thermochemical Module (SI Units)

```
   <cure_kinetics model="ck15" number_of_parameters="46">
      <constraint variable='doc' value='0.001' isMinimum='true' severity_model='1'
initial_severity='1.0' severity_parameters='0.;1.;' />
      <parameter name="HeatOfReaction" parameter_number="1" units="J/kg" value="600000."
/>
      <parameter name="xc1K0" parameter_number="2" units="1/s" value="153900.5" />
      <parameter name="xc1Ea" parameter_number="3" units="J/mol" value="64929.5" />
      <parameter name="xc1l" parameter_number="4" units="none" value="2.347" />
      <parameter name="xc1r" parameter_number="5" units="none" value="1.0" />
      <parameter name="xc1m" parameter_number="6" units="none" value="0.0" />
      <parameter name="xc1n2" parameter_number="7" units="none" value="1.0" />
      <parameter name="xc1b" parameter_number="8" units="none" value="0.1594" />
      <parameter name="xc1n" parameter_number="9" units="none" value="1.413" />
      <parameter name="xi2K0" parameter_number="10" units="1/s" value="1000" />
      <parameter name="xi2Ea" parameter_number="11" units="J/mol" value="0.0" />
      <parameter name="xi2l" parameter_number="12" units="none" value="0.0" />
      <parameter name="xi2r" parameter_number="13" units="none" value="1.0" />
      <parameter name="xi2m" parameter_number="14" units="none" value="0.0" />
      <parameter name="xi2n2" parameter_number="15" units="none" value="0.0" />
      <parameter name="xi2b" parameter_number="16" units="none" value="1.0" />
      <parameter name="xi2n" parameter_number="17" units="none" value="0.0" />
      <parameter name="xc2K0" parameter_number="18" units="1/s" value="1000" />
      <parameter name="xc2Ea" parameter_number="19" units="J/mol" value="0.0" />
      <parameter name="xc2l" parameter_number="20" units="none" value="0.0" />
      <parameter name="xc2r" parameter_number="21" units="none" value="1.0" />
      <parameter name="xc2m" parameter_number="22" units="none" value="0.0" />
      <parameter name="xc2n2" parameter_number="23" units="none" value="0.0" />
      <parameter name="xc2b" parameter_number="24" units="none" value="1.0" />
      <parameter name="xc2n" parameter_number="25" units="none" value="0.0" />
      <parameter name="xeK0" parameter_number="26" units="1/s" value="3.963E+11" />
      <parameter name="xeEa" parameter_number="27" units="J/mol" value="133168.3" />
      <parameter name="xel" parameter_number="28" units="none" value="1.029" />
      <parameter name="xer" parameter_number="29" units="none" value="1.0" />
      <parameter name="xem" parameter_number="30" units="none" value="0.0" />
      <parameter name="xen2" parameter_number="31" units="none" value="1.0" />
      <parameter name="xeb" parameter_number="32" units="none" value="0.0" />
      <parameter name="xen" parameter_number="33" units="none" value="5.586" />
      <parameter name="kd0" parameter_number="34" units="1/s" value="4." />
      <parameter name="B" parameter_number="35" units="none" value="0.21" />
      <parameter name="a1" parameter_number="36" units="1/C" value="4.8E-04" />
      <parameter name="a2" parameter_number="37" units="1/C" value="4.8E-04" />
      <parameter name="Tga1" parameter_number="38" units="C" value="0." />
      <parameter name="Tga2" parameter_number="39" units="C" value="100." />
      <parameter name="b1" parameter_number="40" units="none" value="0.021" />
      <parameter name="b2" parameter_number="41" units="none" value="0.031" />
      <parameter name="Tgb1" parameter_number="42" units="C" value="120." />
      <parameter name="Tgb2" parameter_number="43" units="C" value="195." />
      <parameter name="Tg0" parameter_number="44" units="C" value="-7." />
      <parameter name="Tginf" parameter_number="45" units="C" value="250." />
      <parameter name="Lambda" parameter_number="46" units="none" value="0.78" />
   </cure_kinetics>
   <specific_heat model="cp3" number_of_parameters="13">
      <parameter name="Tg0" parameter_number="1" units="C" value="-7" />
      <parameter name="Tginf" parameter_number="2" units="C" value="250." />
      <parameter name="Lambda" parameter_number="3" units="none" value="0.78" />
      <parameter name="sr0" parameter_number="4" units="J/(kg C2)" value="3.27" />
      <parameter name="srinf" parameter_number="5" units="J/(kg C2)" value="2.00" />
      <parameter name="sg0" parameter_number="6" units="J/(kg C2)" value="3.775" />
      <parameter name="sginf" parameter_number="7" units="J/(kg C2)" value="3.40" />
      <parameter name="cr0" parameter_number="8" units="J/(kg C)" value="1088." />
      <parameter name="crinf" parameter_number="9" units="J/(kg C)" value="1350." />
      <parameter name="cg0" parameter_number="10" units="J/(kg C)" value="730." />
      <parameter name="cginf" parameter_number="11" units="J/(kg C)" value="830." />
      <parameter name="kfac" parameter_number="12" units="none" value="0.278" />
      <parameter name="DTc" parameter_number="13" units="C" value="-1.5" />
   </specific_heat>
   <density model="default" number_of_parameters="5">
      <parameter name="NominalDensity" parameter_number="1" units="kg/m3"
value="1.301E+03" />
```

```
      <parameter name="T0" parameter_number="2" units="C" value="20." />
      <parameter name="Tf" parameter_number="3" units="km/(m3 K)" value="0." />
      <parameter name="a0" parameter_number="4" units="none" value="0." />
      <parameter name="af" parameter_number="5" units="none" value="0." />
   </density>
<!-- everything from here down is not characterized -->
   <conductivity model="default" number_of_parameters="5">
      <parameter name="NominalK" parameter_number="1" units="W/(m K)" value="0.148" />
      <parameter name="T0" parameter_number="2" units="C" value="0." />
      <parameter name="Tf" parameter_number="3" units="W/(m K2)" value="3.430E-04" />
      <parameter name="a0" parameter_number="4" units="none" value="0.0" />
      <parameter name="af" parameter_number="5" units="none" value="6.070E-02" />
   </conductivity>
```

Resin Cure Kinetics

Introduction

A model for cure rate ($\frac{dx}{dt}$) as a function of temperature and degree of cure was developed. Several DSC scans were performed on HexPly 8552 specimens, and the data measured was used to fit the model.

Theoretical

COMPRO model 15 is used to calculate the resin cure kinetics. The mathematical form of this model is:

$$\dot{x} = \left(\frac{1}{\dot{x}_k} + \frac{1}{\dot{x}_d} \right)^{-1}$$

$\dot{x}_k$ is the kinetic component of the reaction, defined as:

$$\dot{x}_k = \left(\frac{1}{\dot{x}_{c_1}} + \frac{1}{\dot{x}_{i_2} + \dot{x}_{c_2}} \right)^{-1} + \dot{x}_e$$

where for each reaction $\dot{x}_{c_1}, \dot{x}_{i_2}, \dot{x}_{c_2}, \dot{x}_e$,

$$\dot{x}_i = K_{0_i} e^{-\frac{E_{a_i}}{RT}} (1-x)^{l_i} \left(\frac{1}{r} - x \right)^{m_i} \left(x^{n_{2_i}} + b_i \right)^{n_i}$$

$\dot{x}_d$ represents the diffusion effects and is defined as:

$$\dot{x}_d = k_{d_0} e^{-\frac{B}{f}}$$

where

$$f = a_f (T - T_g) + b_f$$

and a_f and b_f are defined as:

$$a_f = \begin{cases} a_1 & T_g < T_{g_{a1}} \\ S_a T_g + C_a & T_{g_{a1}} < T_g < T_{g_{a2}} \\ a_2 & T_{g_{a2}} < T_g \end{cases} \quad \text{where} \quad \begin{cases} S_a = \dfrac{a_2 - a_1}{T_{g_{a2}} - T_{g_{a1}}} \\ C_a = a_2 - S_a T_{g_{a2}} \end{cases}$$

$$b_f = \begin{cases} b_1 & T_g < T_{g_{b1}} \\ S_b T_g + C_b & T_{g_{b1}} < T_g < T_{g_{b2}} \\ b_2 & T_{g_{b2}} < T_g \end{cases} \quad \text{where} \quad \begin{cases} S_b = \dfrac{b_2 - b_1}{T_{g_{b2}} - T_{g_{b1}}} \\ C_b = b_2 - S_b T_{g_{b2}} \end{cases}$$

The DeBenedetto equation is used to determine the glass transition temperature, T_g:

$$T_g = T_{g0} + \frac{\lambda x \left(T_{g\infty} - T_{g0}\right)}{1 - \left(1 - \lambda\right)x}$$

In all the equations above:

R is the universal gas constant.
T is the temperature.
x is the degree of cure.
λ, T_{g0}, $T_{g\infty}$, l, r, m, n_2, b, n, k_0, E_a, k_{d_0}, B, a_1, a_2, T_{ga1}, T_{ga2}, b_1, b_2, T_{gb1}, T_{gb2} are model parameters.

Raw Data

The data came from DSC scans using a TA Q1000 instrument. Samples of ~3-6 mg were encapsulated in normal aluminium sample pans, and the thermal analysis was run using a nitrogen purge of 50 ml/min.

The tests consisted of isothermal runs at 10°C increments from 100°C to 190°C; and dynamic scans at 1°C/min to 10°C/min, at 1°C/min increments. In the dynamic tests, the samples were heated at a constant rate in a predefined thermal range. The specimens in the isothermal runs were heated quickly to the test temperature and then held at that temperature for up to 12 hours, until the reaction slowed down significantly due to diffusion. After the prescribed time elapsed, the isothermal samples were cooled down and then subjected to a residual dynamic scan to evaluate the remaining reaction. In interrupted isothermal tests, the hold segment was terminated early, before a significant slow down was observed in the chemical reaction. Cure cycle tests were DSC runs in which the samples were subjected to a recommended cure cycle and the evolution of Tg at various points along the cycle was measured. Overall, a total of 28 tests were performed (11 dynamic, 11 isothermal, 2 interrupted isothermal and 4 cure cycle tests), which were used to fit the cure kinetics model and validate its

predictions. The following tables show a summary of the DSC runs used in this study.

Test	Mass (mg)	Rate (ºC/min)	$Temp_{max}$ (ºC)
8552-MDYN-01cpm-01	4.99	1	300
8552-MDYN-02cpm-01	4.19	2	300
8552-MDYN-02cpm-02	5.3	2	280
8552-MDYN-03cpm-01	5.59	3	300
8552-MDYN-04cpm-01	5.59	4	300
8552-MDYN-05cpm-01	4.79	5	300
8552-MDYN-06cpm-01	4.79	6	300
8552-MDYN-07cpm-01	5.89	7	300
8552-MDYN-08cpm-01	4.09	8	330
8552-MDYN-09cpm-01	5.19	9	330
8552-MDYN-10cpm-01	3.39	10	330

Table 1: Summary of the dynamic tests used in the cure kinetics analysis of HexPly 8552.

Test	Mass (mg)	Hold Temp (ºC)	Hold Time (min)
8552-MISO-100C-01	5.3	100	720
8552-MISO-110C-01	5.7	110	540
8552-MISO-120C-01	4.7	120	480
8552-MISO-130C-01	4.4	130	420
8552-MISO-140C-01	5.2	140	360
8552-MISO-150C-01	5.6	150	360
8552-MISO-160C-01	5.4	160	300
8552-MISO-170C-01	3.6	170	180
8552-MISO-180C-01	5.59	180	180
8552-MISO-180C-02	5.4	180	180
8552-MISO-190C-01	4.49	190	180
8552-160C-INT15	5	160	15
8552-160C-INT30	0	160	30

Table 2: Summary of the isothermal and interrupted tests used in the cure kinetics analysis of HexPly 8552.

Test	Mass (mg)
8552-CC-S1-02	4.6
8552-CC-S3-00-01	5
8552-CC-S3-60-01	4.7
8552-CC-S4-01	4.9

Table 3: Summary of the cure cycle tests used in the cure kinetics analysis of HexPly 8552.

The heat flow measurements for each of the tests are shown along with the baseline and cure rate analysis in the sections that follow.

Analysis

The first step in the analysis was to calculate the "baseline", as is discussed in Barton[1]. In general, the baseline represents the part of the measured heat flow that is unrelated to the curing of the specimen (such as heat lost to the surroundings, or heat that contributed to increasing specimen temperature). In the case of temperature-modulated DSC test (MDSC), the deconvolution of the data not only provides the information traditionally obtainable from conventional DSCs, it also captures the response of the material to the temperature modulation. The total heat flow data (equivalent to the one measured in a non-modulated test) is obtained by averaging the modulated heat flow. The modulation component of the heat flow is used to determine the reversing component of the heat flow (instantaneous heat capacity measure). In this study, the non-reversing heat flow component was used to analyse the curing process of the material when the underlying temperature rate was non-zero. In the zones where temperature was constant (e.g. during hold temperature in isothermal tests), the total heat flow was used in the analysis.

Baseline Calculations for Isothermal Runs

The heat flow measured by the DSC after the reaction slows down significantly due to diffusion at the end of the hold segment is a measure of the "baseline" in isothermal tests. The baseline was found by extending the heat flow at the end of the hold segment back to the start of the scan (Figure 1).

Baseline definition discussed above assumes that no reaction occurs prior to the time that corresponds to the beginning of the baseline. This can introduce some error into the analysis, specifically in the case of high temperature isothermals where a certain amount of curing occurs on the ramp to the hold temperature. This effect was taken into account by using the model

[1] J.M. Barton, "The Application of Differential Scanning Calorimetry (DSC) to the Study of Epoxy Resin Curing Reactions", Advances in Polymer Science 72: Epoxy Resin and Composites I, K. Dusek, Ed., Springer-Verlag, 1985 pp. 111-154.

to estimate the cure on the ramp and reanalysing the isothermal tests with an updated initial degree of cure.

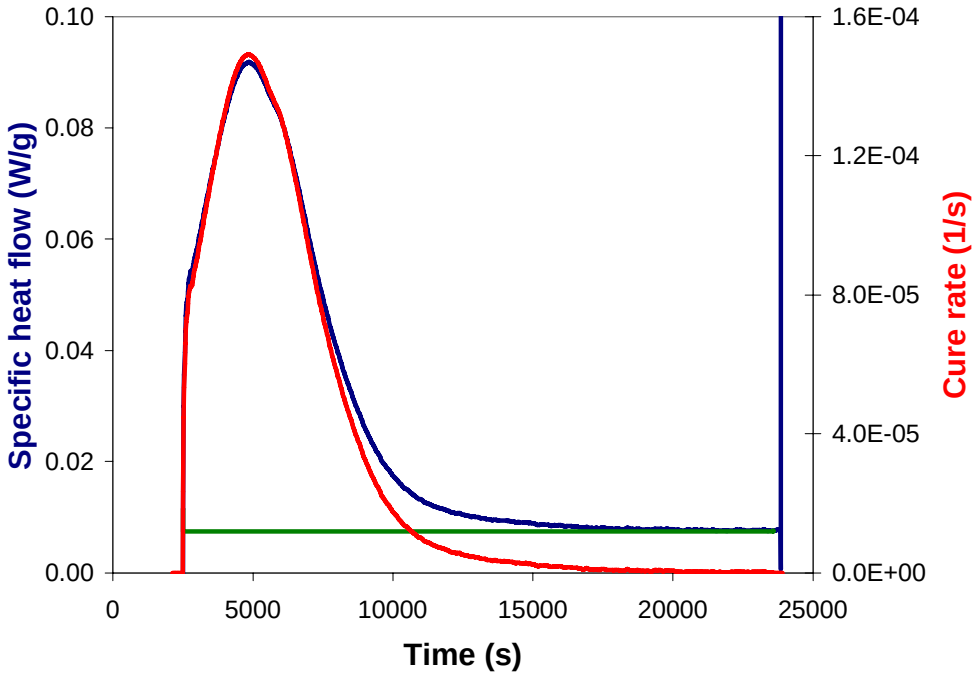

Figure 1. Illustration of baseline definition for isothermal DSC tests (140ºC isothermal scan).

Baseline Calculations for Dynamic Runs

The baseline for the dynamic runs and the residual scans of the isothermal tests were calculated using the non-reversing component of the specific heat flow[1]. All dynamic scans exhibit a characteristic local minimum in the specific heat flow, and this point was taken as the start of the reaction. A linear baseline is usually extended from this point to the end of the reaction, where the heat flow measured reduces back to its initial level. However, in the cases where material degradation occurs before the reaction is completed, the tail end of the heat flow response shows a different behaviour. In the case of HexPly 8552, the heat flow starts to increase at the end of reaction, indicating the presence of an exothermic reaction. This is associated with material degradation, and thus a bilinear baseline is chosen to account for the degradation of material at higher temperatures (see Figure 2).

[1] L. C. Thomas, "Modulated DSC Basics; Calculation and Calibration of MDSC Signals", TA Instrument Modulated DSC Paper Series. Paper #2.

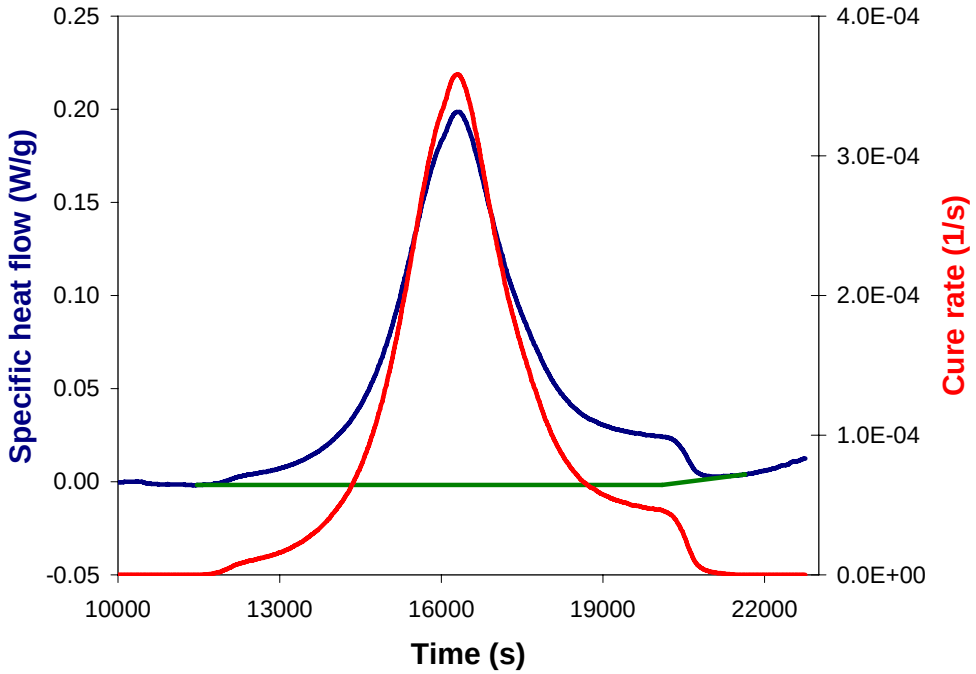

Figure 2. Illustration of baseline for dynamic and residual DSC scans (1ºC/min dynamic scan).

Heat of Reaction

Once the baselines were established, the heat of reaction (HR) generated in each of the tests was determined. The heat of reaction is found by integrating the difference between the specific heat flow ($\dot{q}$) and the baseline ($\dot{q}_{baseline}$) over the time the reaction occurs:

$$H_T = \int (\dot{q} - \dot{q}_{baseline}) dt$$

The total HR in each test is comprised of several components:

HR_{Ramp} : HR released during the ramp segment of the DSC tests.

HR_{Hold} : HR released during the hold segment of the DSC tests.

$HR_{preTest}$: HR released due to the cure advancement in material before the start of the test (material handling, mixing, storing, etc.)

HR_{Test} : The total HR measured through various stages of the DSC test ($HR_{Ramp} + HR_{Hold}$).

HR_{Total} : The total HR of the material ($HR_{preTest} + HR_{Test}$).

HR_{Iso}^{avg} : The average of the total HR measured through various stages of the isothermal DSC tests.

HR_{Dyn}^{avg} : The average of the total HR measured through various stages of the dynamic DSC tests.

HR_{Model} : Model HR; the nominal total HR value used in the model.

The non-zero components of the total HRs for all the tests are shown in Table 44 and Table 55, and plotted in Figure 3.

Test	Heat of Reaction (J/g)		
	Pre-Test	Ramp	Total
8552-MDYN-01cpm-01	0.00	558.91	558.91
8552-MDYN-02cpm-01	0.00	575.43	575.43
8552-MDYN-02cpm-02	0.00	601.65	601.65
8552-MDYN-03cpm-01	0.00	594.88	594.88
8552-MDYN-04cpm-01	0.00	621.82	621.82
8552-MDYN-05cpm-01	0.00	596.98	596.98
8552-MDYN-06cpm-01	0.00	616.41	616.41
8552-MDYN-07cpm-01	0.00	582.98	582.98
8552-MDYN-08cpm-01	0.00	630.07	630.07
8552-MDYN-09cpm-01	0.00	614.07	614.07
8552-MDYN-10cpm-01	0.00	583.62	583.62

Table 4: Heat of reaction calculated for the dynamic DSC tests.

Test	Heat of Reaction (J/g)			
	Iso-Ramp	Hold	Ramp	Total
8552-MISO-100C-01	2.00	295.95	270.47	568.42
8552-MISO-110C-01	2.00	334.88	235.30	572.18
8552-MISO-120C-01	3.00	357.40	206.01	566.41
8552-MISO-130C-01	3.50	403.40	171.32	578.21
8552-MISO-140C-01	4.50	413.43	147.17	565.10
8552-MISO-150C-01	6.50	432.63	118.29	557.42
8552-MISO-160C-01	10.00	466.01	95.26	571.27
8552-MISO-170C-01	12.00	479.84	79.00	570.84
8552-MISO-180C-01	16.50	473.10	55.43	545.03
8552-MISO-180C-02	15.00	486.49	53.05	554.54
8552-MISO-190C-01	19.00	502.82	34.88	556.70
8552-160C-INT15	8.50	99.40	445.77	553.66
8552-160C-INT30	8.50	274.09	275.24	557.83

Table 5: Heat of reaction calculated for the isothermal DSC tests.

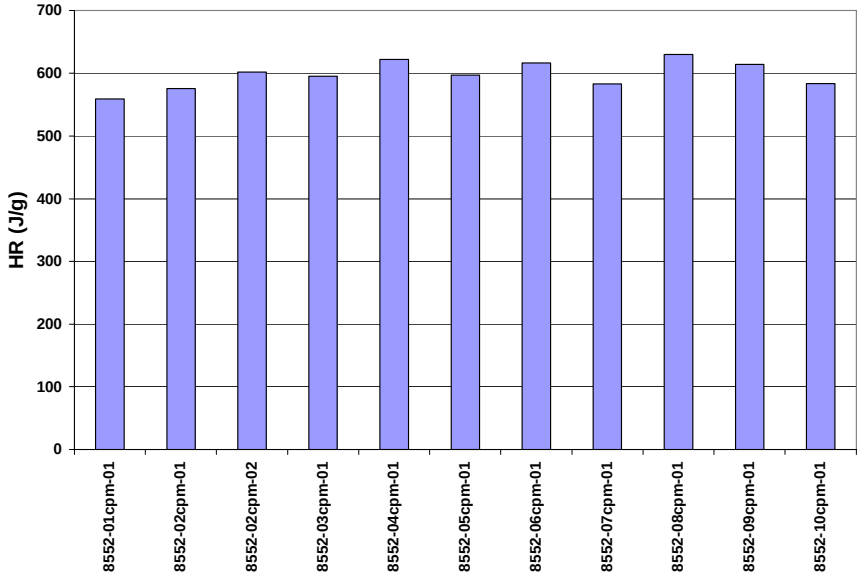

Figure 3. Heat of reaction calculated from the dynamic DSC tests.

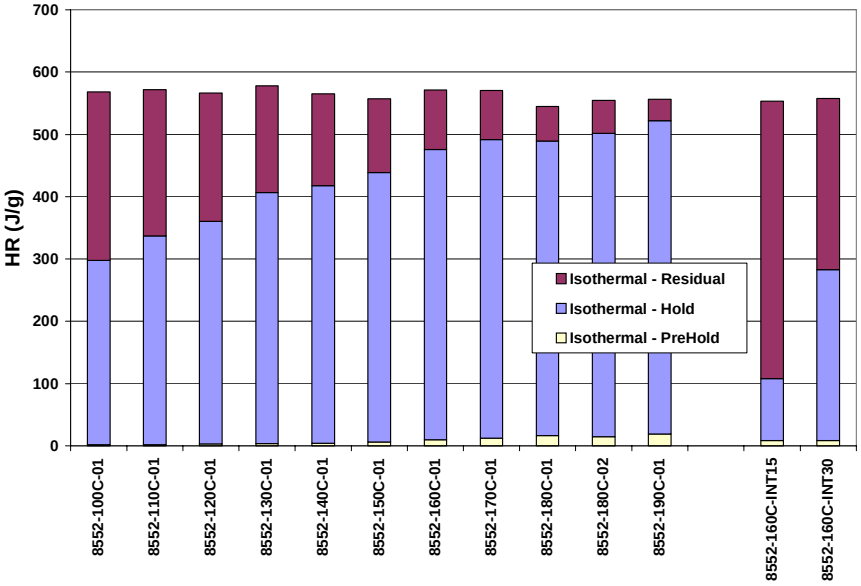

Figure 4. Heat of reaction calculated from the isothermal DSC tests.

Based on the HR values measured in the dynamic and isothermal tests, the following values were calculated:

$$HR_{Dyn}^{avg} = 598 \text{ J/g}$$
$$HR_{Iso}^{avg} = 564 \text{ J/g}$$

The difference between the isothermal and dynamic HR values can be associated to the error embedded in the HR measurement on the hold and ramp segments of the DSC tests, by using the total and reversing heat flow signals, respectively. The model HR was set at:

$$HR_{Model} = 600 \text{ J/g}$$

Calculation of Degree of Cure and Resin Cure Rate

With the baseline heat flow and the total heat of reaction known, the degree of cure was determined by reanalyzing the specific heat flow data. The degree of cure was found by dividing the heat evolved from the start of the reaction at time t_i to the current time, t, by the total heat of reaction.

$$x(t) = \frac{\int_{t_i}^{t} (\dot{q} - \dot{q}_{baseline}) dt}{H_T}$$

The resin cure rate is then determined by considering the degree of cure as a function of time:

$$\frac{dx}{dt} = \frac{\left(x_t - x_{t-\Delta t}\right)}{\Delta t}$$

The specific heat flow, baselines, and cure rates are shown below, along with separate plots of degree of cure and cure rates for all the DSC tests.

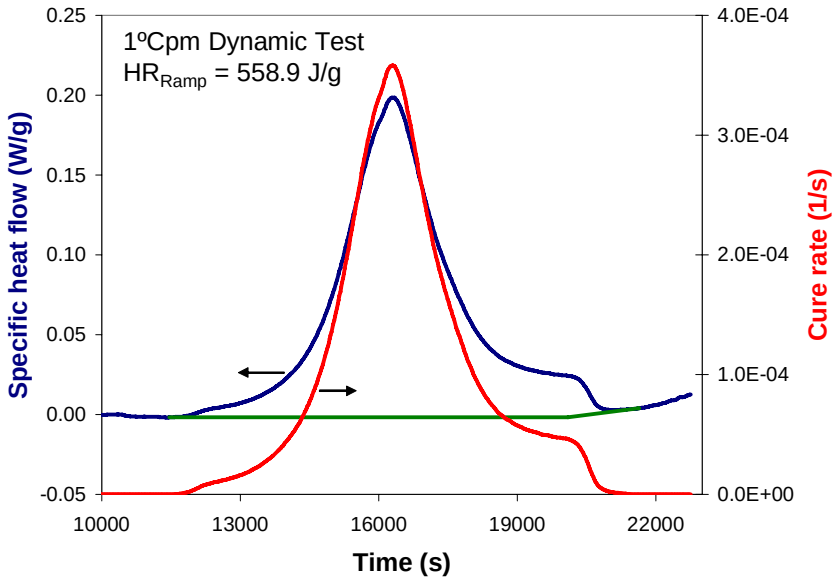

Figure 4. Specific heat flow and resin cure rate for the 1°C/min dynamic scan.

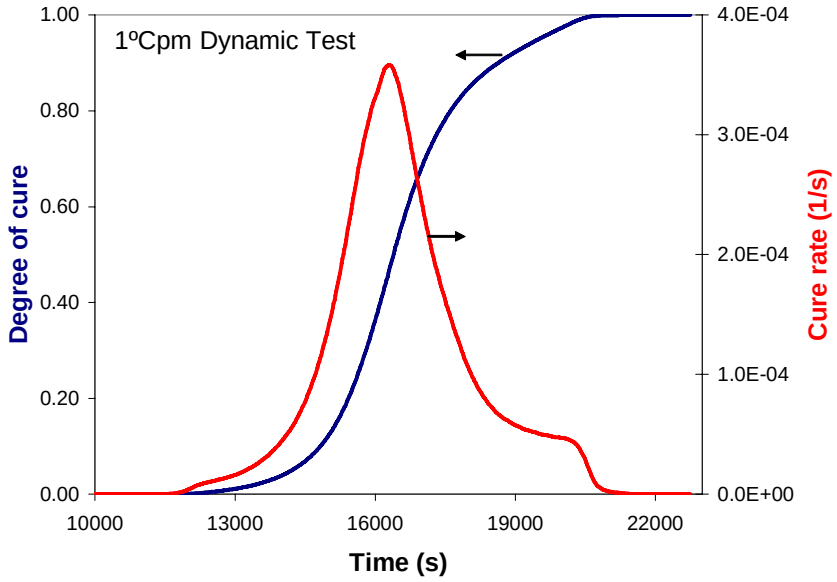

Figure 6. Degree of cure and cure rate for the 1°C/min dynamic scan.

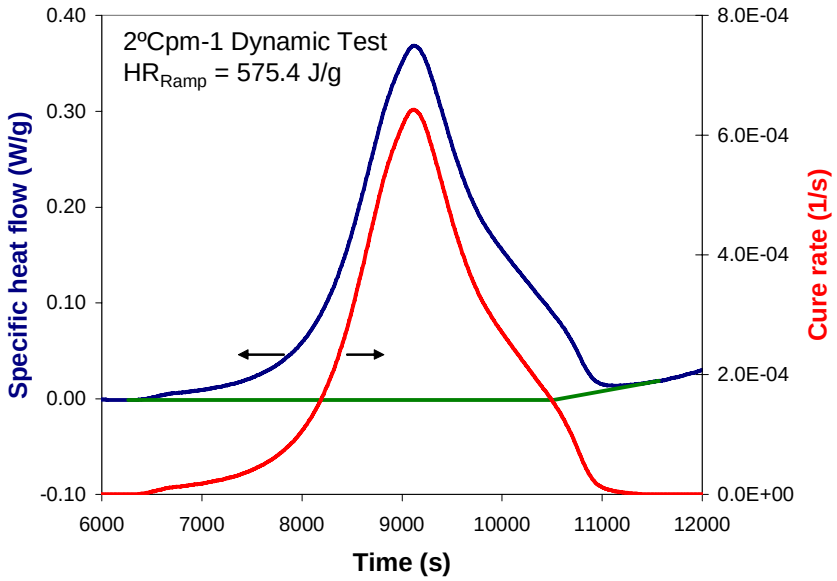

Figure 7. Specific heat flow and resin cure rate for the 2°C/min (1) dynamic scan.

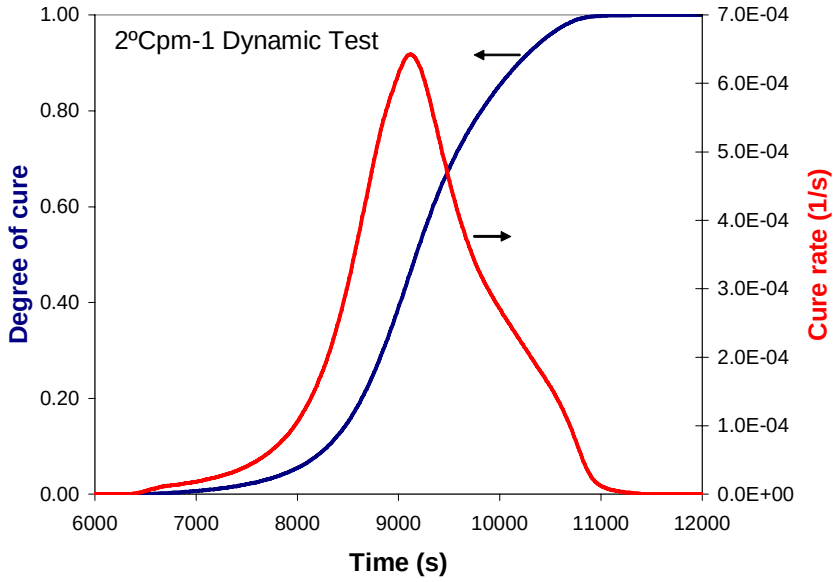

Figure 8. Degree of cure and cure rate for the 2°C/min (1) dynamic scan.

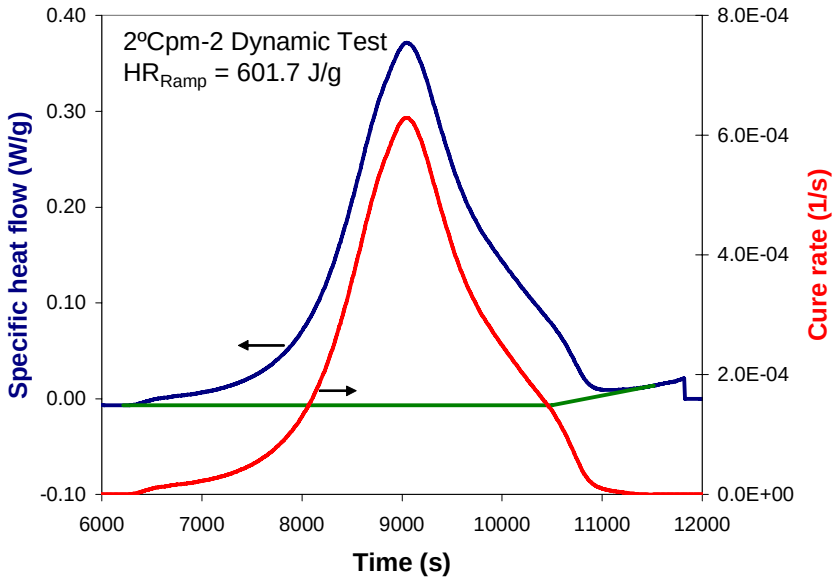

Figure 9. Specific heat flow and resin cure rate for the 2°C/min (2) dynamic scan.

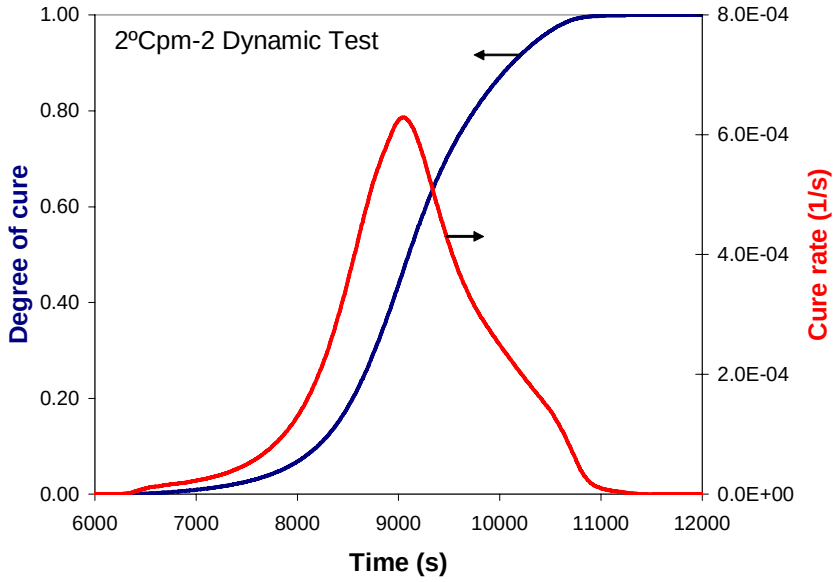

Figure 10. Degree of cure and cure rate for the 2°C/min (2) dynamic scan.

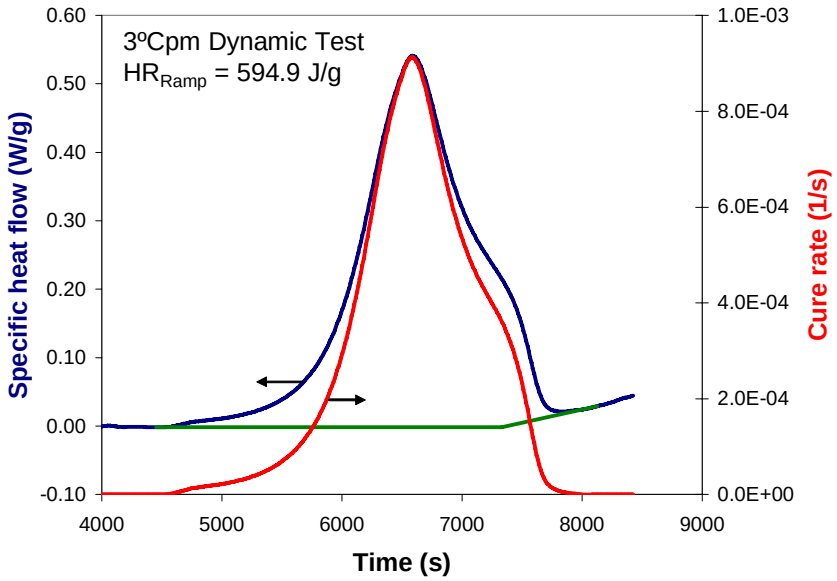

Figure 11. Specific heat flow and resin cure rate for the 3°C/min dynamic scan.

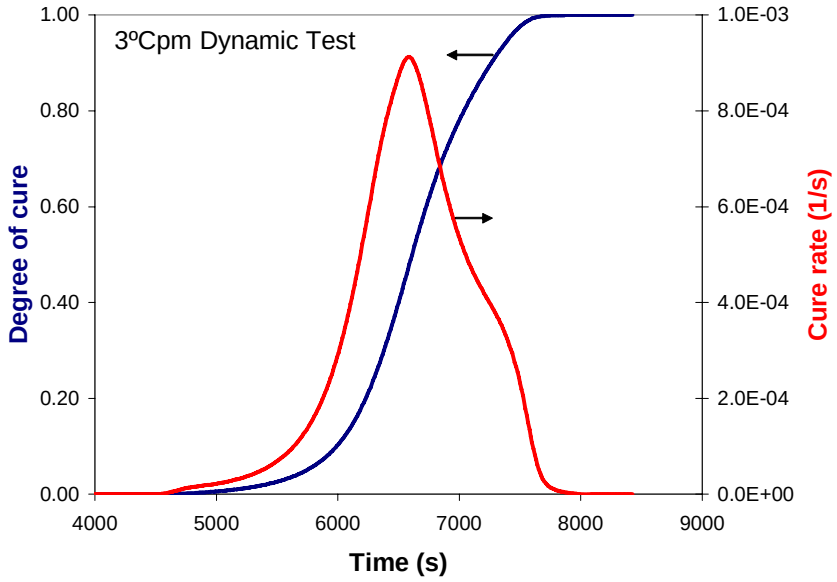

Figure 12. Degree of cure and cure rate for the 3°C/min dynamic scan.

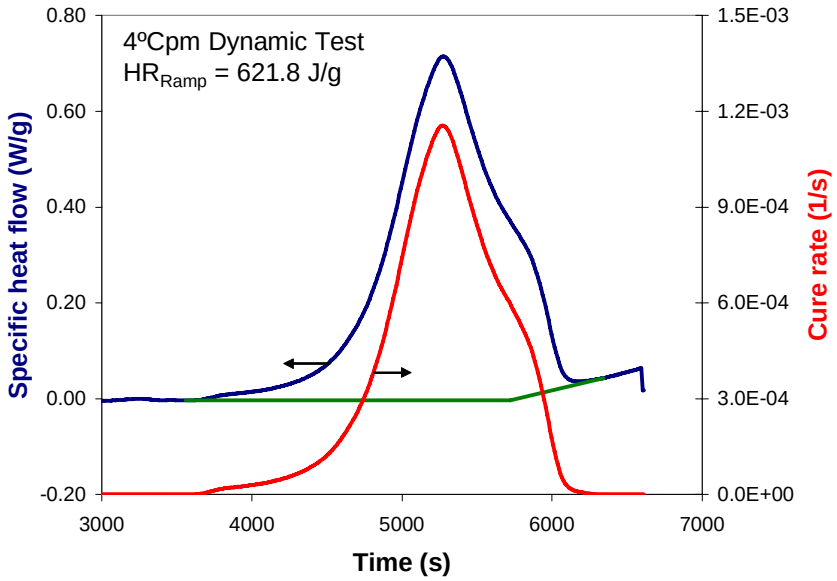

Figure 13. Specific heat flow and resin cure rate for the 4°C/min dynamic scan.

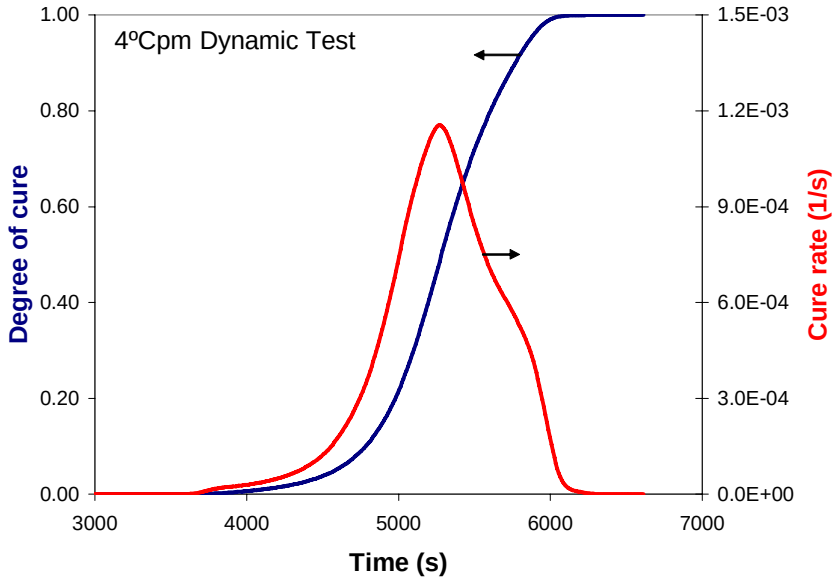

Figure 14. Degree of cure and cure rate for the 4°C/min dynamic scan.

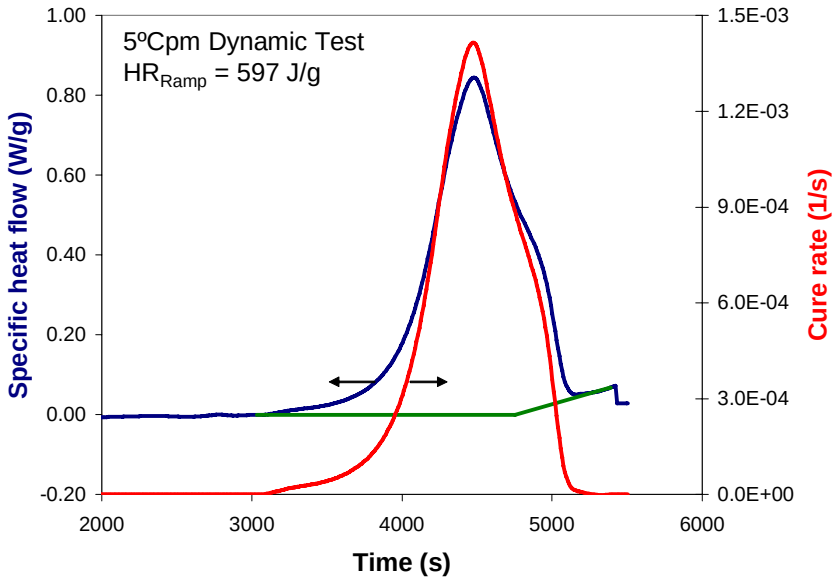

Figure 15. Specific heat flow and resin cure rate for the 5°C/min dynamic scan.

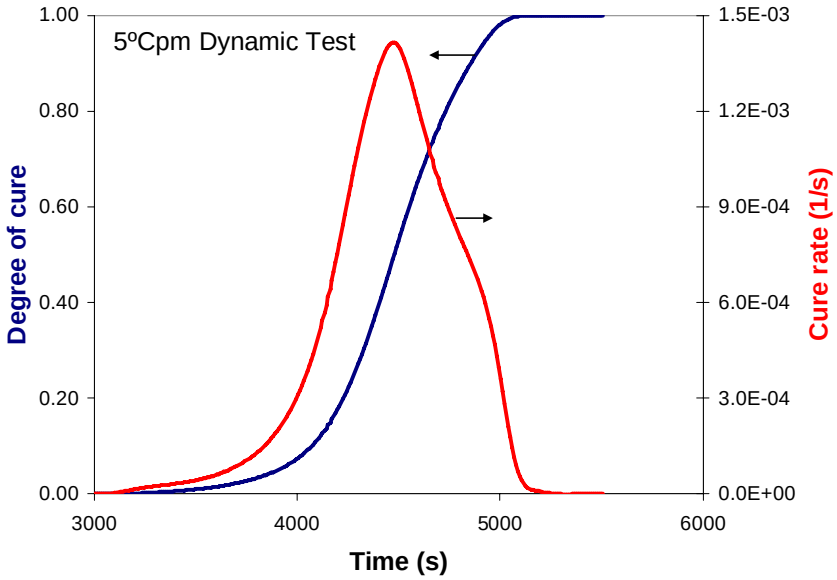

Figure 16. Degree of cure and cure rate for the 5°C/min dynamic scan.

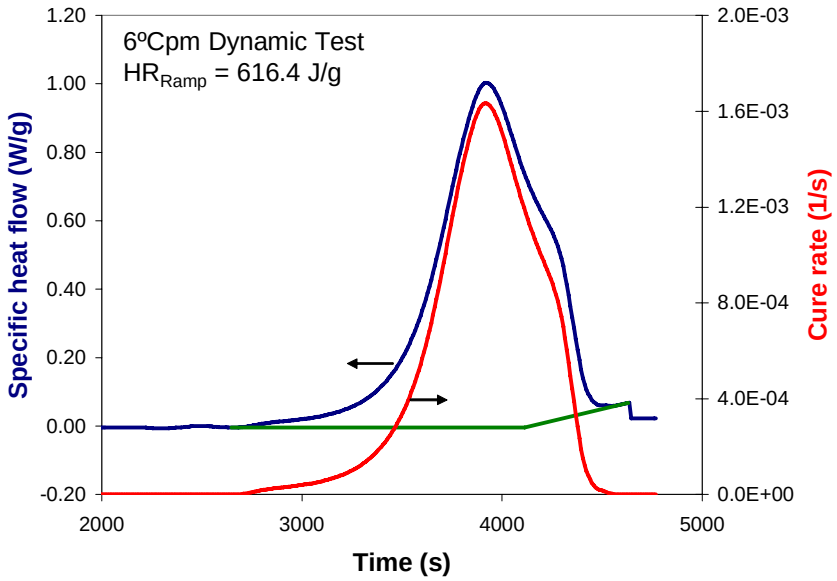

Figure 17. Specific heat flow and resin cure rate for the 6°C/min dynamic scan.

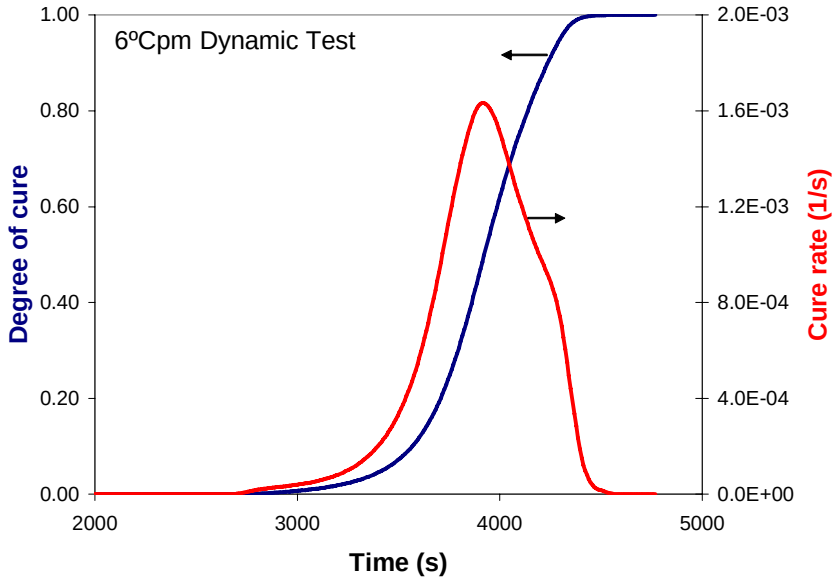

Figure 18. Degree of cure and cure rate for the 6°C/min dynamic scan.

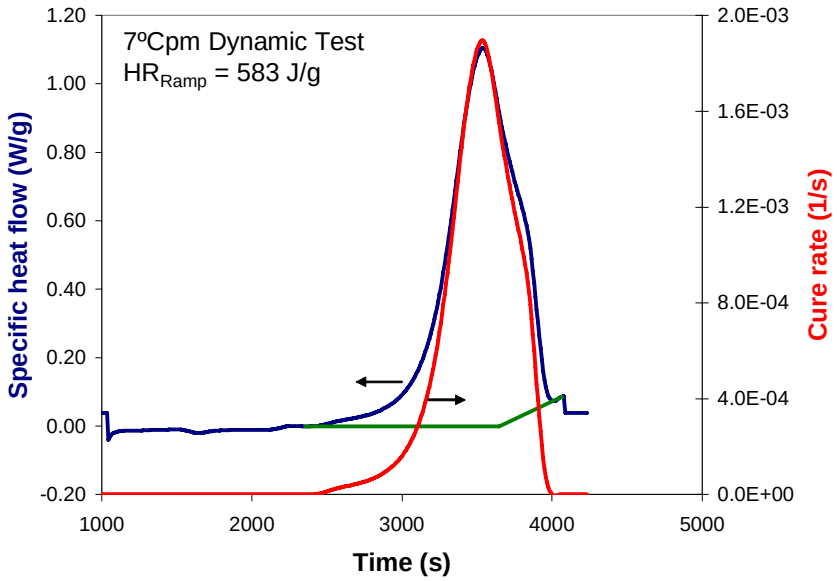

Figure 19. Specific heat flow and resin cure rate for the 7°C/min dynamic scan.

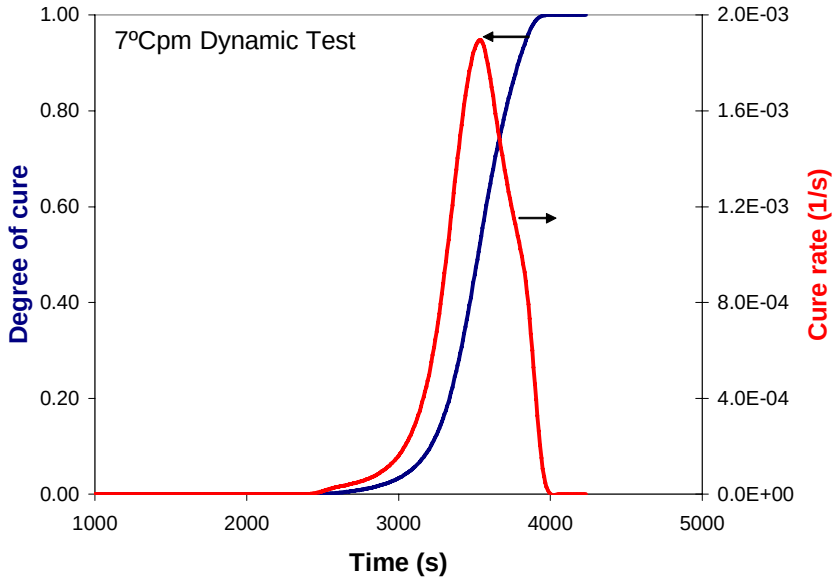

Figure 20. Degree of cure and cure rate for the 7°C/min dynamic scan.

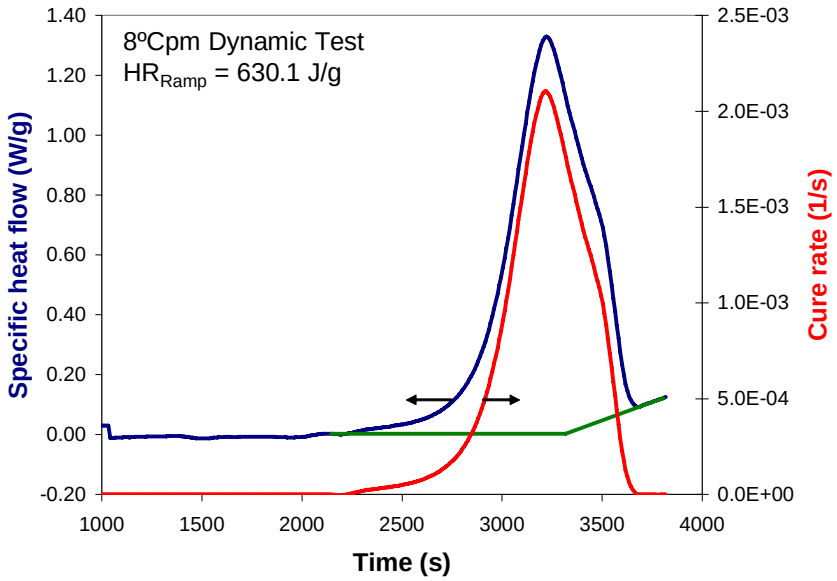

Figure 21. Specific heat flow and resin cure rate for the 8°C/min dynamic scan.

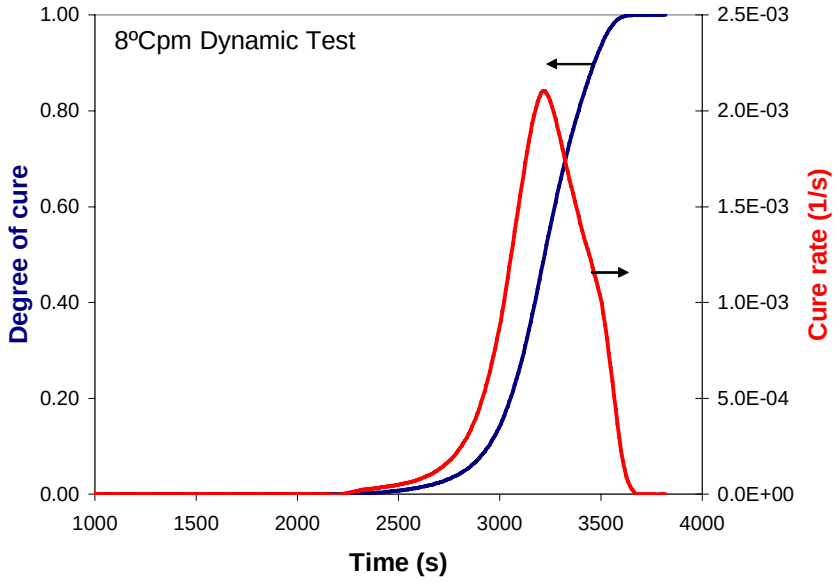

Figure 22. Degree of cure and cure rate for the 8°C/min dynamic scan.

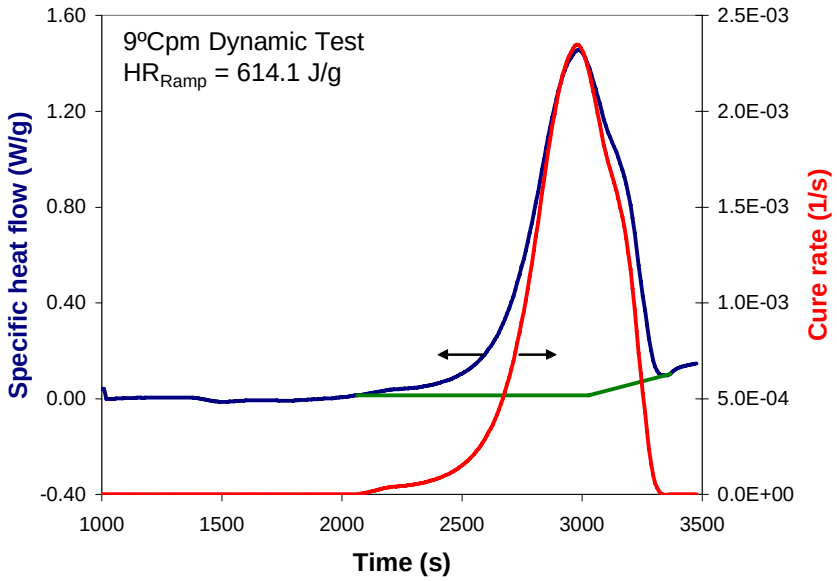

Figure 23. Specific heat flow and resin cure rate for the 9°C/min dynamic scan.

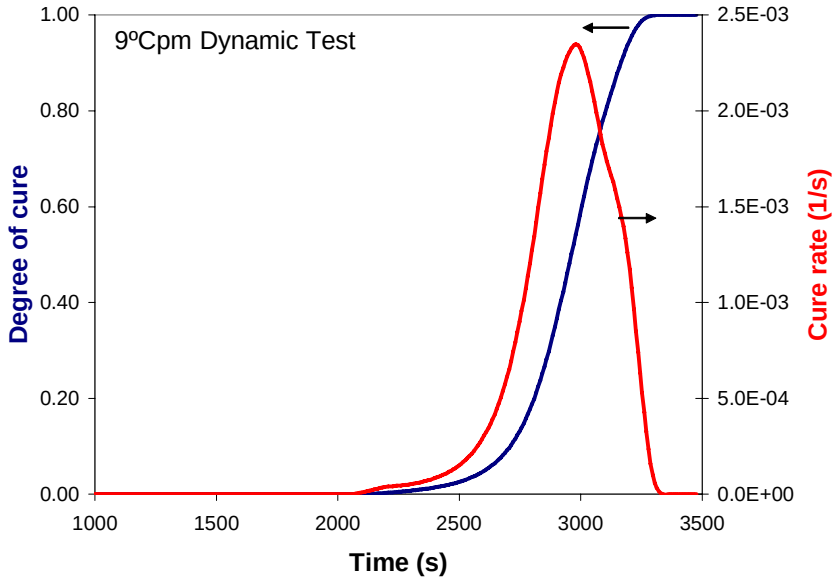

Figure 24. Degree of cure and cure rate for the 9°C/min dynamic scan.

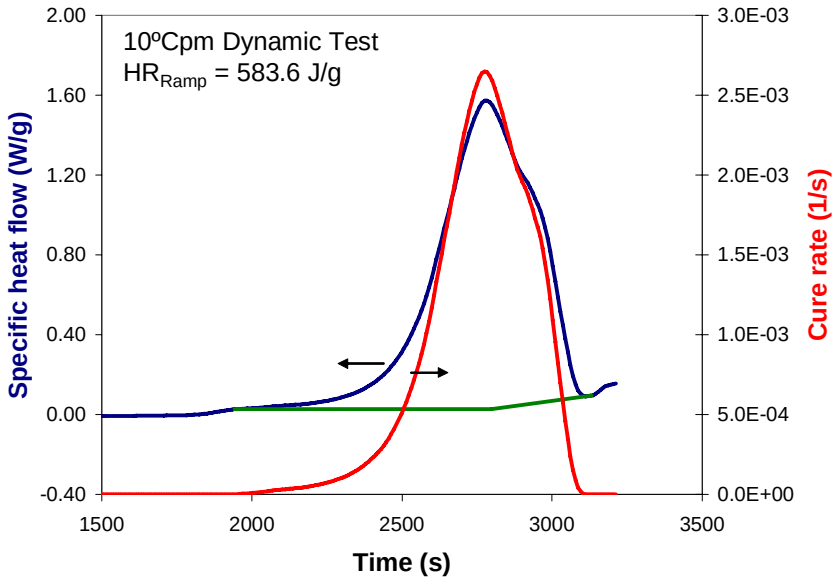

Figure 25. Specific heat flow and resin cure rate for the 10°C/min dynamic scan.

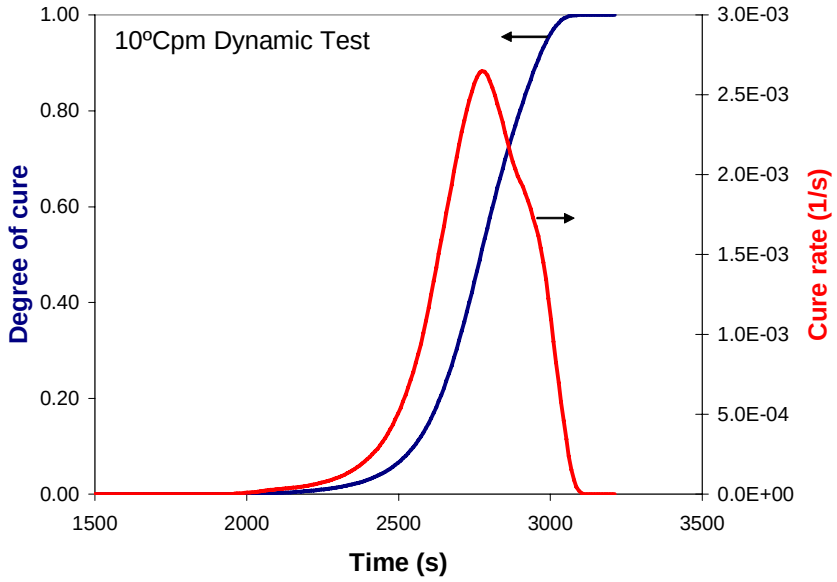

Figure 26. Degree of cure and cure rate for the 10°C/min dynamic scan.

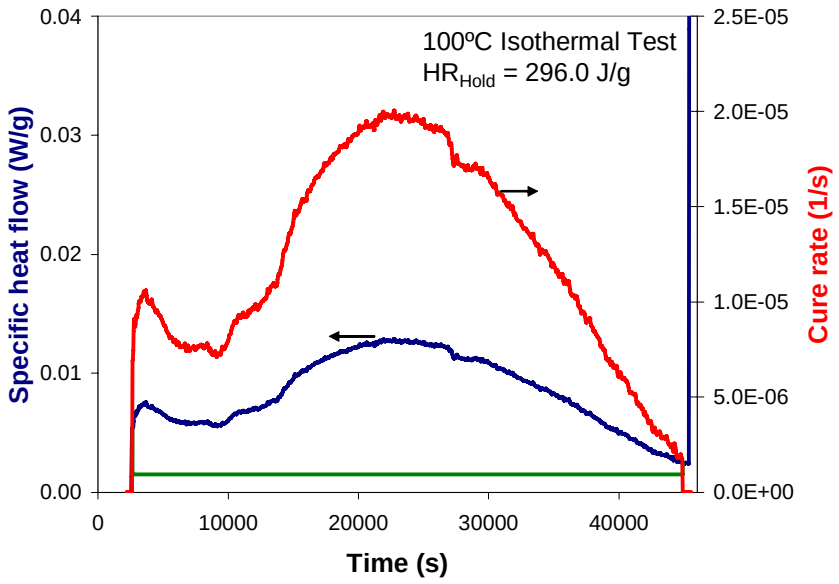

Figure 27. Specific heat flow and resin cure rate for the 100°C isothermal scan.

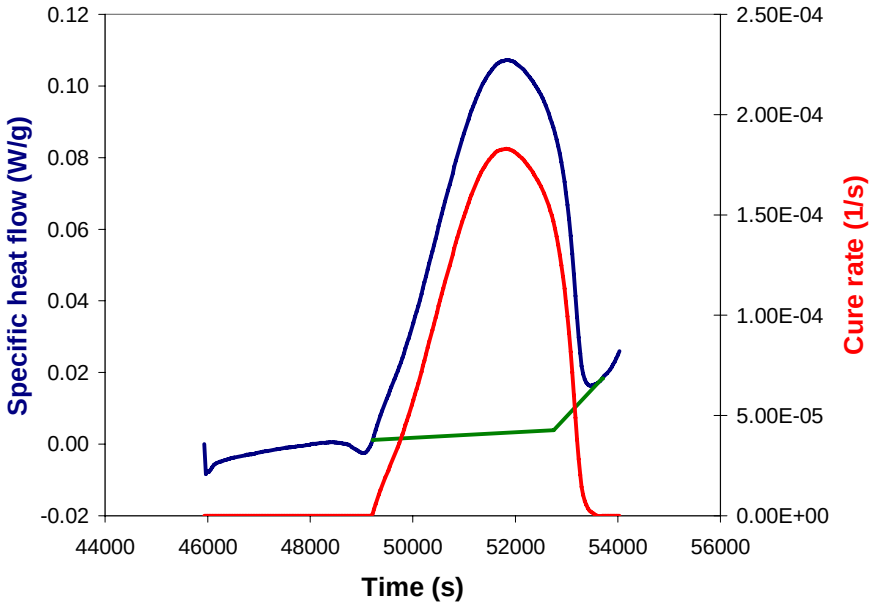

Figure 28. Specific heat flow and resin cure rate for the residual ramp of the 100°C isothermal scan.

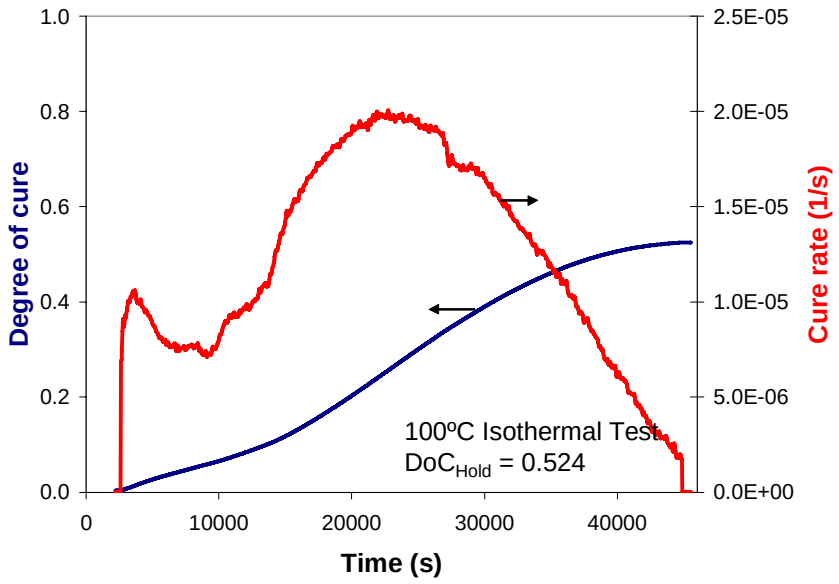

Figure 29. Degree of cure and cure rate for the 100°C isothermal scan.

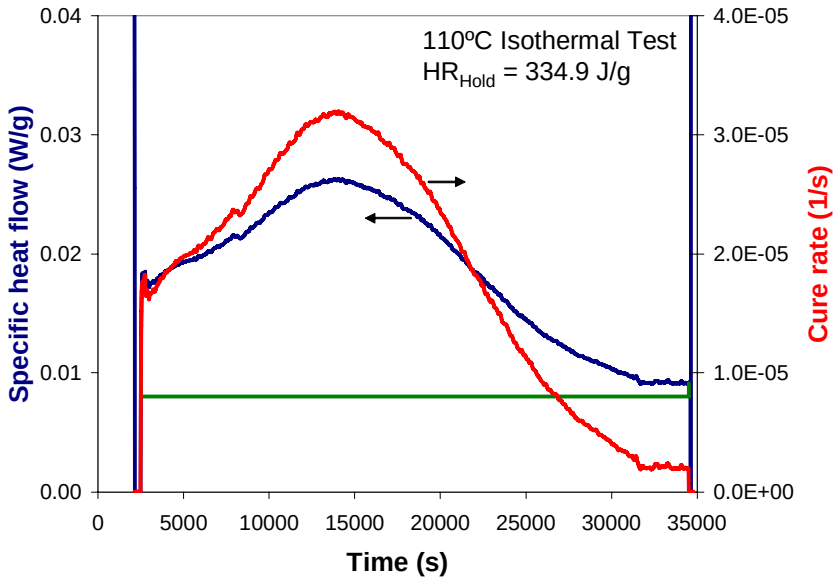

Figure 30. Specific heat flow and resin cure rate for the 110°C isothermal scan.

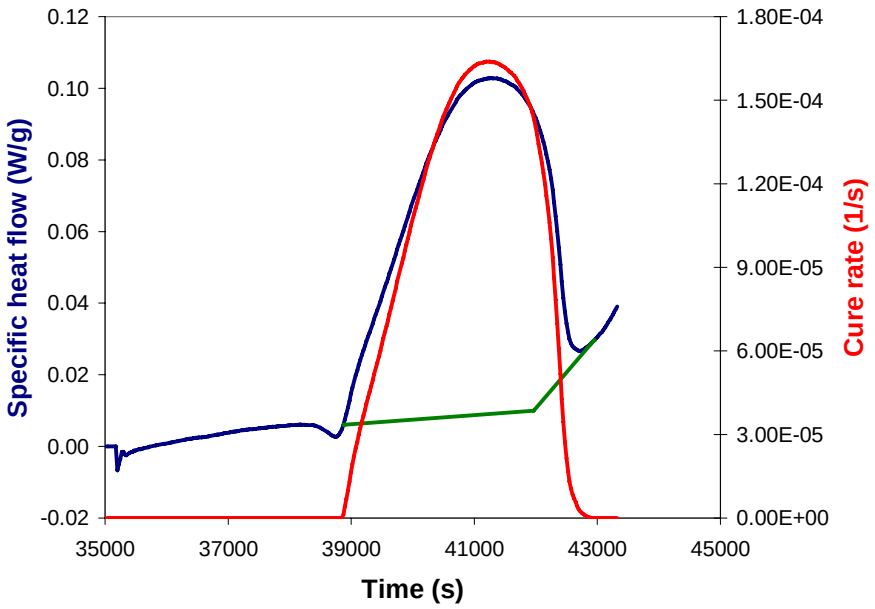

Figure 31. Specific heat flow and resin cure rate for the residual ramp of the 110°C isothermal scan.

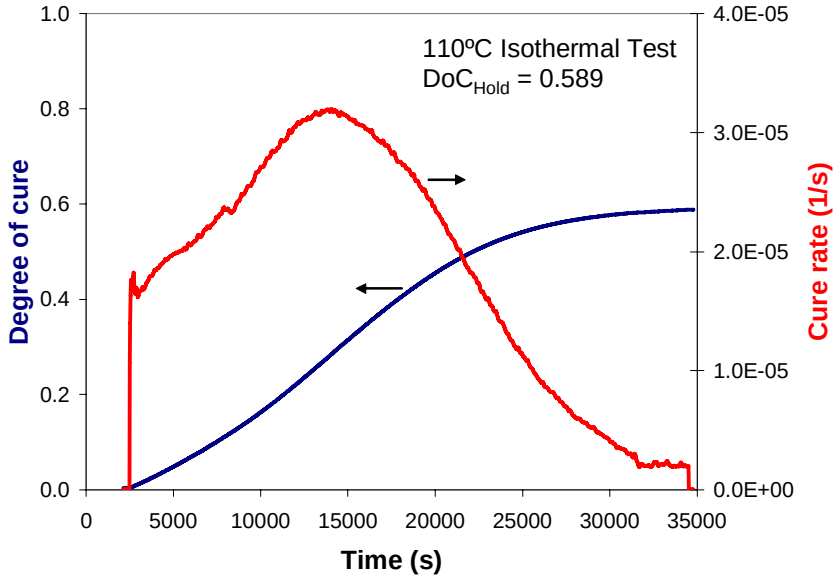

Figure 32. Degree of cure and cure rate for the 110°C isothermal scan.

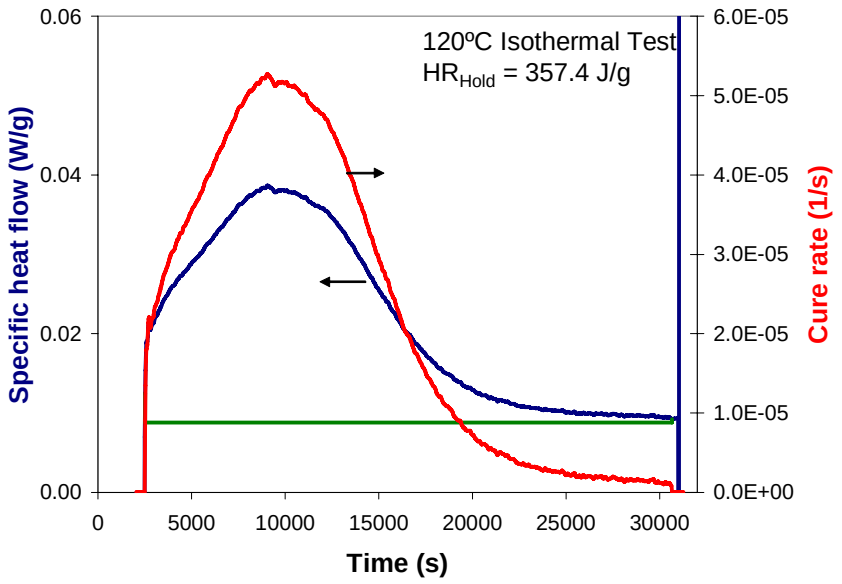

Figure 33. Specific heat flow and resin cure rate for the 120°C isothermal scan.

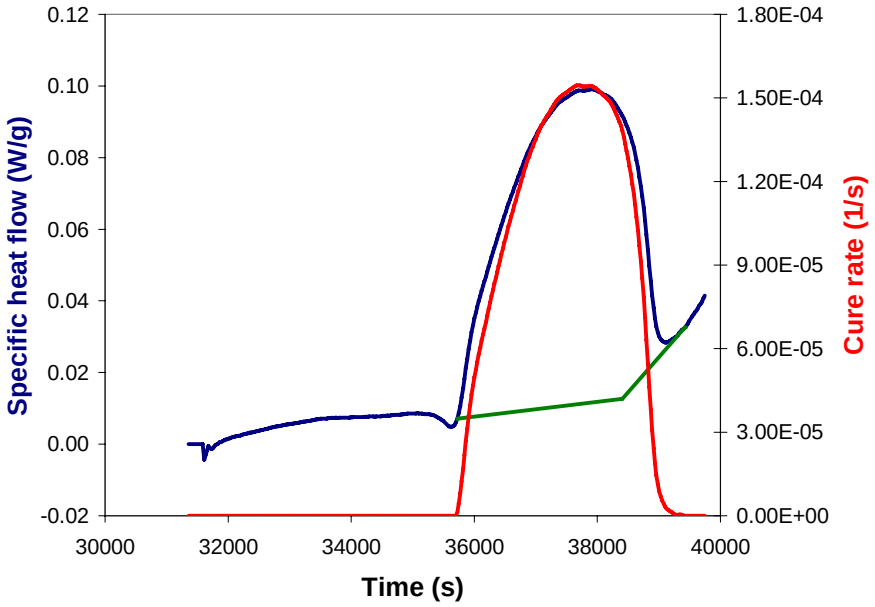

Figure 34. Specific heat flow and resin cure rate for the residual ramp of the 120°C isothermal scan.

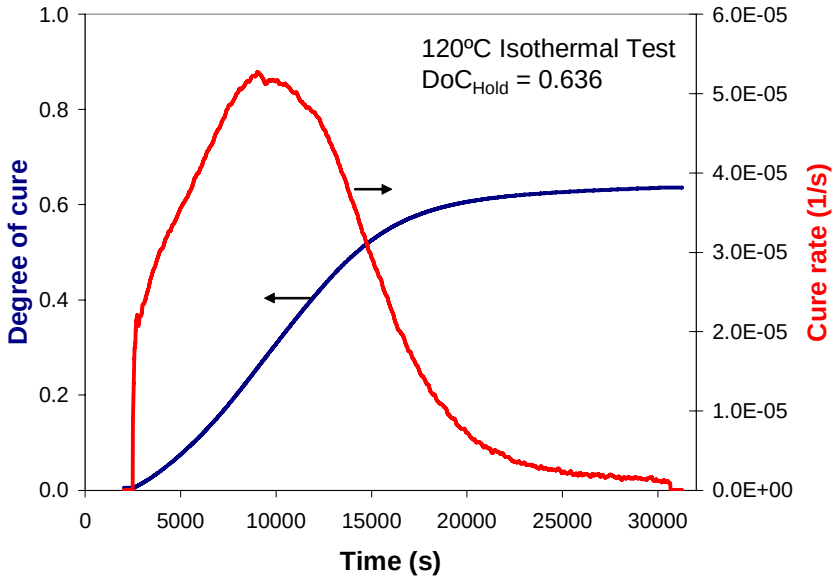

Figure 35. Degree of cure and cure rate for the 120°C isothermal scan.

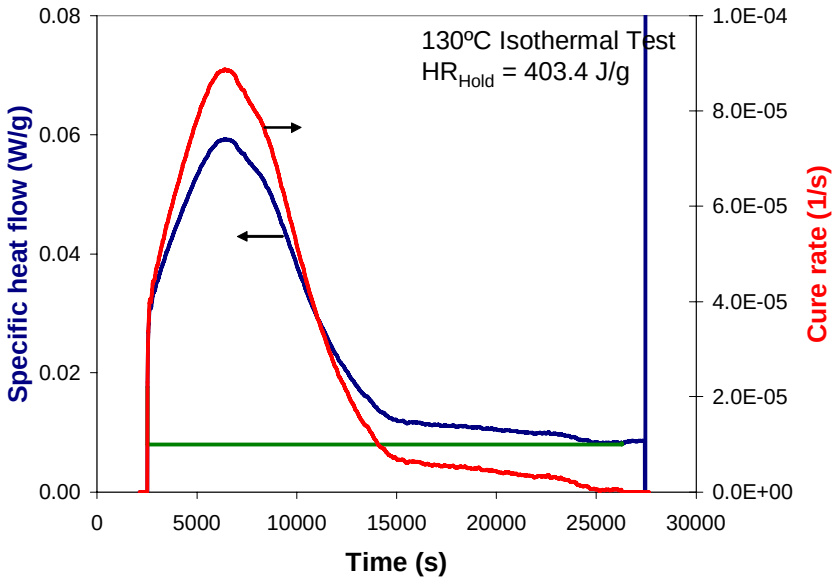

Figure 36. Specific heat flow and resin cure rate for the 130°C isothermal scan.

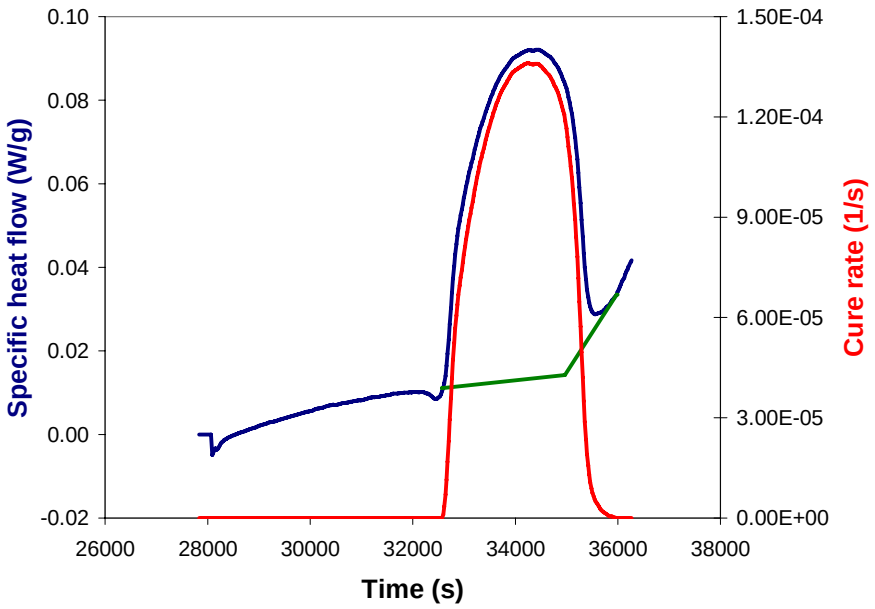

Figure 37. Specific heat flow and resin cure rate for the residual ramp of the 130°C isothermal scan.

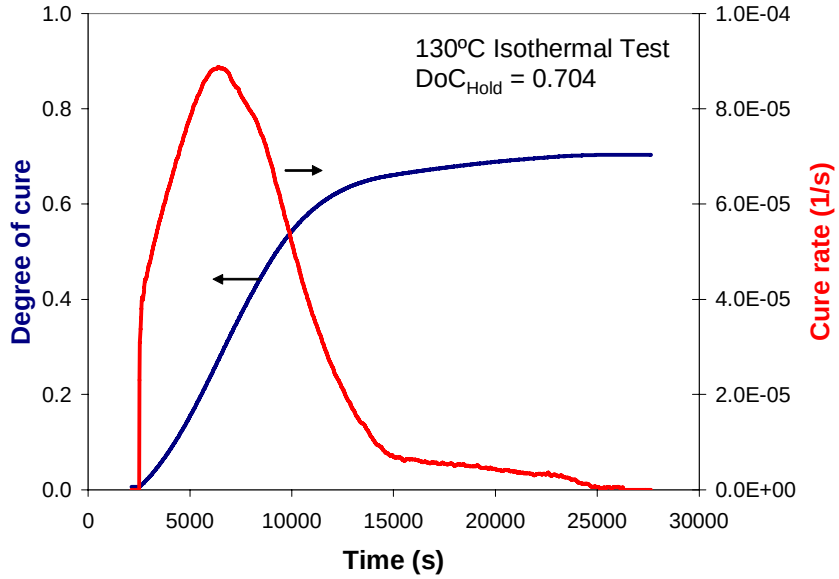

Figure 38. Degree of cure and cure rate for the 130°C isothermal scan.

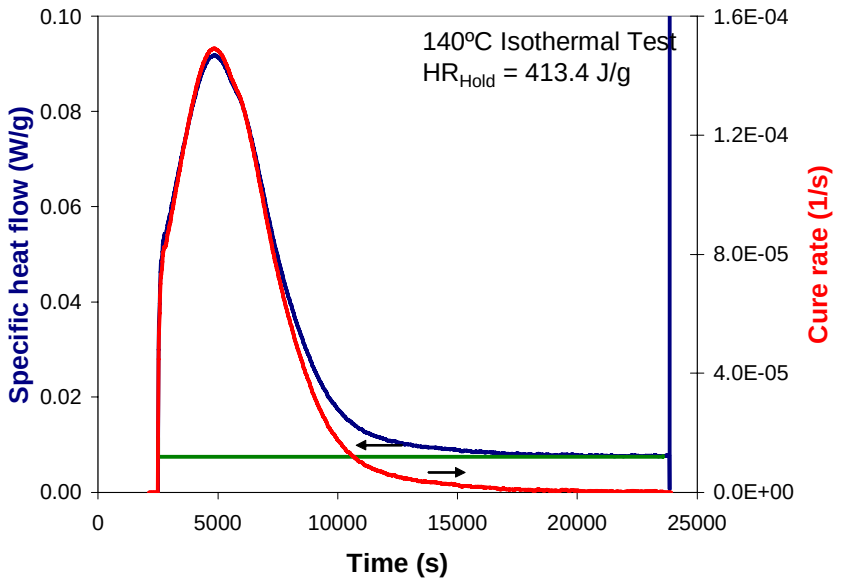

Figure 39. Specific heat flow and resin cure rate for the 140°C isothermal scan.

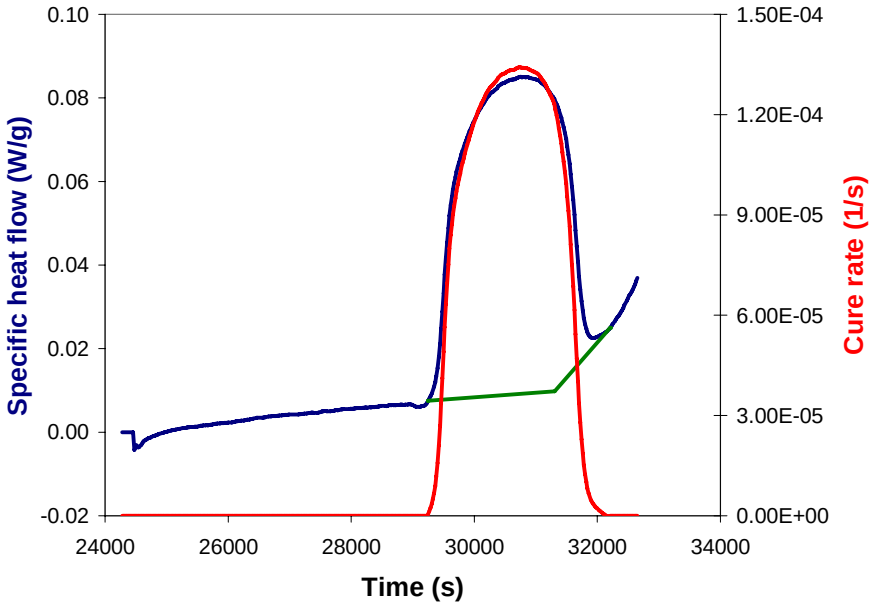

Figure 40. Specific heat flow and resin cure rate for the residual ramp of the 140°C isothermal scan.

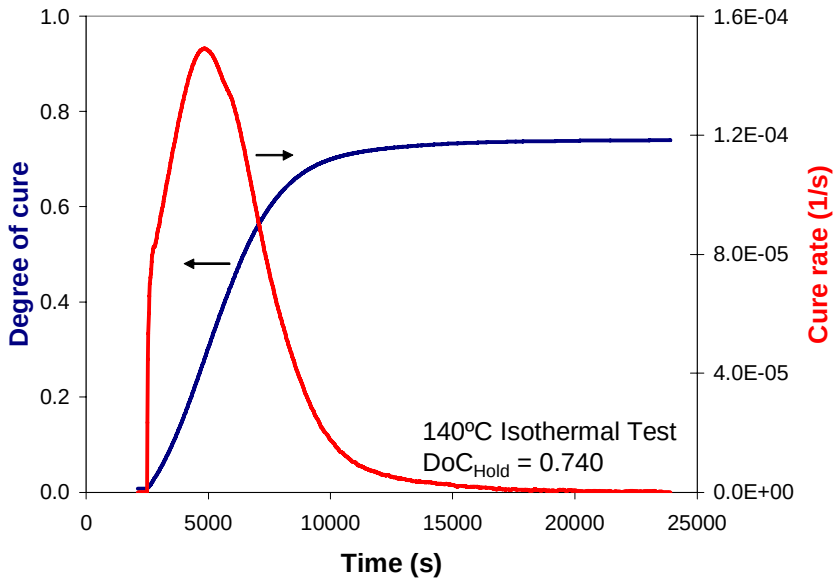

Figure 41. Degree of cure and cure rate for the 140°C isothermal scan.

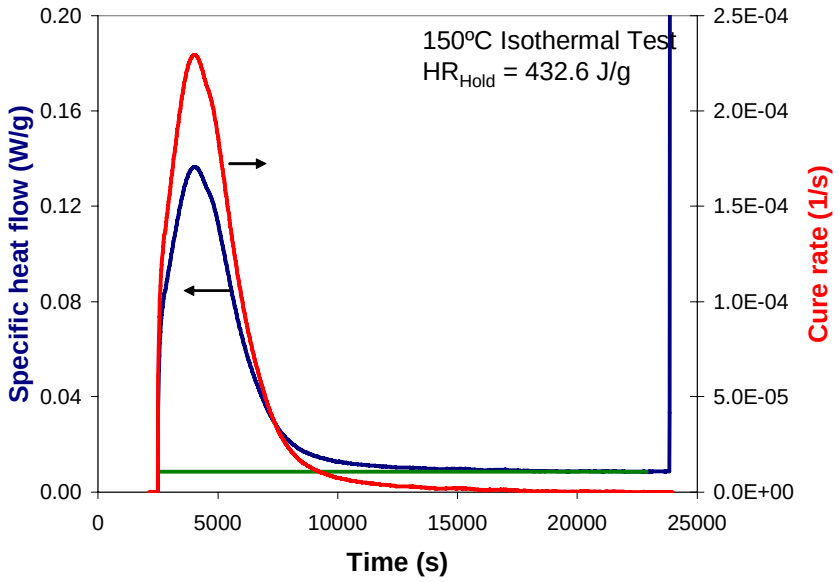

Figure 42. Specific heat flow and resin cure rate for the 150°C isothermal scan.

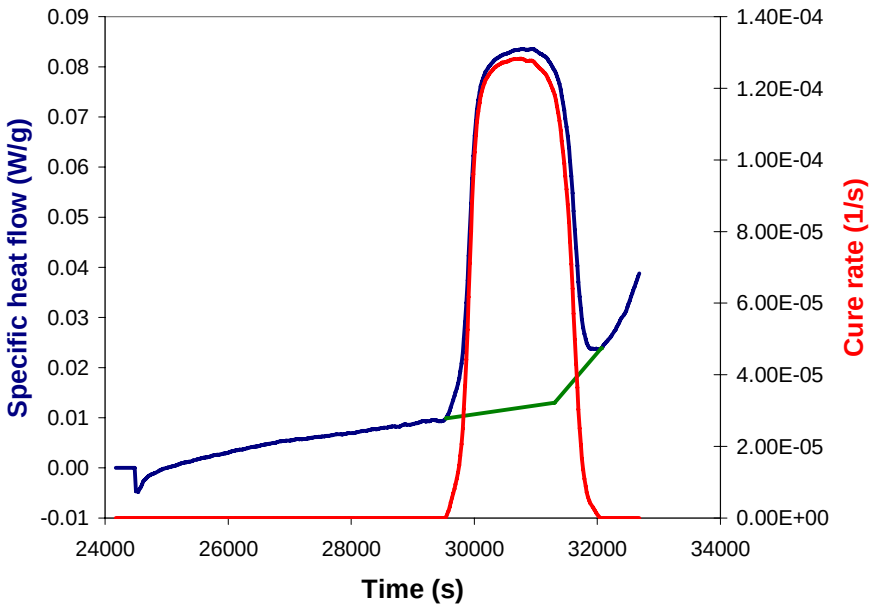

Figure 43. Specific heat flow and resin cure rate for the residual ramp of the 150°C isothermal scan.

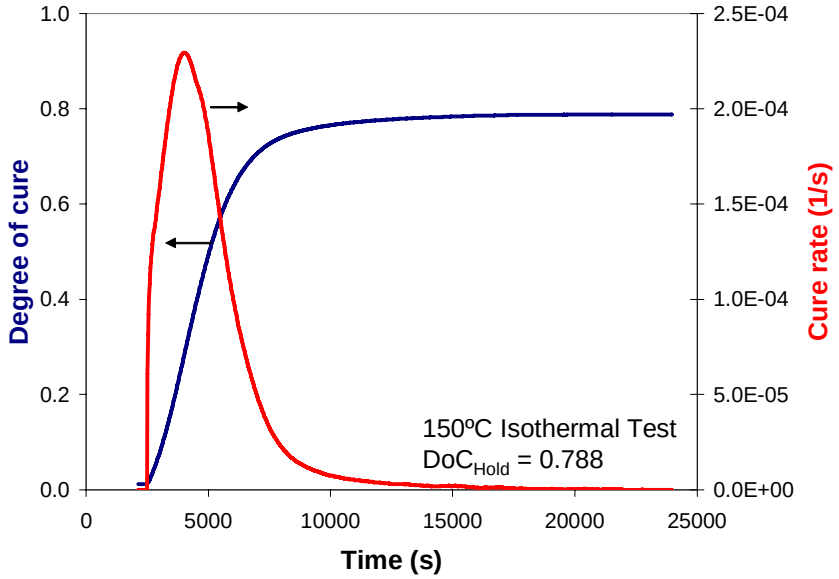

Figure 44. Degree of cure and cure rate for the 150°C isothermal scan.

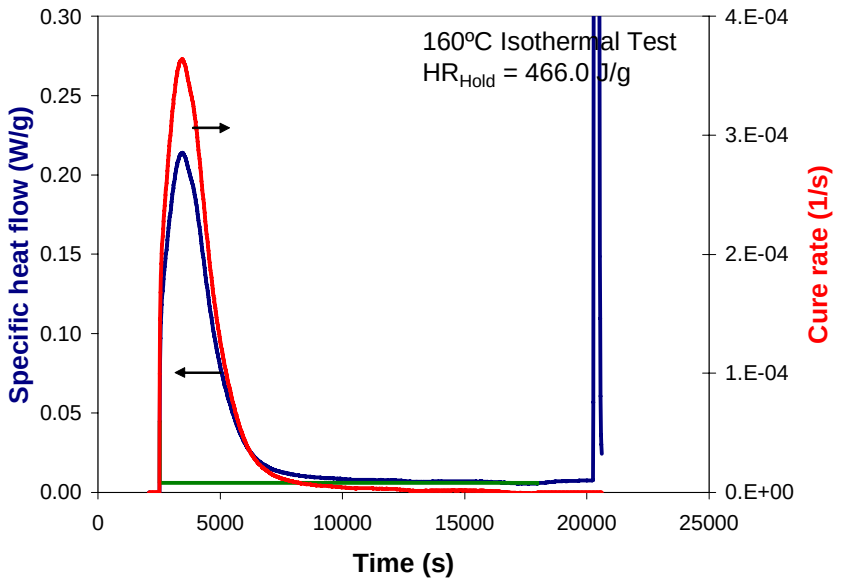

Figure 45. Specific heat flow and resin cure rate for the 160°C isothermal scan.

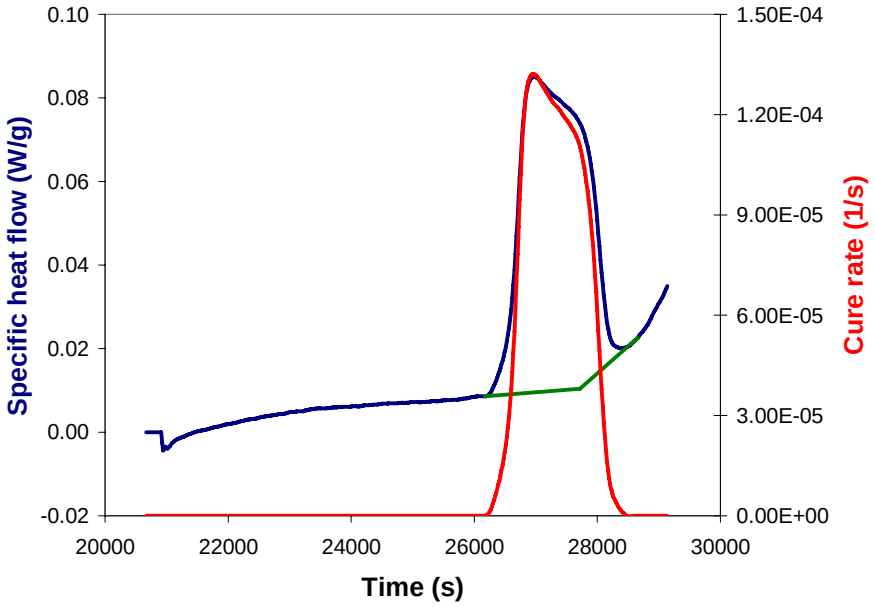

Figure 46. Specific heat flow and resin cure rate for the residual ramp of the 160°C isothermal scan.

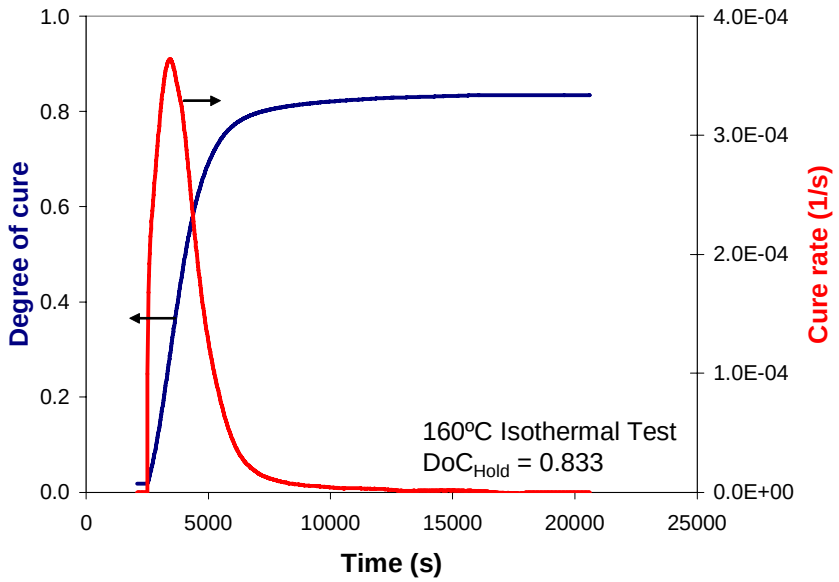

Figure 47. Degree of cure and cure rate for the 160°C isothermal scan.

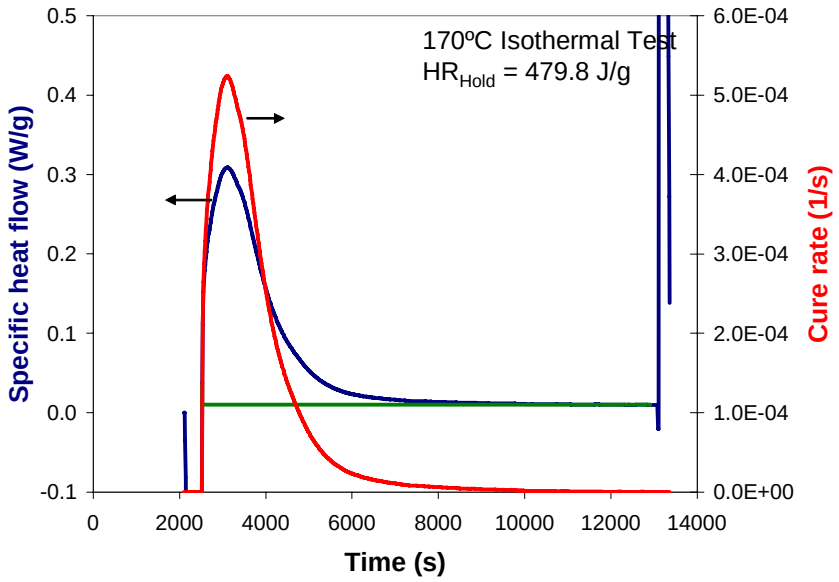

Figure 48. Specific heat flow and resin cure rate for the 170°C isothermal scan.

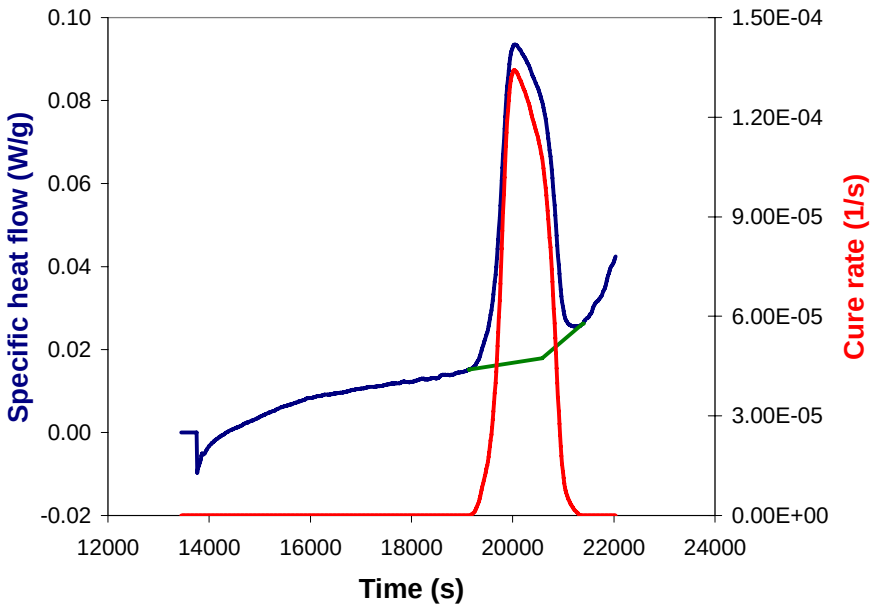

Figure 49. Specific heat flow and resin cure rate for the residual ramp of the 170°C isothermal scan.

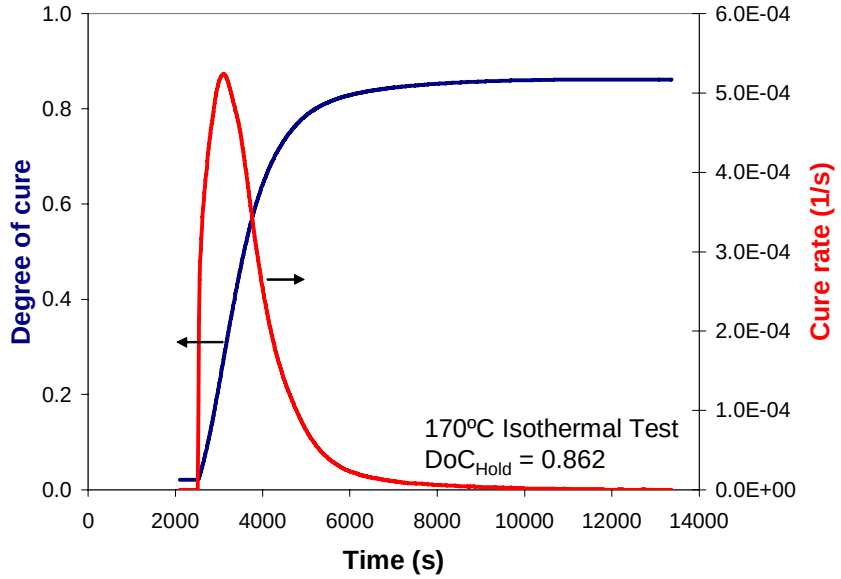

Figure 50. Degree of cure and cure rate for the 170°C isothermal scan.

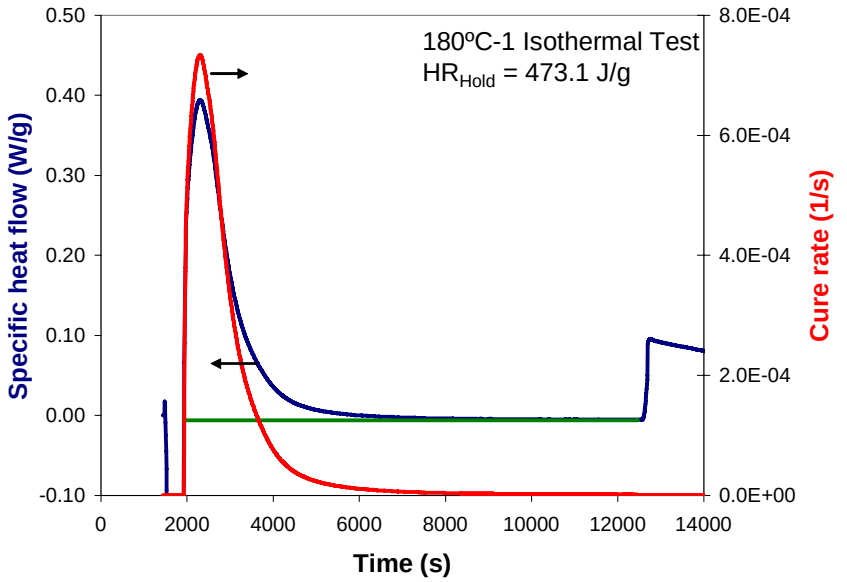

Figure 51. Specific heat flow and resin cure rate for the 180°C (1) isothermal scan.

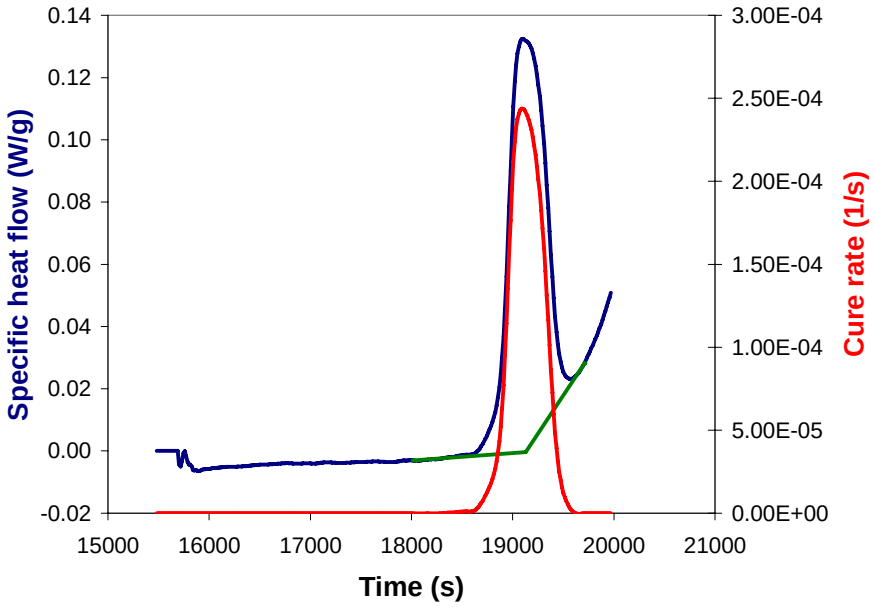

Figure 52. Specific heat flow and resin cure rate for the residual ramp of the 180°C (1) isothermal scan.

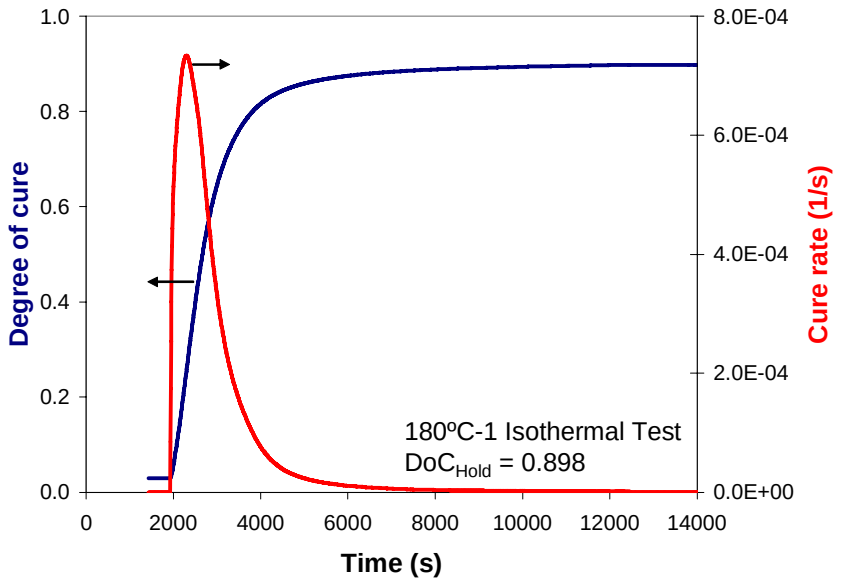

Figure 53. Degree of cure and cure rate for the 180°C (1) isothermal scan.

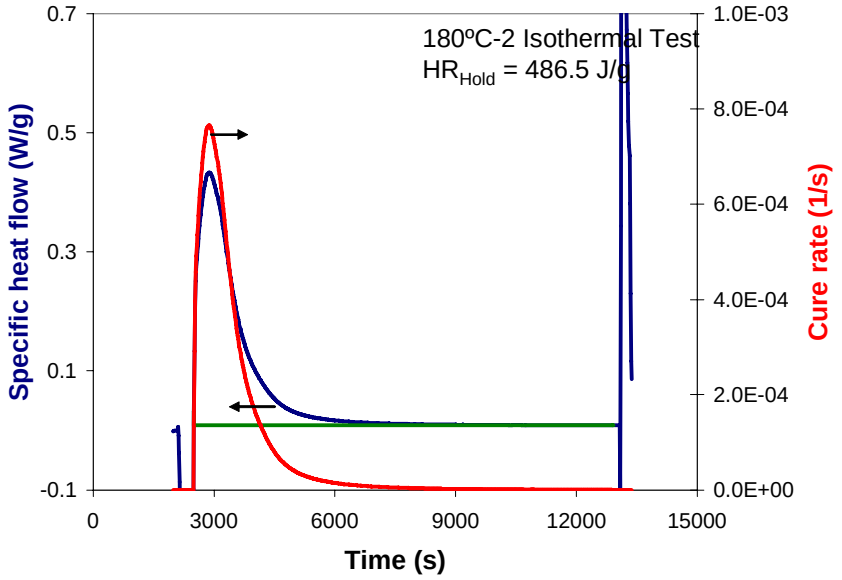

Figure 54. Specific heat flow and resin cure rate for the 180°C (2) isothermal scan.

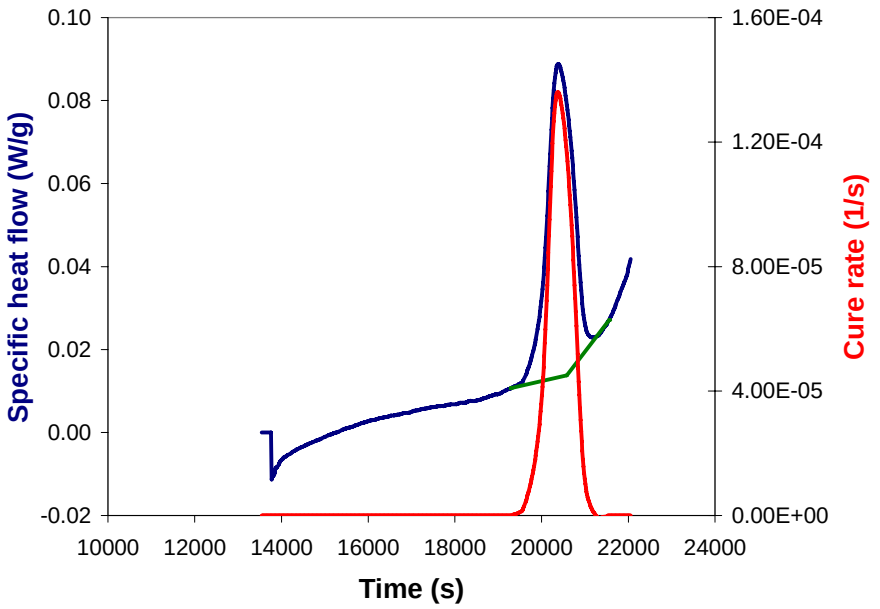

Figure 55. Specific heat flow and resin cure rate for the residual ramp of the 180°C (2) isothermal scan.

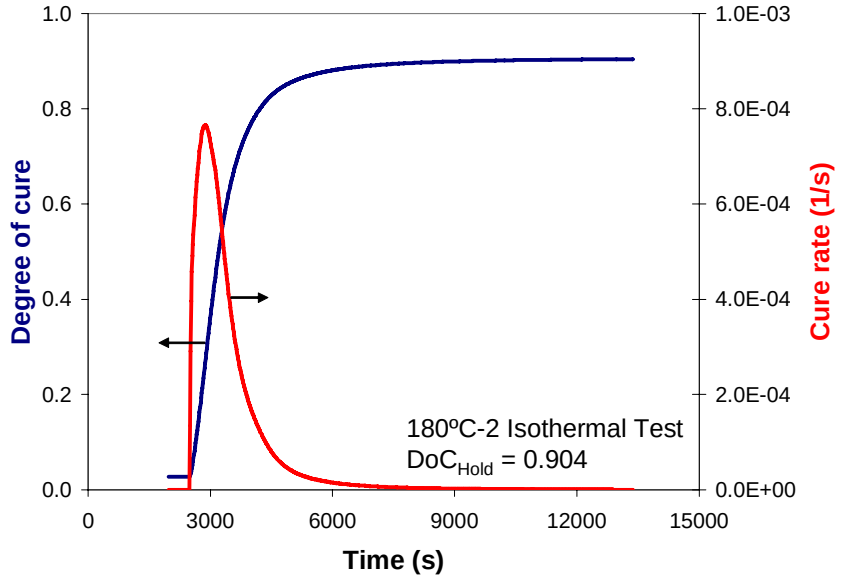

Figure 56. Degree of cure and cure rate for the 180°C (2) isothermal scan.

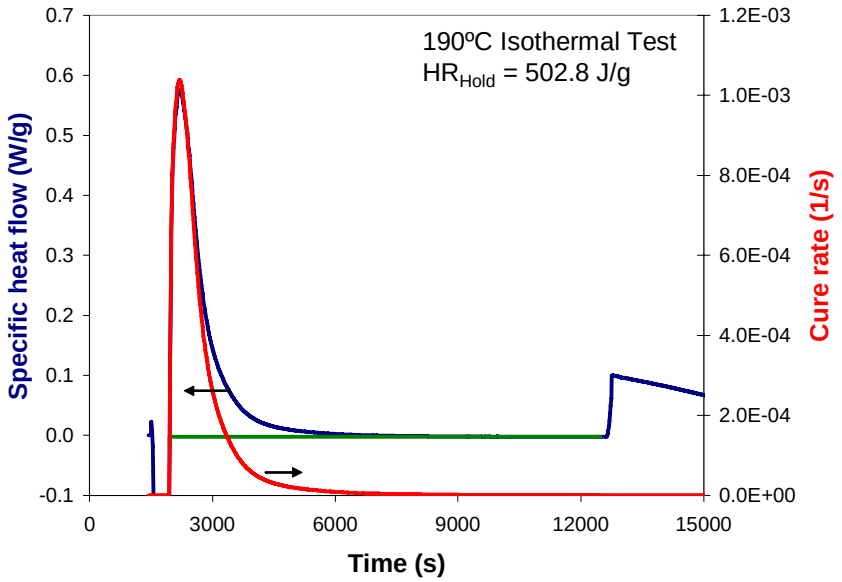

Figure 57. Specific heat flow and resin cure rate for the 190°C isothermal scan.

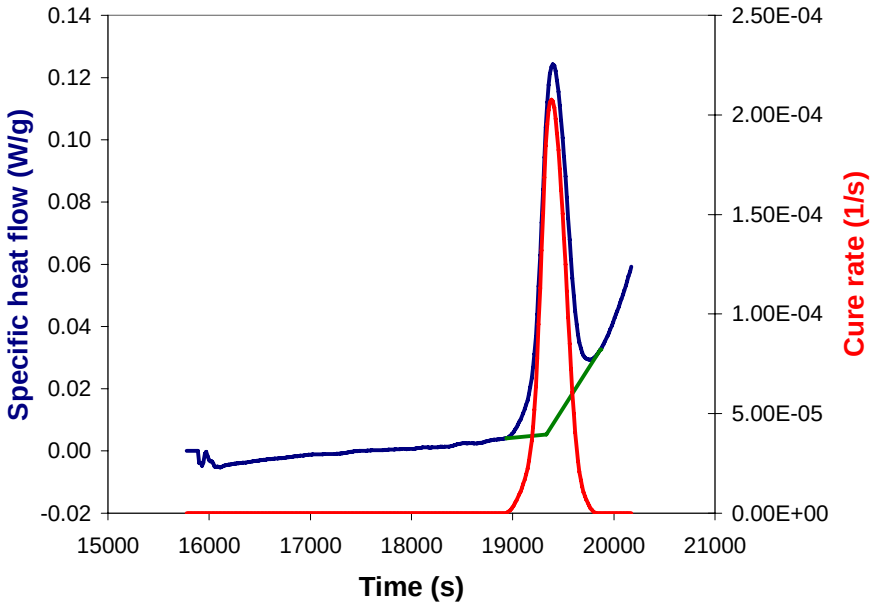

Figure 58. Specific heat flow and resin cure rate for the residual ramp of the 190°C isothermal scan.

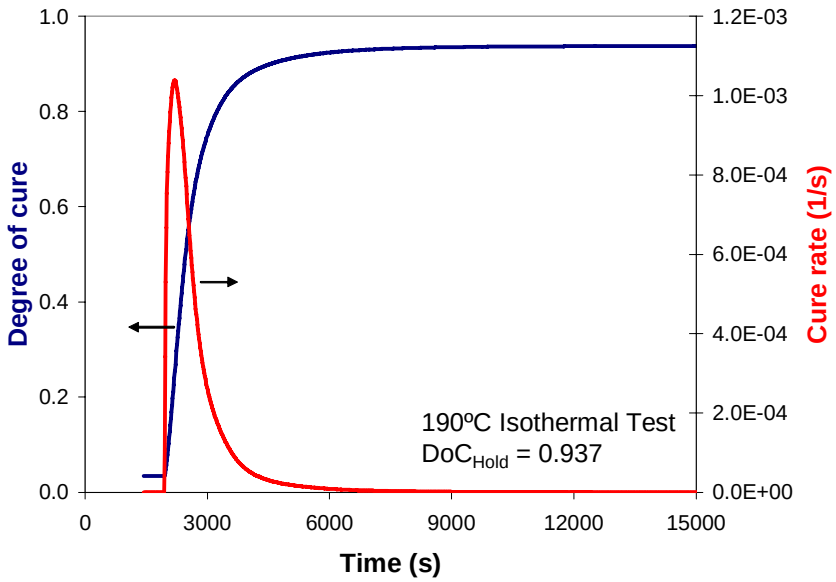

Figure 59. Degree of cure and cure rate for the 190°C isothermal scan.

Glass Transition Temperature

Cure kinetics model 15 requires the glass transition temperature (T_g) of the material at a given degree of cure. To determine T_g, the inflection point of the heat capacity response was considered as the temperature at which the material transitions from glassy to rubbery during heat-up or cool-down segments of the DSC tests. In the dynamic tests, T_g measurement at the end of the test was not possible, as the material seemed to have degraded due to the high temperatures it was exposed to during the test. This was also the case for the residual dynamic scans of the isothermal tests. The corresponding values of the degree of cure were determined in an iterative procedure using the values of heat of reaction measured at different stages of the test and the DeBenedetto equation. The final results of this analysis are provided in Table 66 to Table 8.

Table 6: Glass transition temperature (Tg) data measured for the dynamic tests.

Test	Initial		Final	
	DoC	Tg (ºC)	DoC	Tg (ºC)
8552-MDYN-01cpm-01	0.00	-8.84	1.00	197.26
8552-MDYN-02cpm-01	0.00	-8.15	1.00	205.79
8552-MDYN-02cpm-02	0.00	-10.09	1.00	217.28
8552-MDYN-03cpm-01	0.00	-7.36	1.00	204.15
8552-MDYN-04cpm-01	0.00	-6.66	1.00	203.67
8552-MDYN-05cpm-01	0.00	-7.68	1.00	203.58
8552-MDYN-06cpm-01	0.00	-7.28	1.00	203.48
8552-MDYN-07cpm-01	0.00	-2.70	1.00	203.05
8552-MDYN-08cpm-01	0.00	-7.08	1.00	162.63
8552-MDYN-09cpm-01	0.00	-5.78	1.00	162.28
8552-MDYN-10cpm-01	0.00	-2.99	1.00	167.96

[1]Degree of cure is calculated using DeBenedetto equation

Table 7: Glass transition temperature (Tg) data measured for isothermal tests.

Test	Initial		Post-Hold	
	DoC	Tg (ºC)	DoC	Tg (ºC)
8552-MISO-100C-01	0.00	-12.57	0.52	108.21
8552-MISO-110C-01	0.00	-14.36	0.59	126.05
8552-MISO-120C-01	0.00	-13.94	0.64	142.72
8552-MISO-130C-01	0.00	-13.48	0.70	165.85
8552-MISO-140C-01	0.00	-12.55	0.74	169.27
8552-MISO-150C-01	0.00	-12.71	0.79	182.65
8552-MISO-160C-01	0.00	-14.44	0.83	195.99
8552-MISO-170C-01	0.00	-14.31	0.86	204.91
8552-MISO-180C-01	0.00	-	0.90	226.65
8552-MISO-180C-02	0.00	-13.53	0.90	218.09
8552-MISO-190C-01	0.00	-	0.94	217.58

[1]Degree of cure is calculated using DeBenedetto equation
[2]Degree of cure is calculated from heat of reaction

Table 8: Glass transition temperature (Tg) data measured for interrupted isothermal tests.

Test	Initial		Post-Hold	
	DoC	Tg (ºC)	DoC	Tg (ºC)
8552-160C-INT15	0.00	-14.34	0.00	208.53
8552-160C-INT30	0.00	-13.97	0.00	214.27

[1]Degree of cure is calculated using DeBenedetto equation
[2]Degree of cure is calculated from heat of reaction

The DeBenedetto equation (below) was fit to the data in order to determine its parameters.

$$T_g = T_{go} + \frac{\lambda x}{1-(1-\lambda)x}(T_{g\infty} - T_{go})$$

The final DeBenedetto fit along with the fitted glass transition temperature and degree of cure data are shown in the figure below:

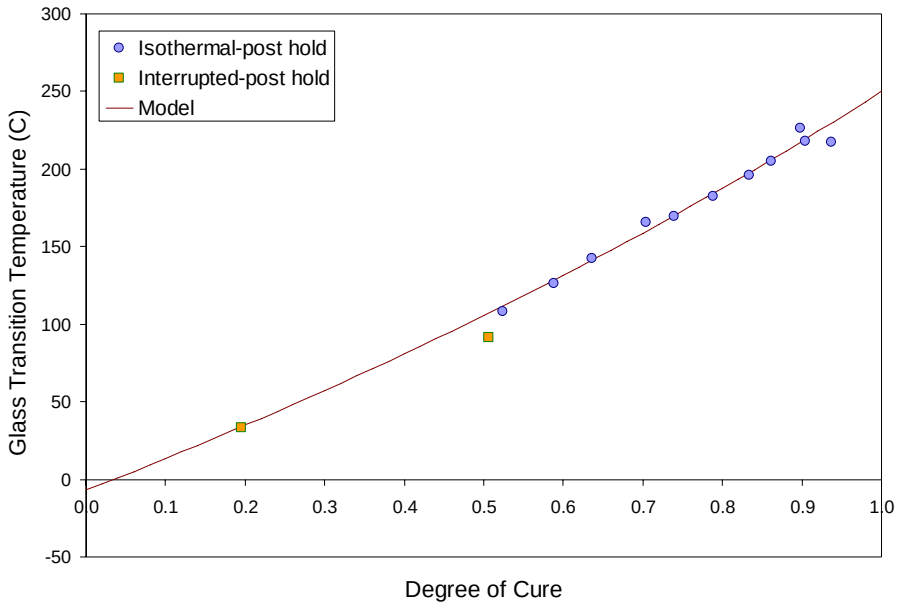

Figure 60. T_g data from the isothermal and interrupted isothermal tests, and the resulting model based on the DeBenedetto equation.

Curve Fit Calculations

The cure kinetics model constants were determined by fitting the model to the experimental data. Model fitting was performed using ODRPACK[1], a minimization software based on the weighted orthogonal distance regression.

Process maps generated for this cure kinetics model can be found in the Appendix.

Quality of Fit

The following figures show a comparison of the degree of cure and cure rate from experimental data and as predicted by the model. Model predictions for high temperature isothermals tests not included in the fitting procedure are also shown.

[1] P. T. Boggs, R. H. Byrd, J. E. Rogers, and R. B. Schnabel, "User's Reference Guide for ODRPACK Version 2.01 – Software for Weighted Orthogonal Distance Regression", NISTIR 4834, June 1992.

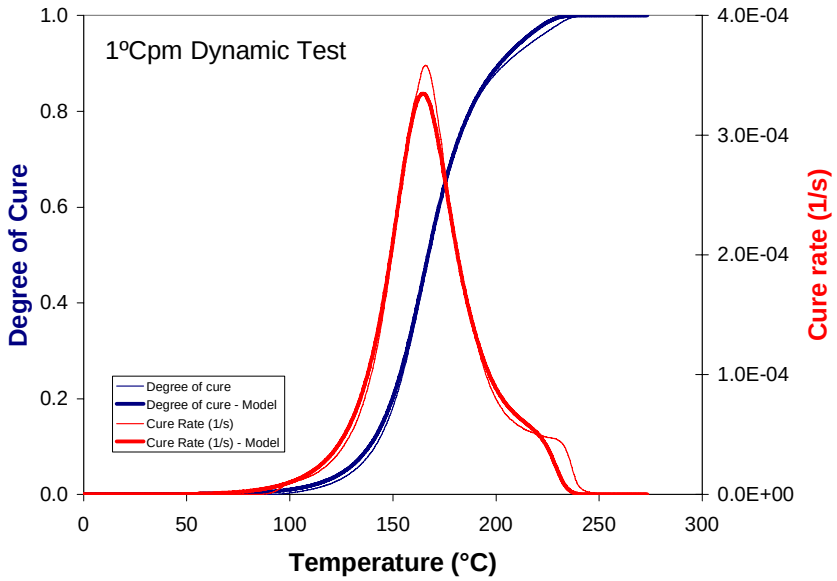

Figure 7. Degree of cure and cure rate for the 1°C/min dynamic scan compared to model predictions.

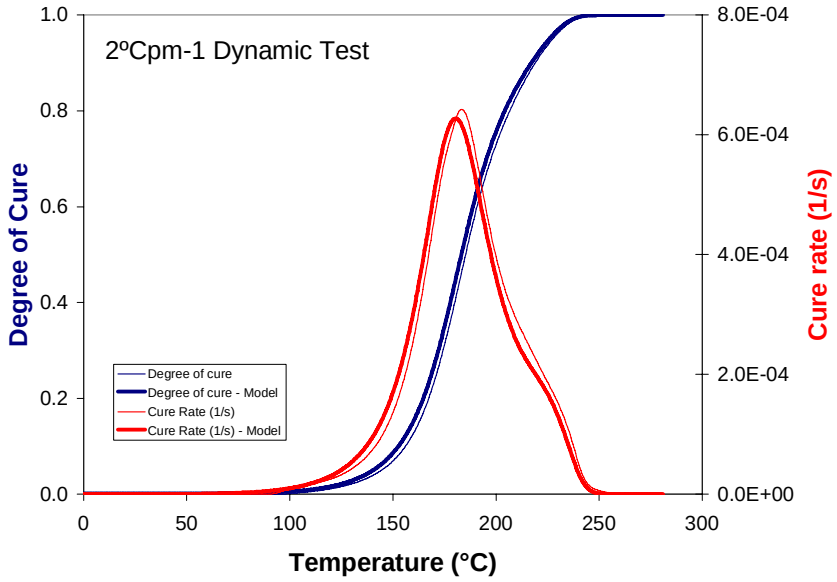

Figure 81. Degree of cure and cure rate for the 2°C/min (1) dynamic scan compared to model predictions.

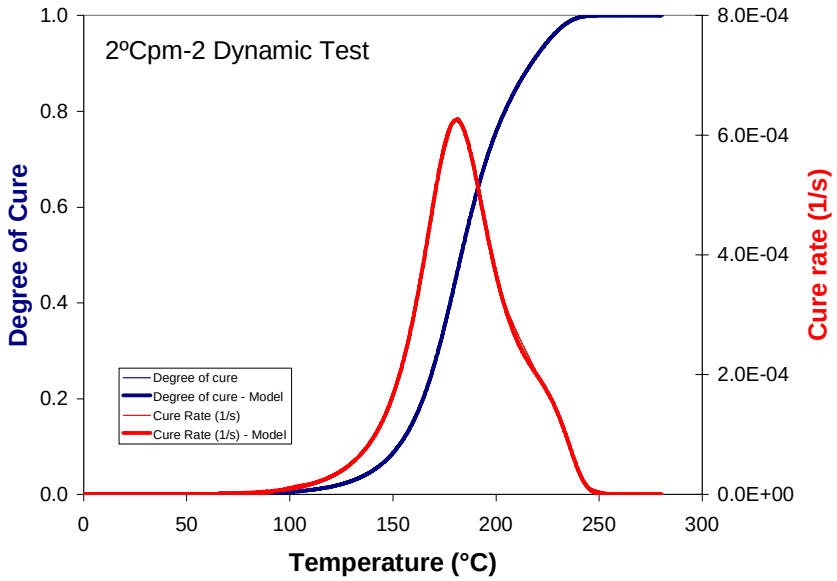

Figure 92. Degree of cure and cure rate for the 2°C/min (2) dynamic scan compared to model predictions.

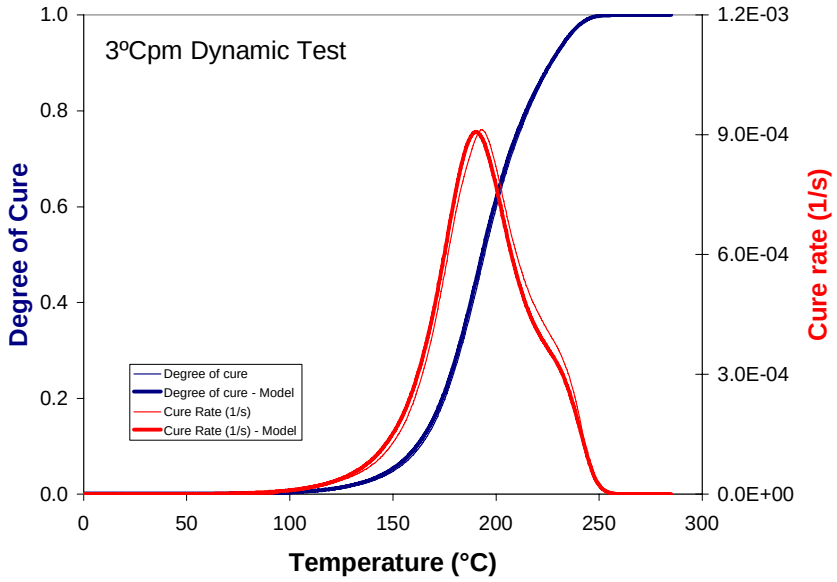

Figure 103. Degree of cure and cure rate for the 3°C/min dynamic scan compared to model predictions.

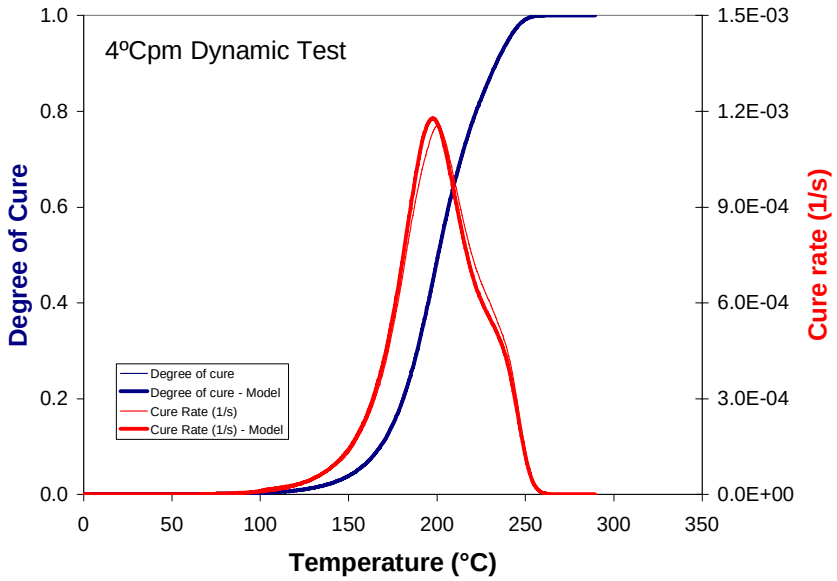

Figure 114. Degree of cure and cure rate for the 4°C/min dynamic scan compared to model predictions.

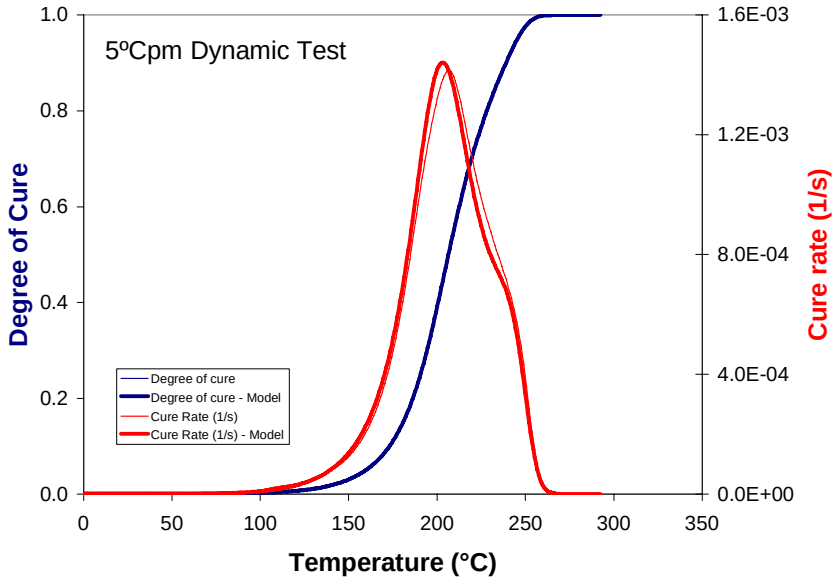

Figure 125. Degree of cure and cure rate for the 5°C/min dynamic scan compared to model predictions.

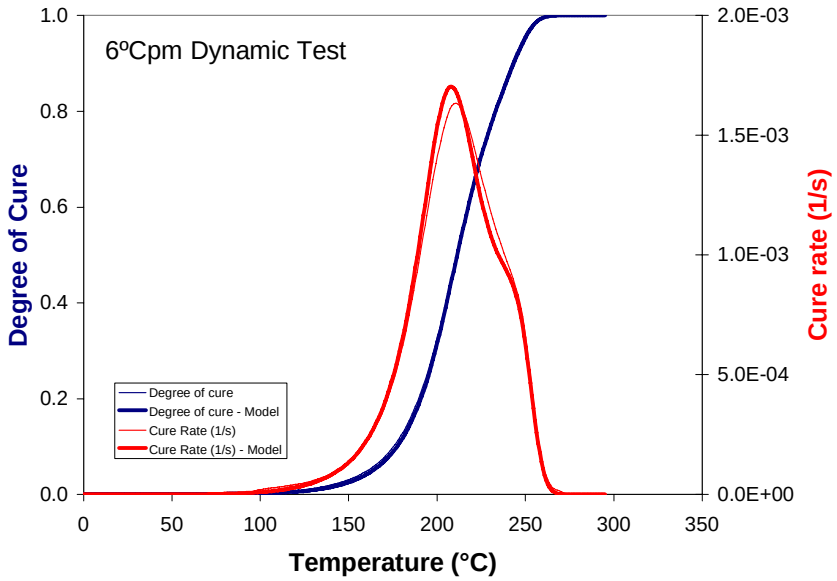

Figure 136. Degree of cure and cure rate for the 6°C/min dynamic scan compared to model predictions.

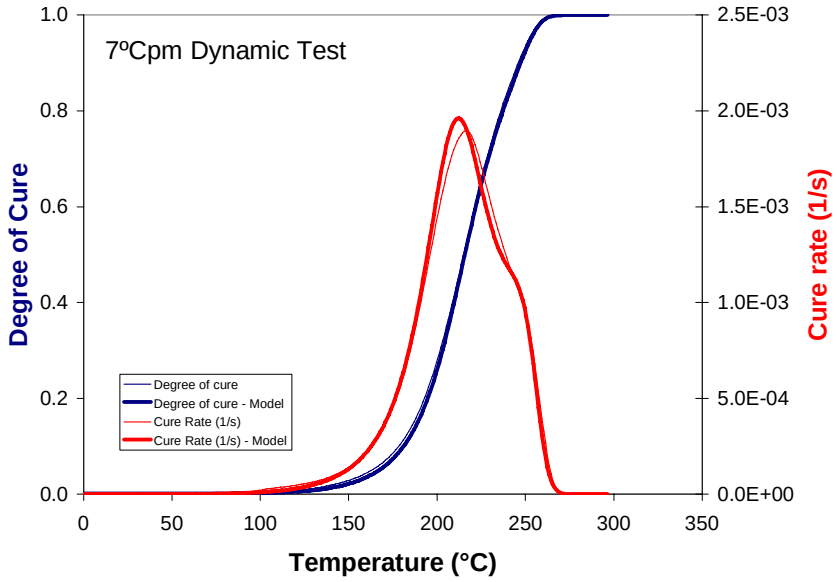

Figure 147. Degree of cure and cure rate for the 7°C/min dynamic scan compared to model predictions.

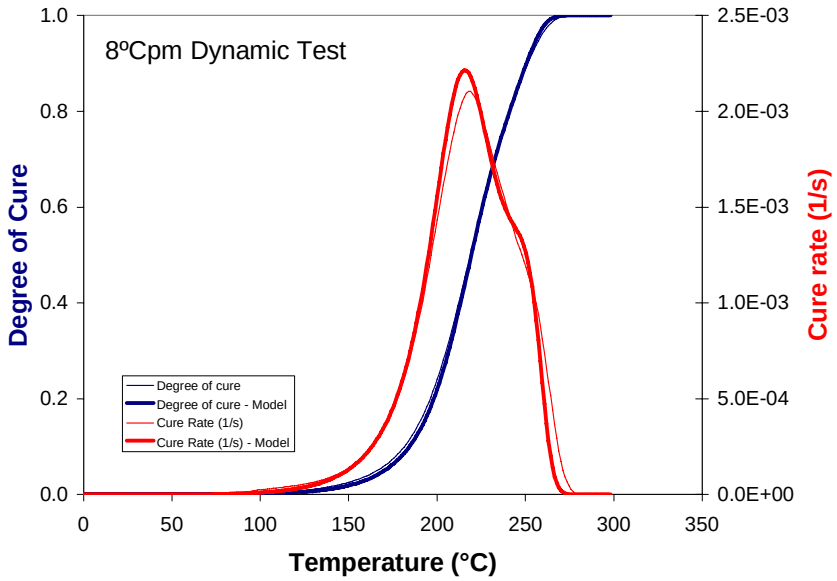

Figure 158. Degree of cure and cure rate for the 8°C/min dynamic scan compared to model predictions.

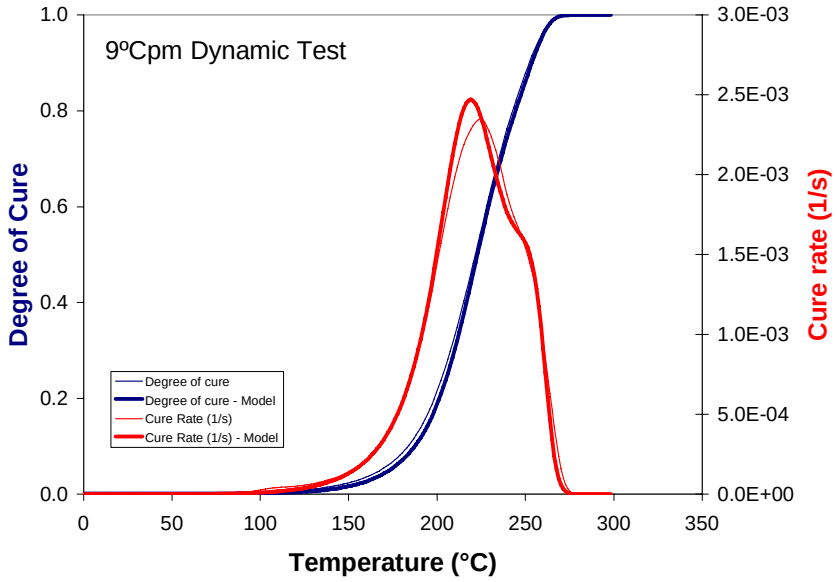

Figure 169. Degree of cure and cure rate for the 9°C/min dynamic scan compared to model predictions.

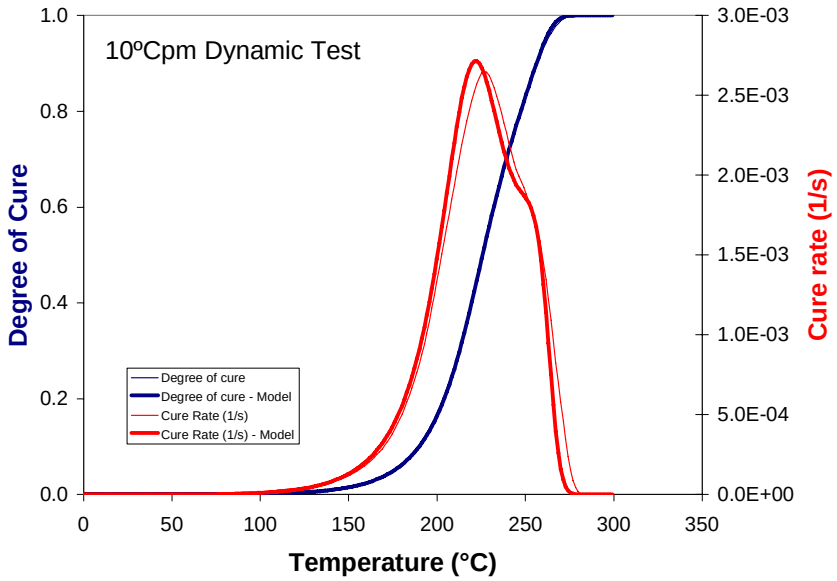

Figure 80. Degree of cure and cure rate for the 10°C/min dynamic scan compared to model predictions.

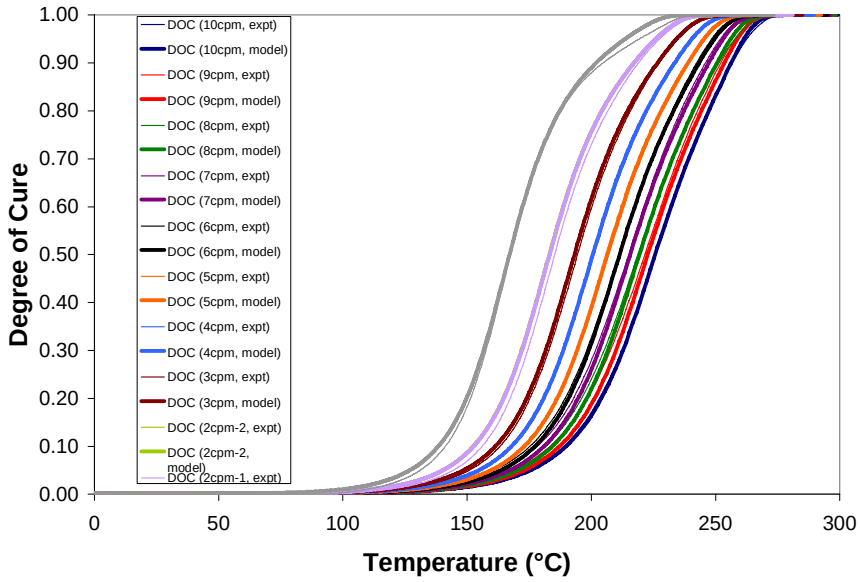

Figure 81. Comparisons of the degree of cure between the model and experiments for the dynamic DSC tests.

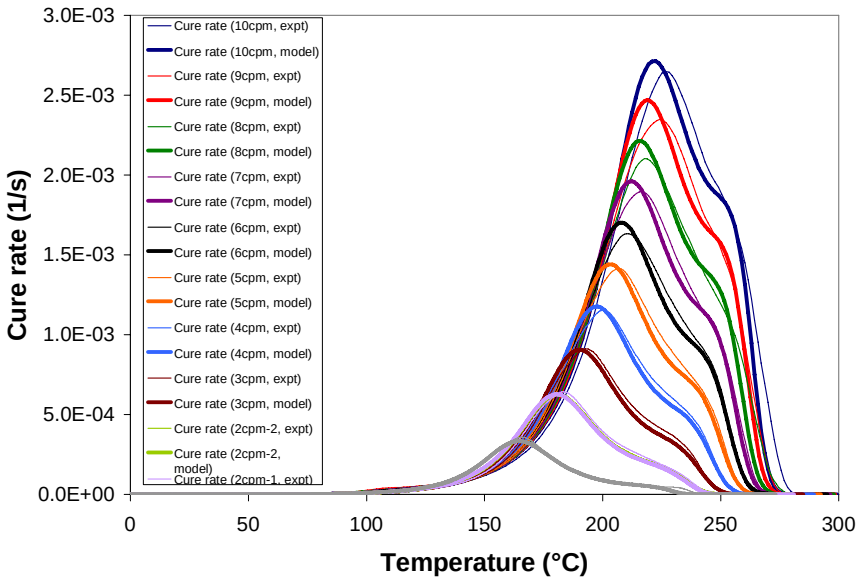

Figure 82. Comparisons of the cure rate between the model and experiments for the dynamics DSC tests.

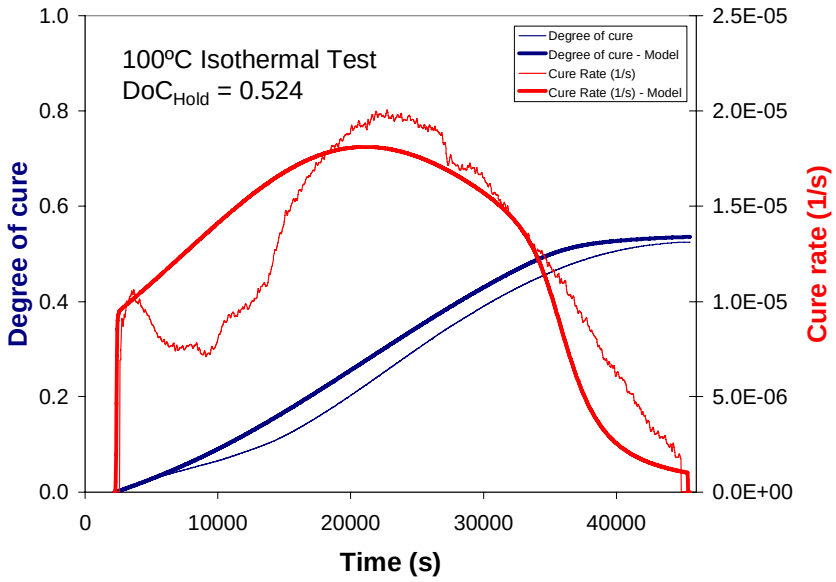

Figure 83. Degree of cure and cure rate for the 100°C isothermal scan compared to model predictions.

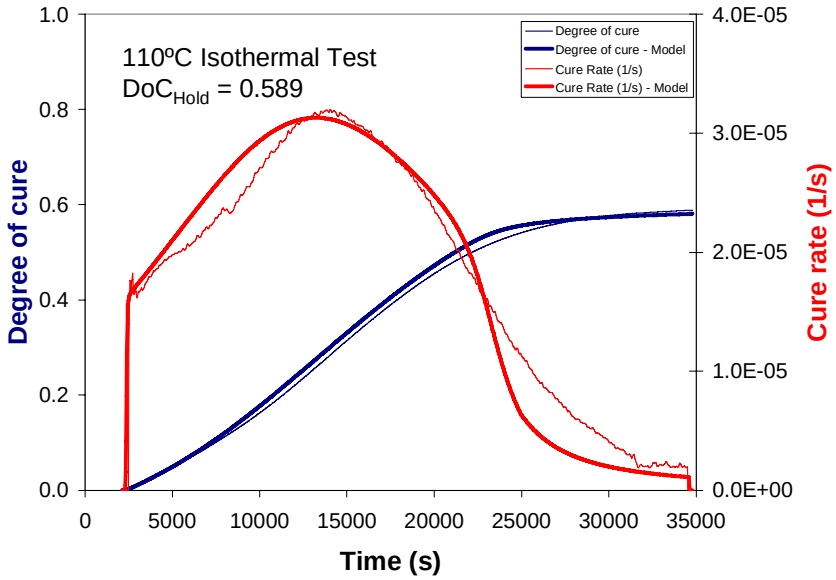

Figure 84. Degree of cure and cure rate for the 110°C isothermal scan compared to model predictions.

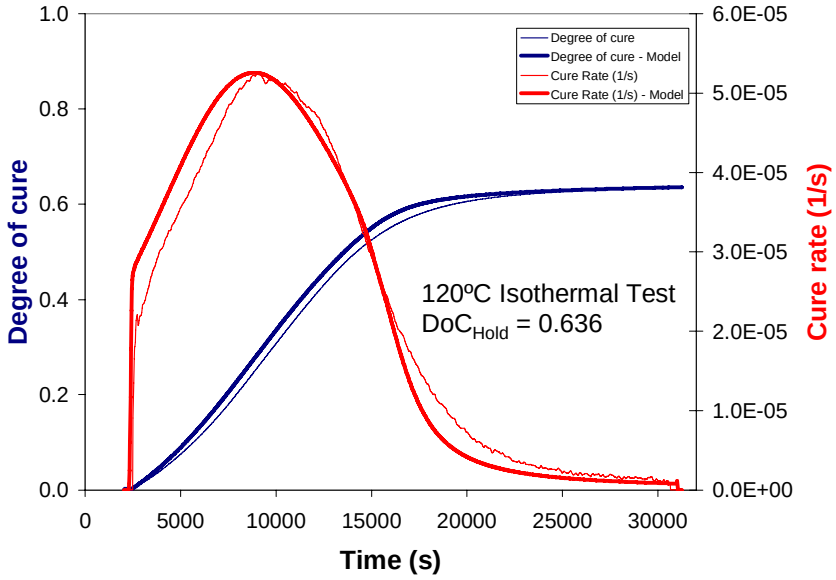

Figure 85. Degree of cure and cure rate for the 120°C isothermal scan compared to model predictions.

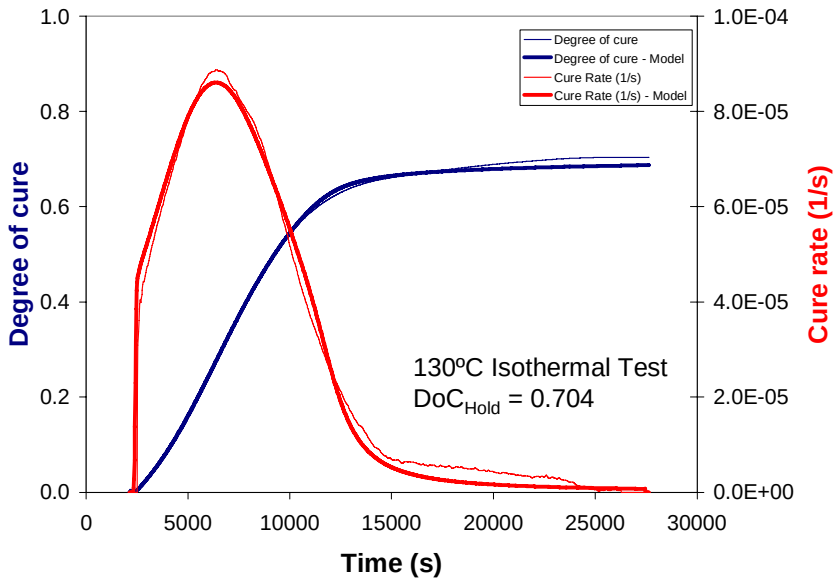

Figure 86. Degree of cure and cure rate for the 130°C isothermal scan compared to model predictions.

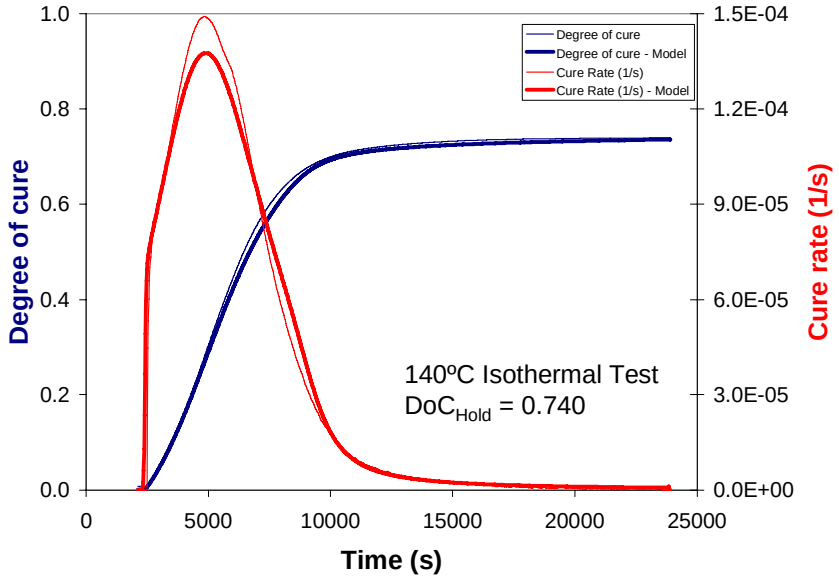

Figure 87. Degree of cure and cure rate for the 140°C isothermal scan compared to model predictions.

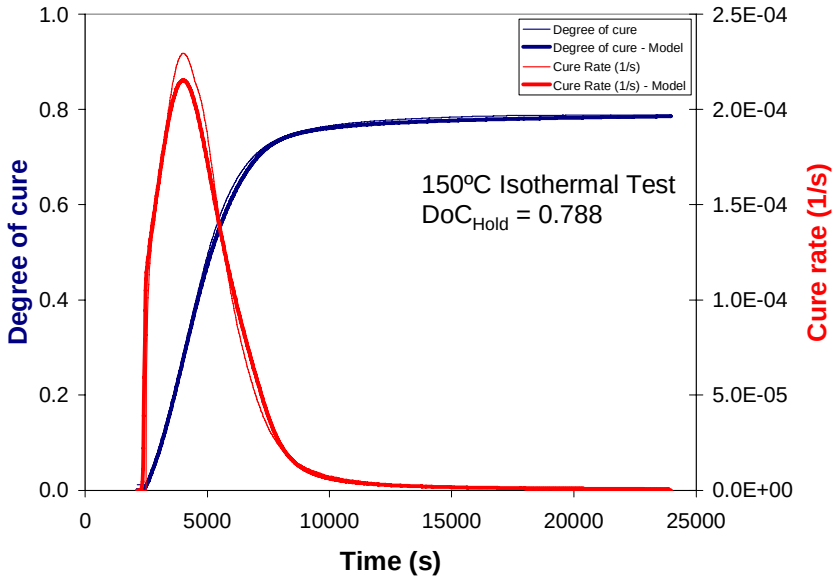

Figure 88. Degree of cure and cure rate for the 150°C isothermal scan compared to model predictions.

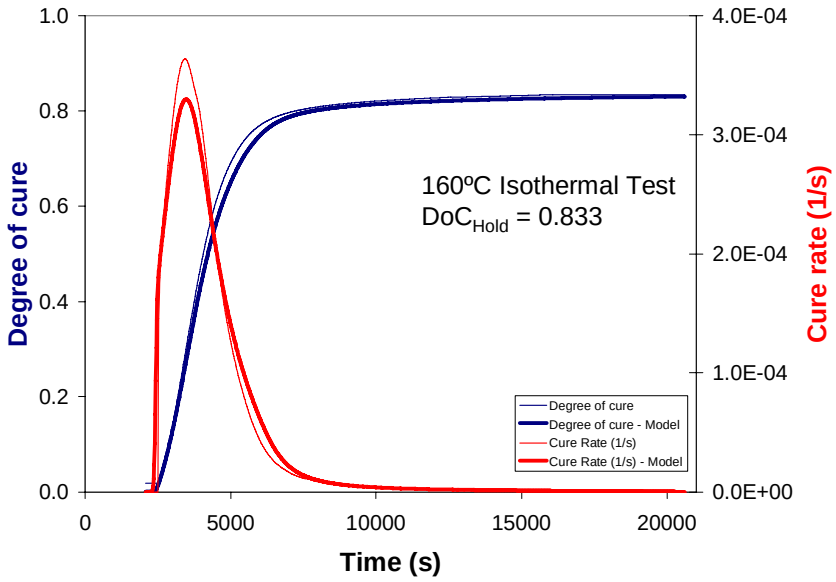

Figure 89. Degree of cure and cure rate for the 160°C isothermal scan compared to model predictions.

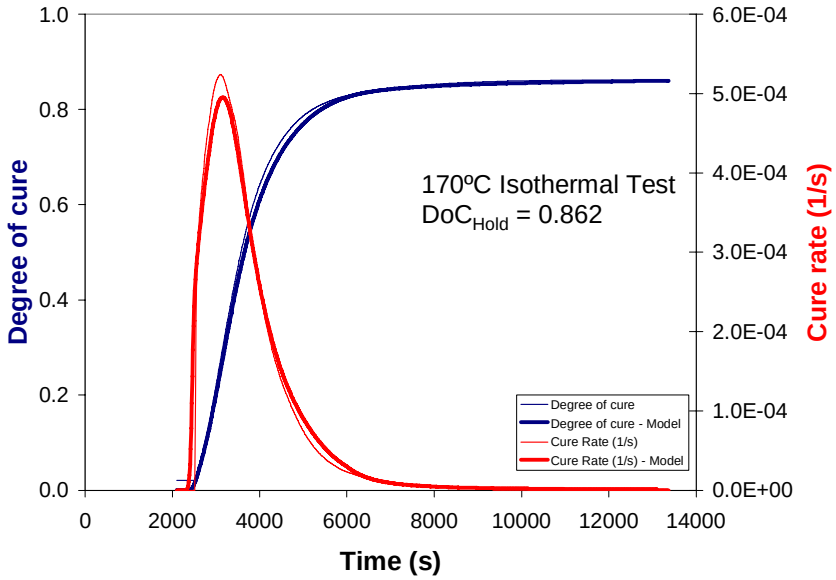

Figure 90. Degree of cure and cure rate for the 170°C isothermal scan compared to model predictions.

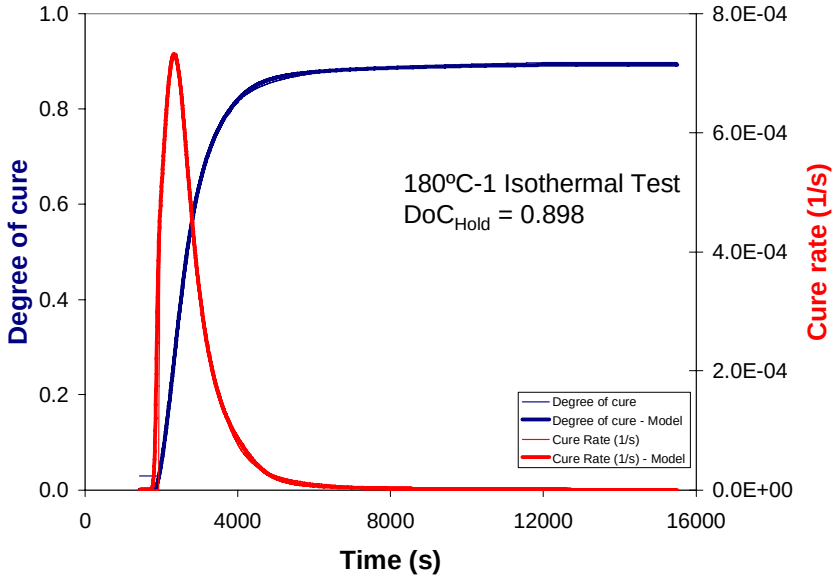

Figure 91. Degree of cure and cure rate for the 180°C (1) isothermal scan compared to model predictions.

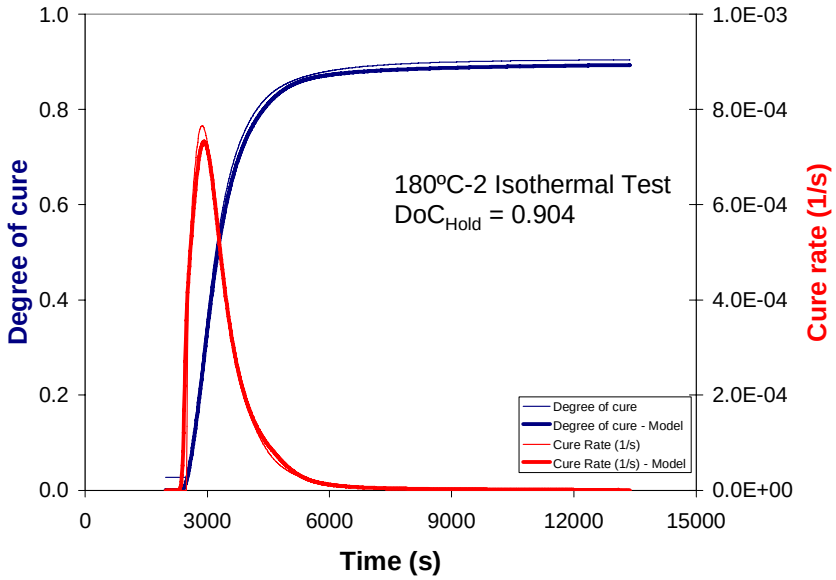

Figure 92. Degree of cure and cure rate for the 180°C (2) isothermal scan compared to model predictions.

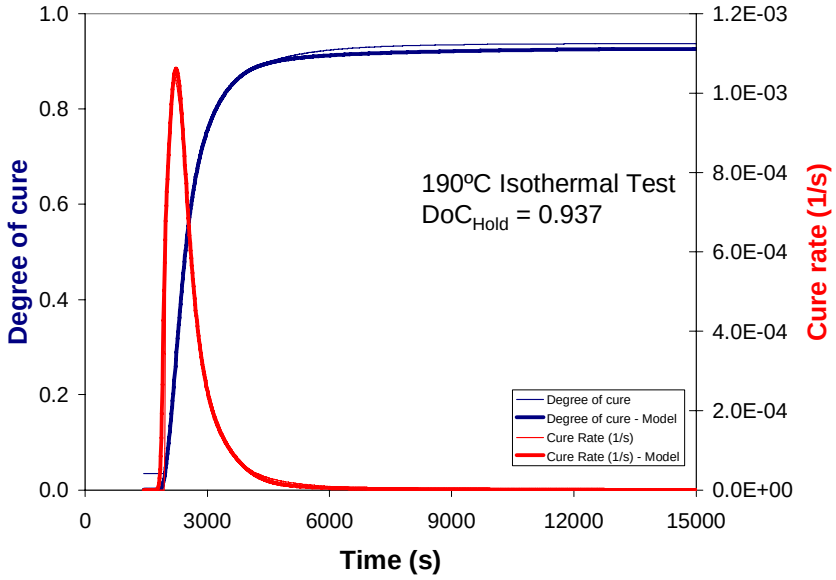

Figure 93. Degree of cure and cure rate for the 190°C isothermal scan compared to model predictions.

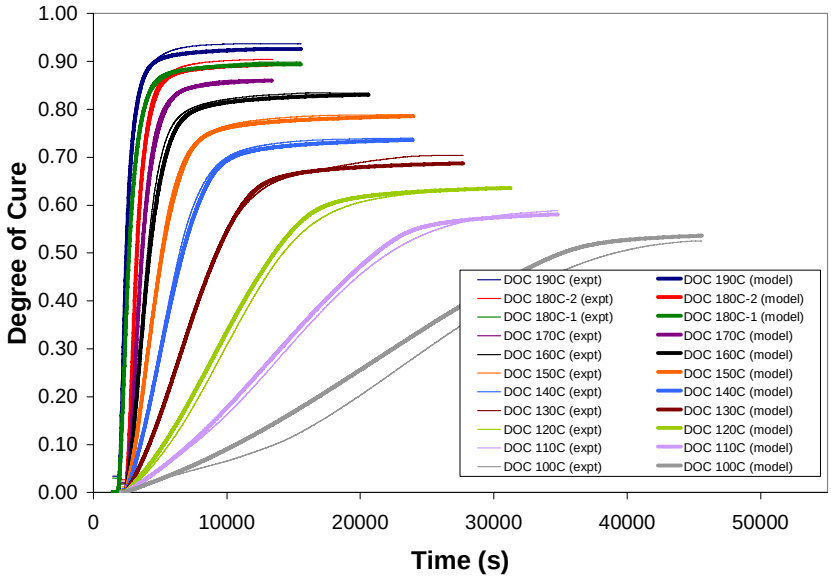

Figure 94. Comparisons of the degree of cure between the model and experiments for the isothermal DSC tests.

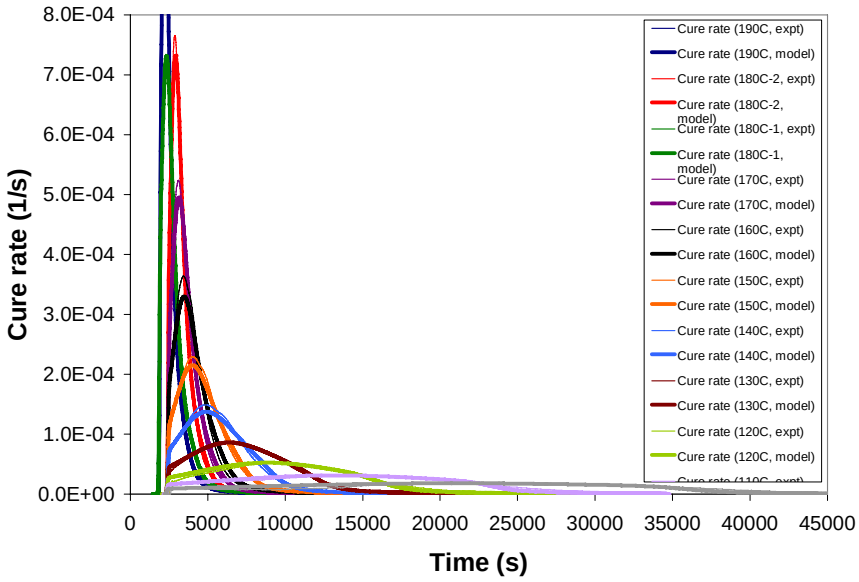

Figure 95. Comparisons of the cure rate between the model and experiments for the isothermal DSC tests.

A recommended cure cycle (provided by Company) was used to validate the prediction of the cure kinetics model in capturing the resin cure advancement (Figure). The Tg values measured were then compared against the prediction of the model (Figure) and good agreement was observed.

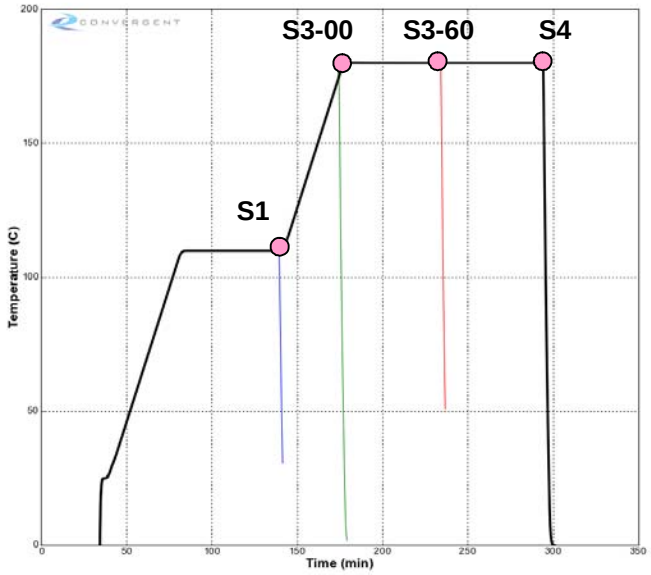

Figure 96. Cure Cycle (CC) used for validating the cure kinetics model, along with the labels used for the interrupted tests.

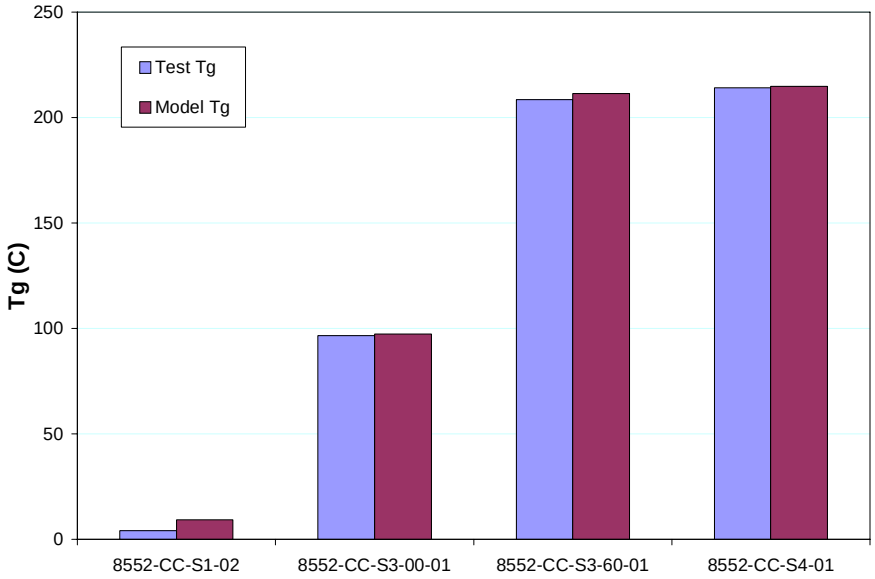

Figure 97. Glass transition values measured from the Cure Cycle tests compared to the model predictions.

Comments

The cure kinetics model developed above is validated within the range of temperatures defined below:

Isothermal Tests $100°C < Temperature < 190°C$

Dynamic Tests $-90°C < Temperature < 275°C$

and $1°C/\min < Temperature\ Rate < 10°C/\min$

Fibre Volume Fraction and Density

Introduction

The fibre volume fraction, V_f, and composite density were not modeled in this project. The values chosen are thus best estimates from other sources.

Theoretical

The equation used was:

$$\rho_c = V_f \rho_f + (1 - V_f)\rho_r$$

The COMPRO density model equations are:

$$\rho_r = \rho_{r(0)} + \alpha_{\rho r}(T - T_0) + b_{\rho r}(x - x_0)$$
$$\rho_f = \rho_{f(0)} + a_{\rho f}(T - T_0)$$

Raw Data

No tests were performed. A value of 1.301 g/cm^3 was taken from the material datasheet as the resin density.

The fibre volume fraction was found to be 0.55, based on the resin and fibre densities, along with a resin content (by weight) of 38% (taken from the material datasheet).

Analysis

In the absence of experimental data, the density of fibre and composite are assumed to be invariant in both temperature and degree of cure. This assumption will not have any significant effect on the other properties.

Goodness of Fit

Not Applicable.

Comments

Not Applicable.

Specific Heat

Introduction

The specific heat capacity model considered for this material is calculated as a function of temperature and degree of cure.

Theoretical

The specific heat capacity is assumed to be varying between rubbery and glassy values as a function of $T - T_g$. The glassy and rubbery heat capacity values are functions of resin temperature and degree of cure. The mathematical form of such heat capacity model, as implemented in COMPRO is:

$$C_p = C_{p_r} + \frac{C_{p_g} - C_{p_r}}{1 + e^{k\left[\left(T - T_g\right) - \Delta T_c\right]}}$$

where

$$C_{p_i} = \left(1 - x\right)C_{p_{i0}} + xC_{p_{i\infty}} \qquad \left(i = r, g\right)$$

and

$$C_{p_{ij}} = s_{ij}T + c_{ij} \qquad \left(i = r, g \quad \text{and} \quad j = 0, \infty\right)$$

Raw Data

Using a Thermal Analysis Q1000 Differential Scanning Calorimetry (DSC), modulated dynamic and isothermal DSC tests were performed. A direct measurement of the modulated DSC tests is the total heat capacity of the sample, which is further divided into reversing and non-reversing components. The reversing component is the signal corresponding the material's instantaneous heat capacity.

Eleven dynamic DSC tests (see Table 1) were used in model fitting. A small amount of scatter was observed in the experimental data for the measurement of the heat capacity (Figure 98). The tests were adjusted to align the initial glassy response. The adjusted heat capacity responses are plotted in Figure .

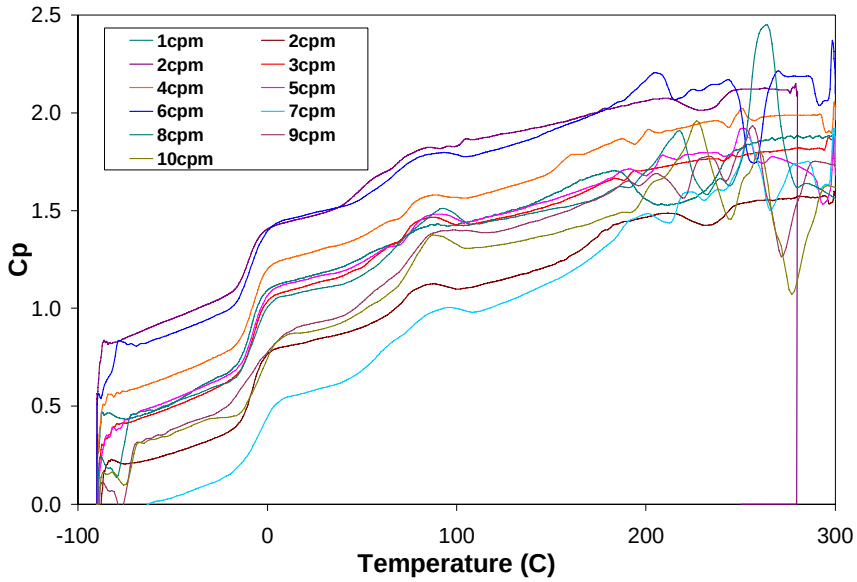

Figure 98. Heat capacity (Cp) data of all dynamic DSC tests, prior to any adjustments

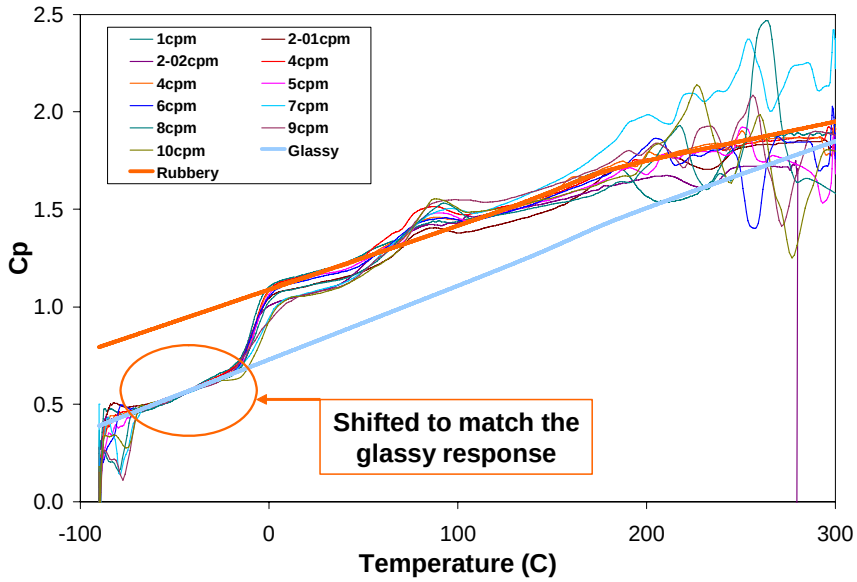

Figure 99. Heat capacity (Cp) data of all dynamic DSC tests, after adjusting the outlying tests.

The raw data after shifting is presented in Figure 170 to **Error! Reference source not found.**0 for individual tests.

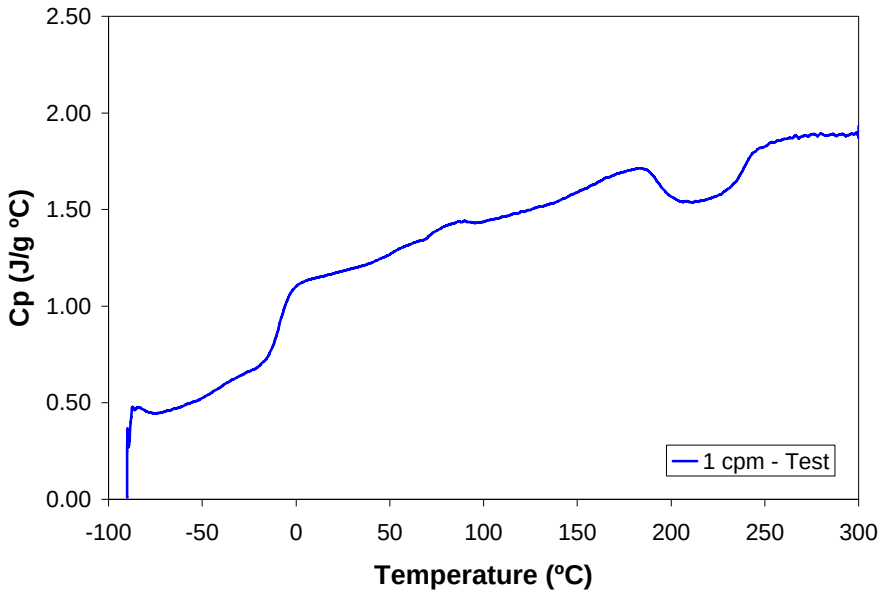

Figure 170. Heat capacity (Cp) test data of the 1ºC/min dynamic DSC test.

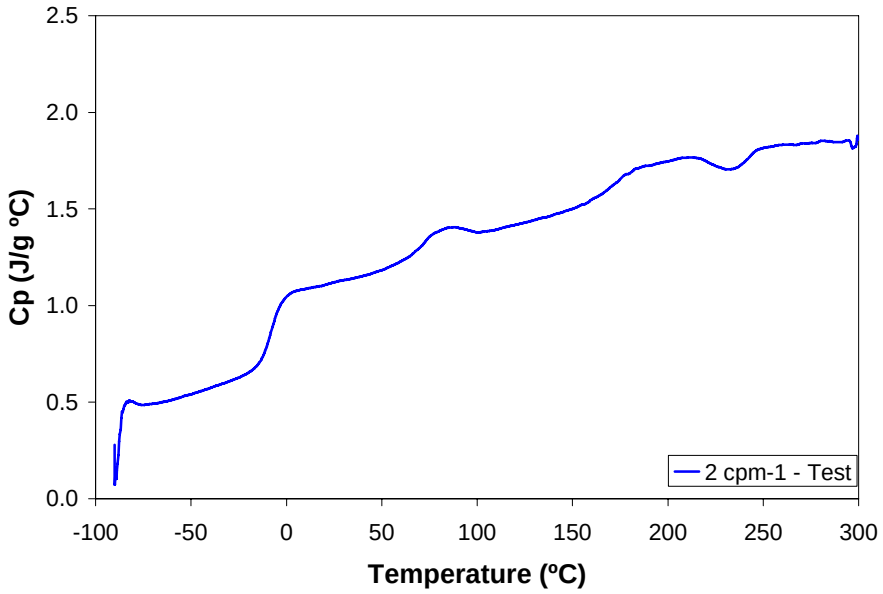

Figure 181. Heat capacity (Cp) test data of the 2ºC/min (1) dynamic DSC test.

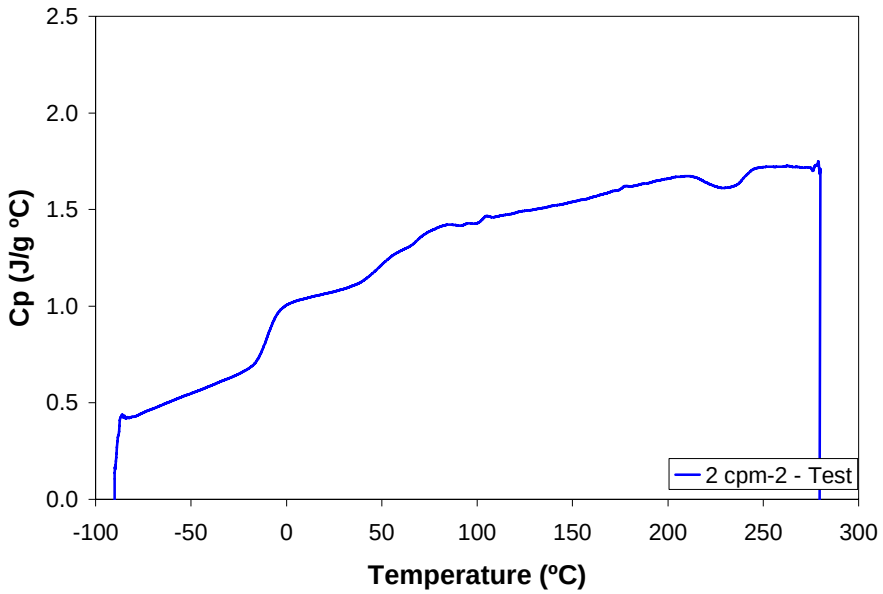

Figure 192. Heat capacity (Cp) test data of the 2ºC/min (2) dynamic DSC test.

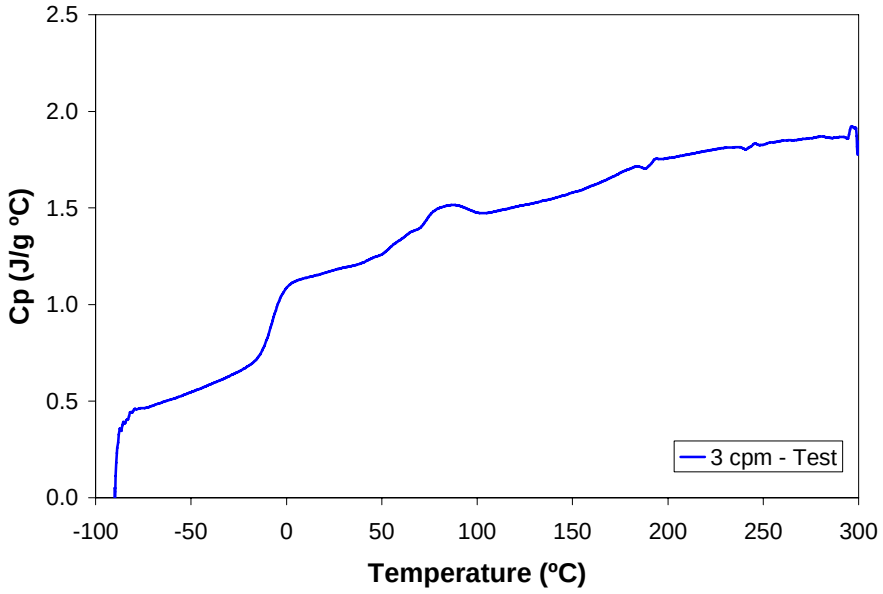

Figure 203. Heat capacity (Cp) test data of the 3ºC/min dynamic DSC test.

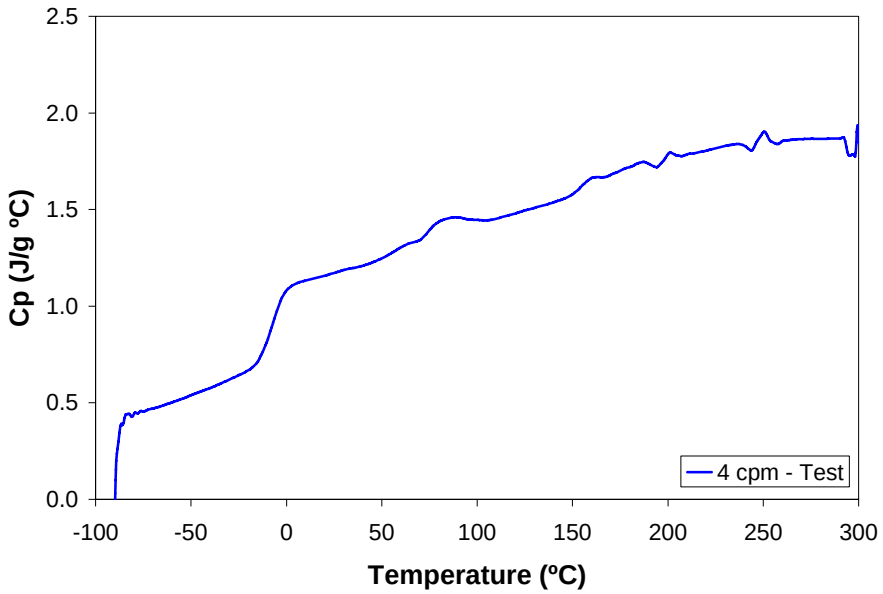

Figure 214. Heat capacity (Cp) test data of the 4ºC/min dynamic DSC test.

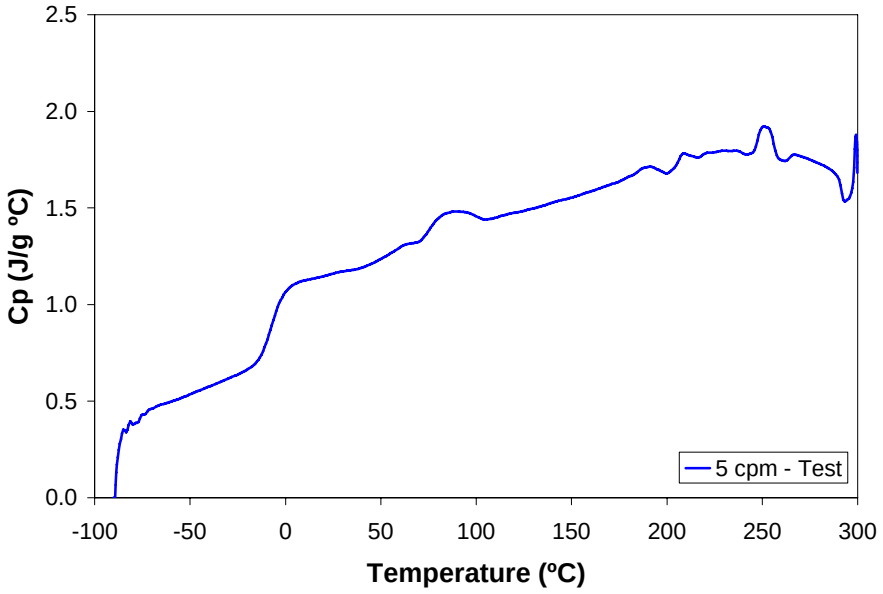

Figure 225. Heat capacity (Cp) test data of the 5ºC/min dynamic DSC test.

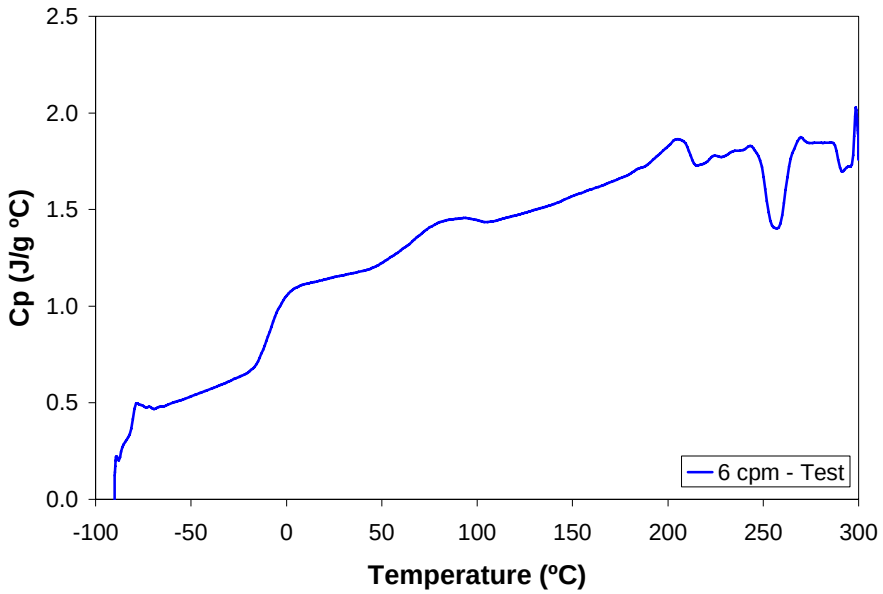

Figure 236. Heat capacity (Cp) test data of the 6ºC/min dynamic DSC test.

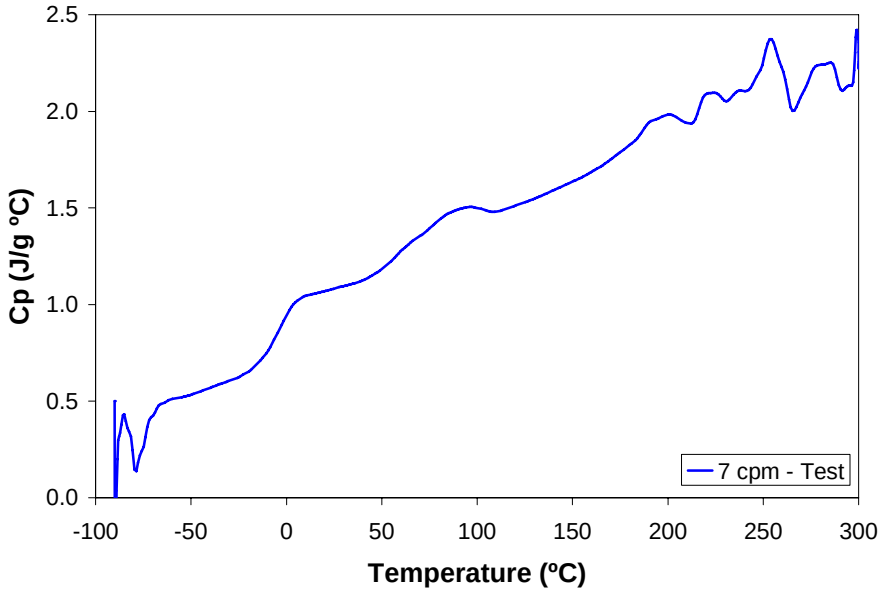

Figure 247. Heat capacity (Cp) test data of the 7ºC/min dynamic DSC test.

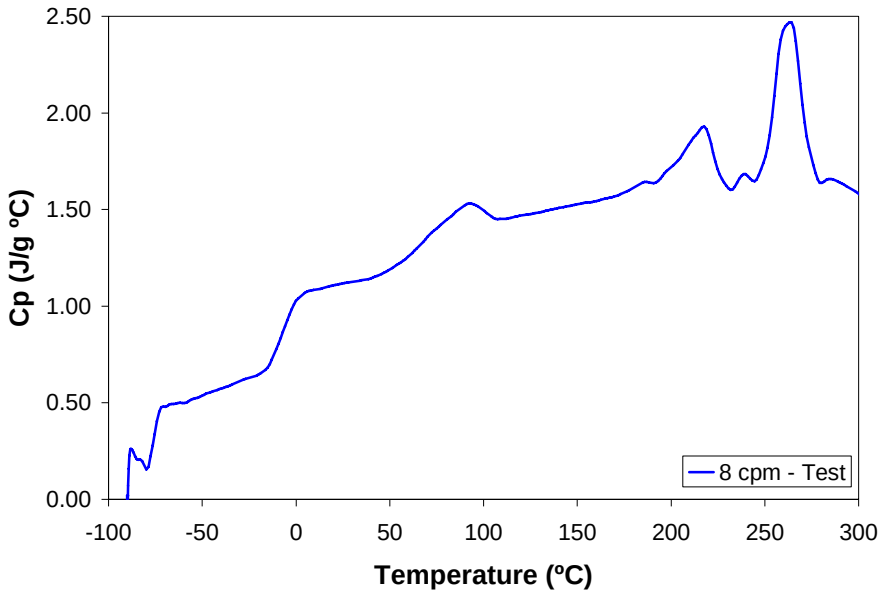

Figure 258. Heat capacity (Cp) test data of the 8ºC/min dynamic DSC test.

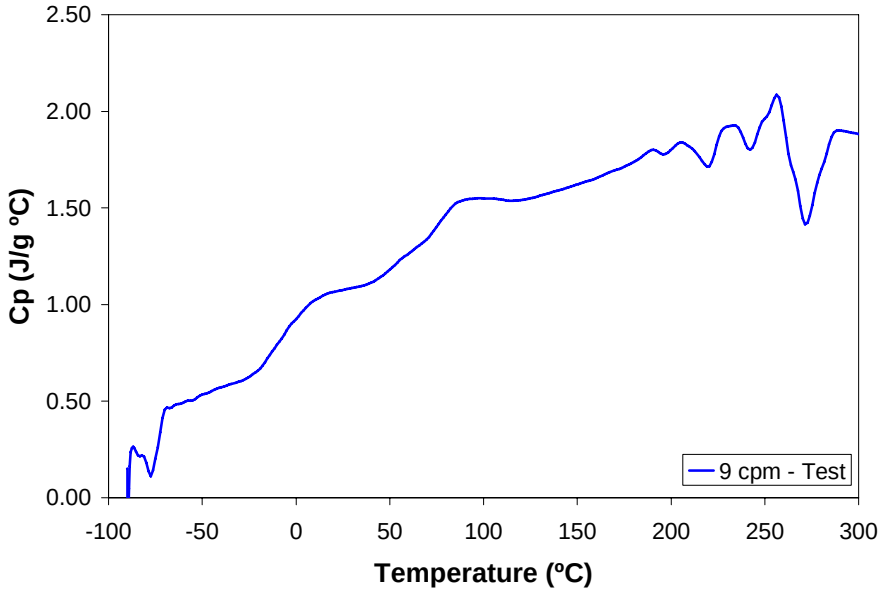

Figure 269. Heat capacity (Cp) test data of the 9ºC/min dynamic DSC test.

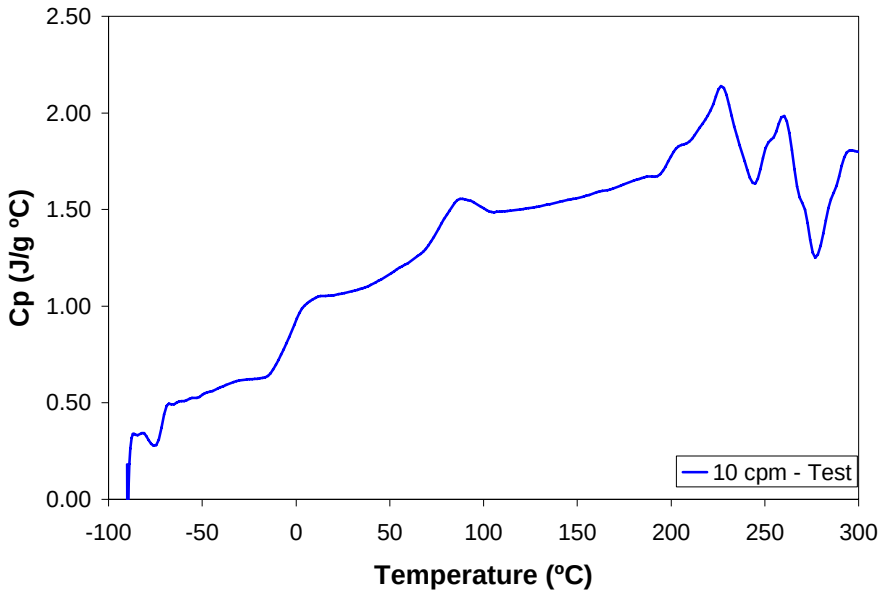

Figure 2710. Heat capacity (Cp) test data of the 10ºC/min dynamic DSC test.

Analysis

The Cp model equation was fit to the data from dynamic DSC runs. The data was examined separately as a function of degree of cure and temperature, and the Cp equation parameters were fit. In this process, the predictions of the cure kinetics model (developed earlier, see page 17) were used to determine the resin cure advancement during the tests.

Quality of Fit

Using the fitted Cp model parameters (COMPRO model), the model fit is shown in the plots below for the dynamic tests, both as a function of temperature and degree of cure.
The Cp model predictions against the measured values in eleven of the isothermal tests are also provided, in order to gauge the accuracy of the Cp model. Good agreement was observed between the experimental data and the model predictions.

Variation with temperature – Dynamic Tests

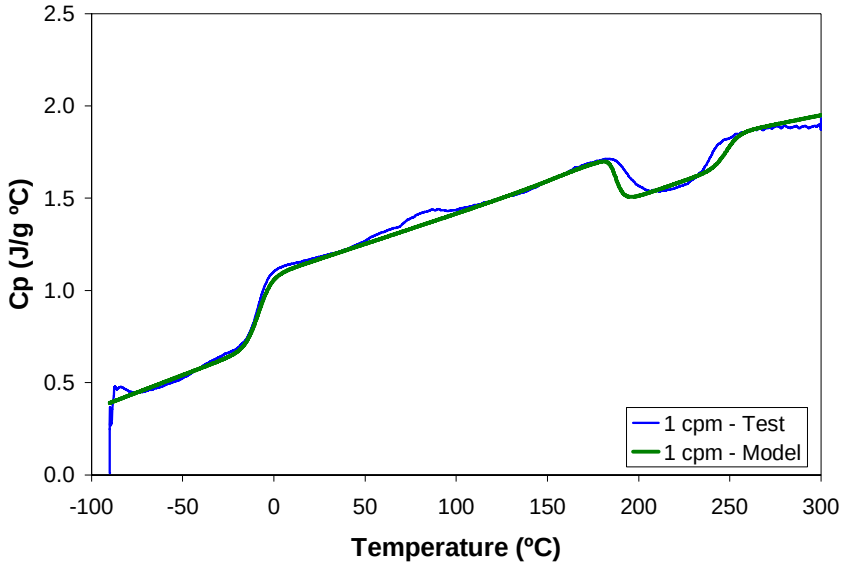

Figure 281. Heat capacity COMPRO model fit to the 1ºC/min dynamic test.

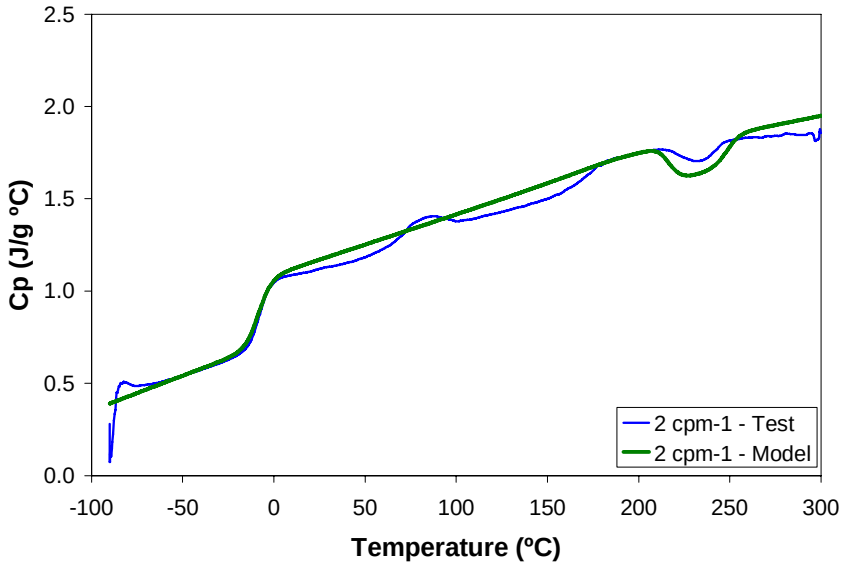

Figure 292. Heat capacity COMPRO model fit to the 2ºC/min (1) dynamic test.

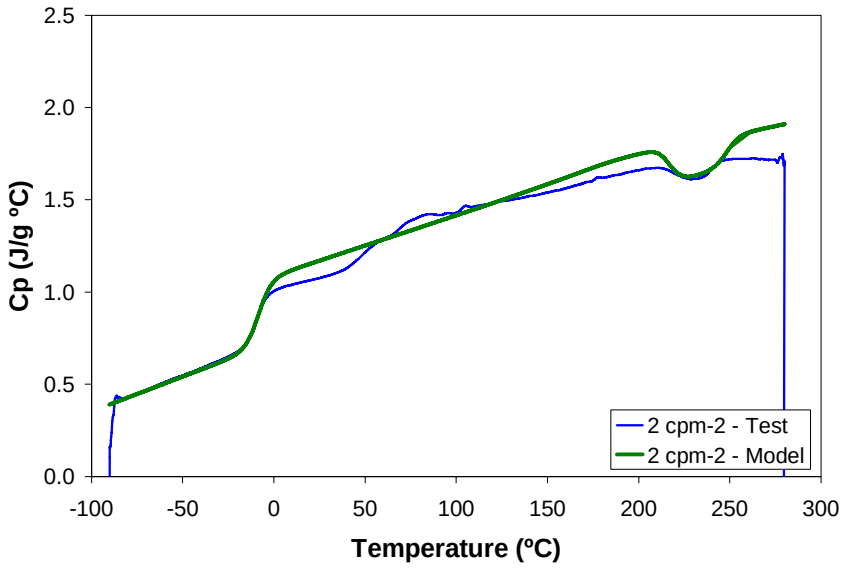

Figure 303. Heat capacity COMPRO model fit to the 2ºC/min (2) dynamic test.

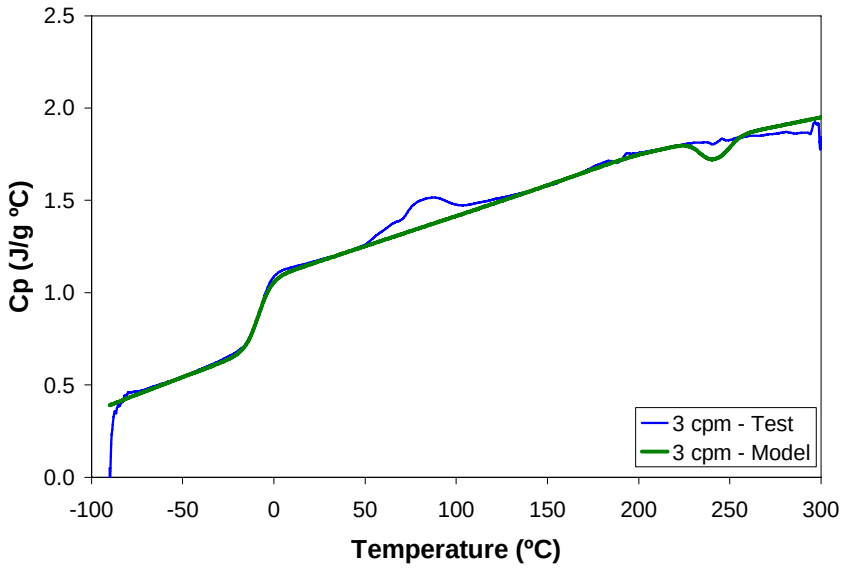

Figure 314. Heat capacity COMPRO model fit to the 3ºC/min dynamic test.

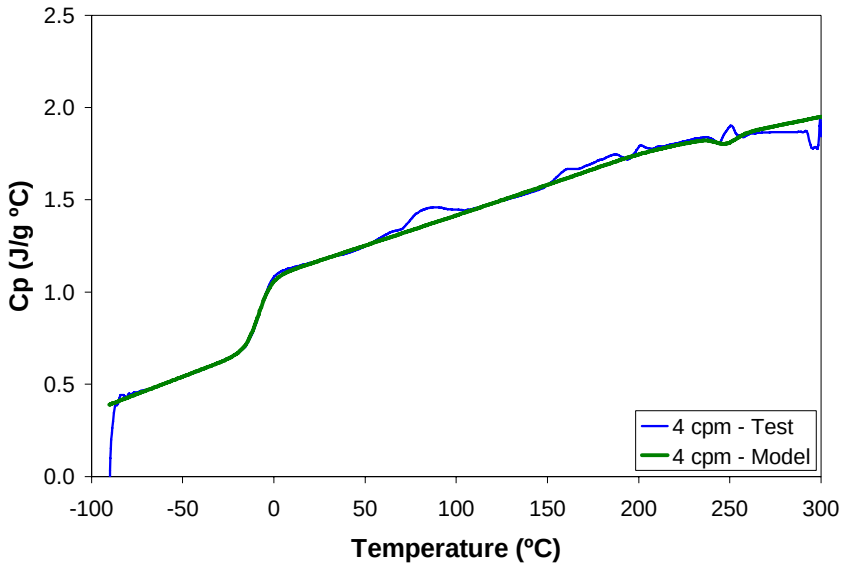

Figure 325. Heat capacity COMPRO model fit to the 4ºC/min dynamic test.

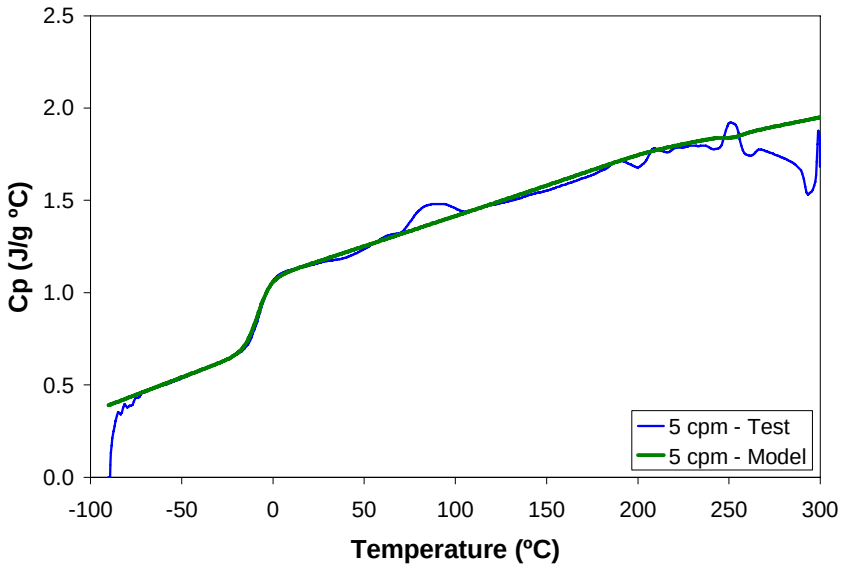

Figure 336. Heat capacity COMPRO model fit to the 5?ºC/min dynamic test.

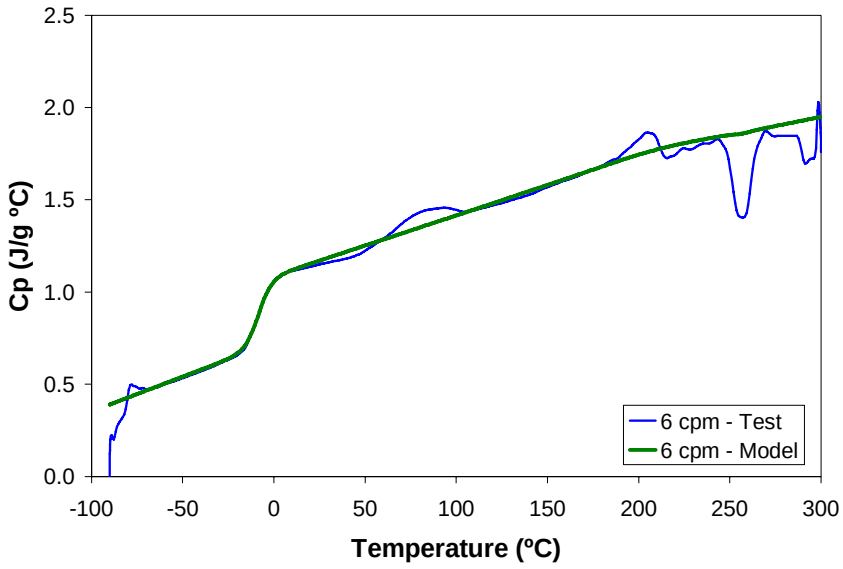

Figure 347. Heat capacity COMPRO model fit to the 6ºC/min dynamic test.

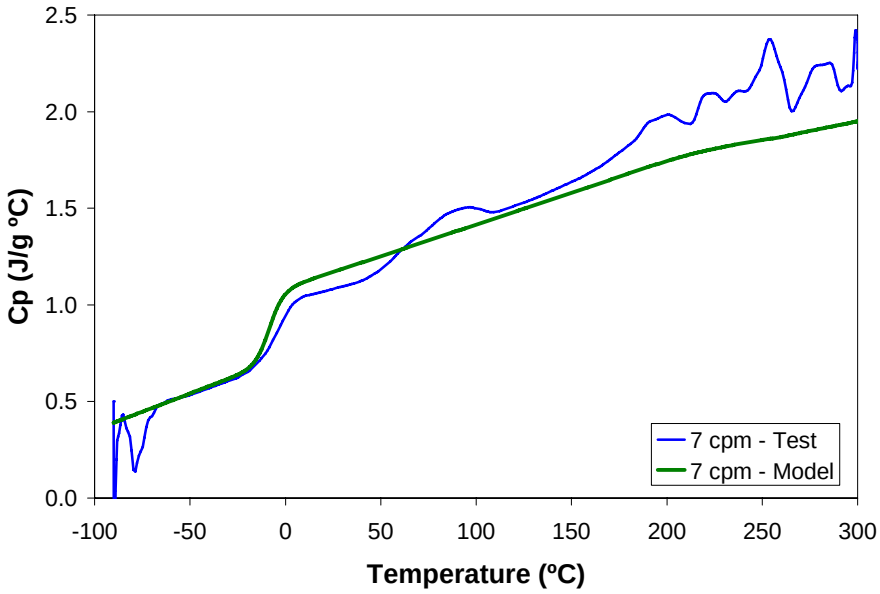

Figure 358. Heat capacity COMPRO model fit to the 7ºC/min dynamic test.

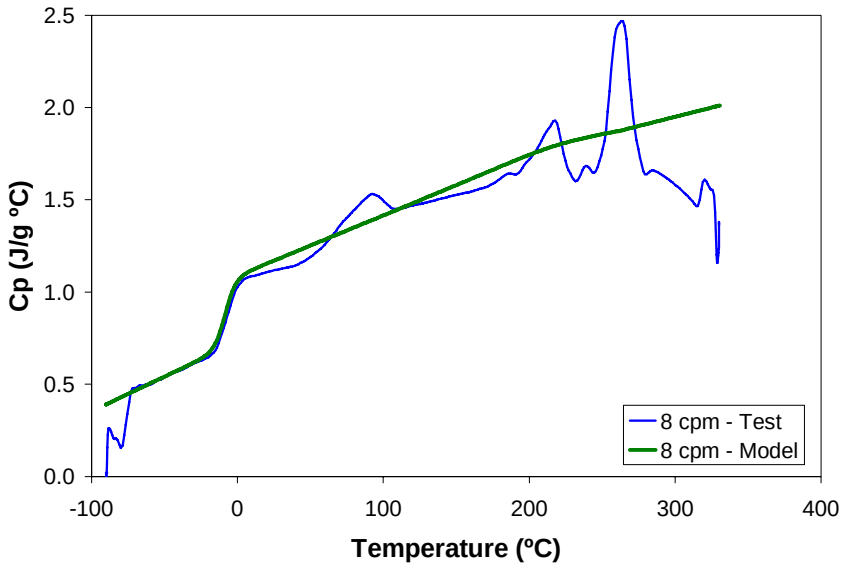

Figure 369. Heat capacity COMPRO model fit to the 8ºC/min dynamic test.

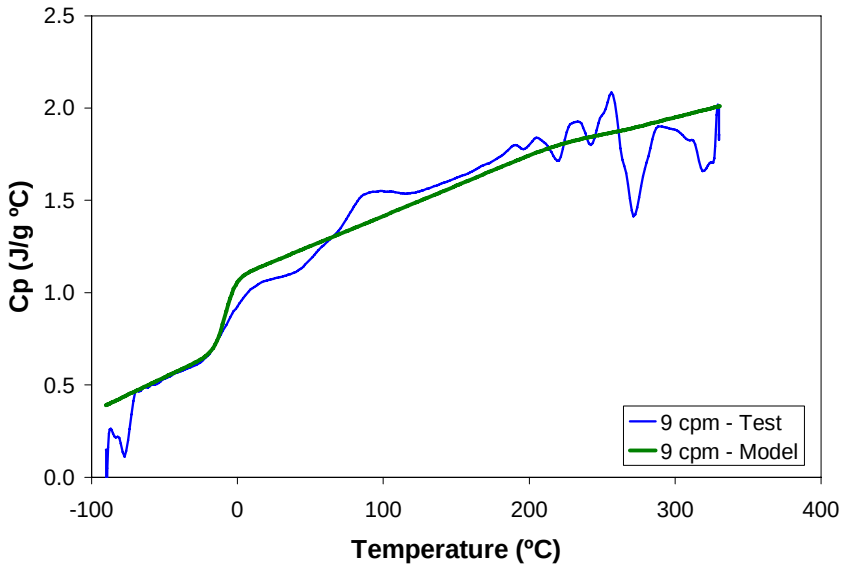

Figure 3720. Heat capacity COMPRO model fit to the 9ºC/min dynamic test.

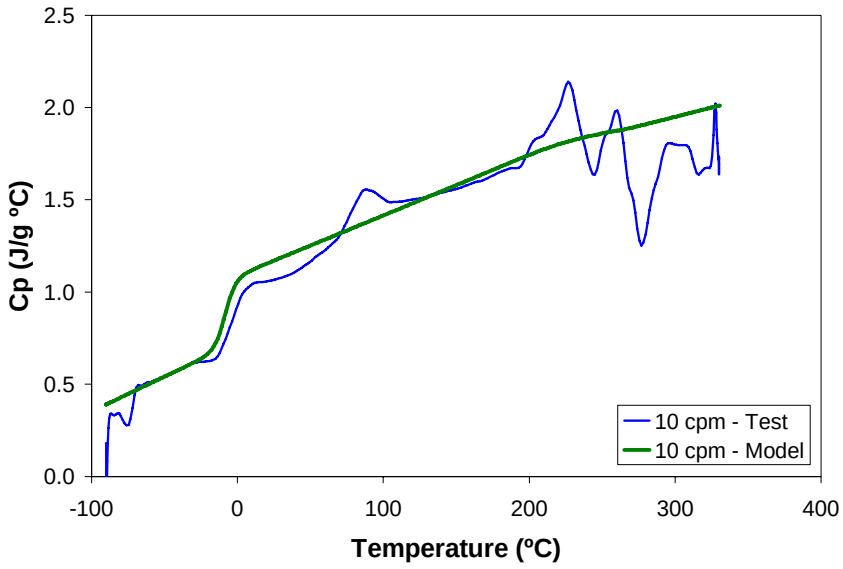

Figure 3821. Heat capacity COMPRO model fit to the 10°C/min dynamic test.

Variation with degree of cure – Dynamic Tests

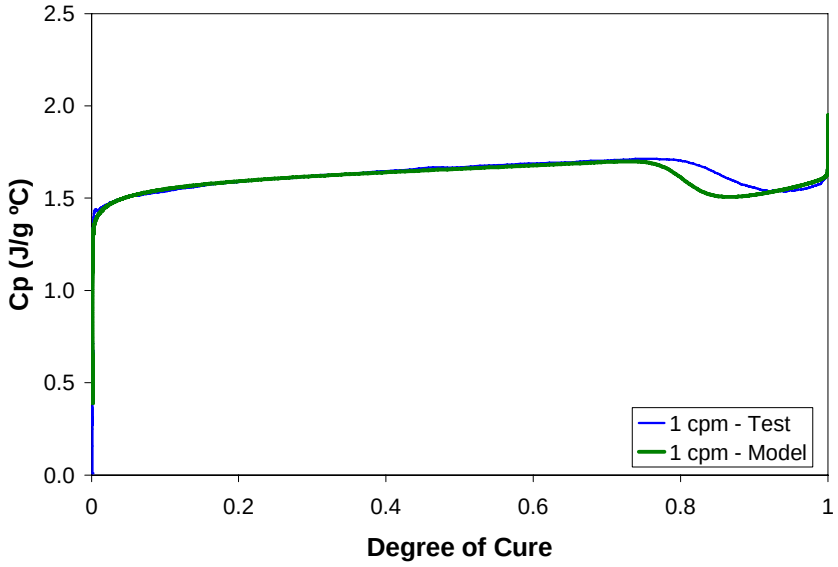

Figure 392. Heat capacity COMPRO model fit to the 1°C/min dynamic test.

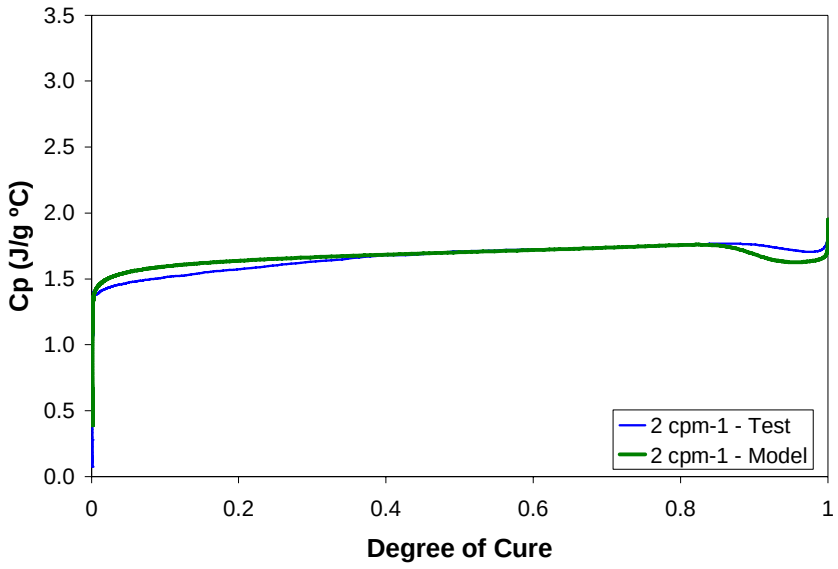

Figure 403. Heat capacity COMPRO model fit to the 2ºC/min (1) dynamic test.

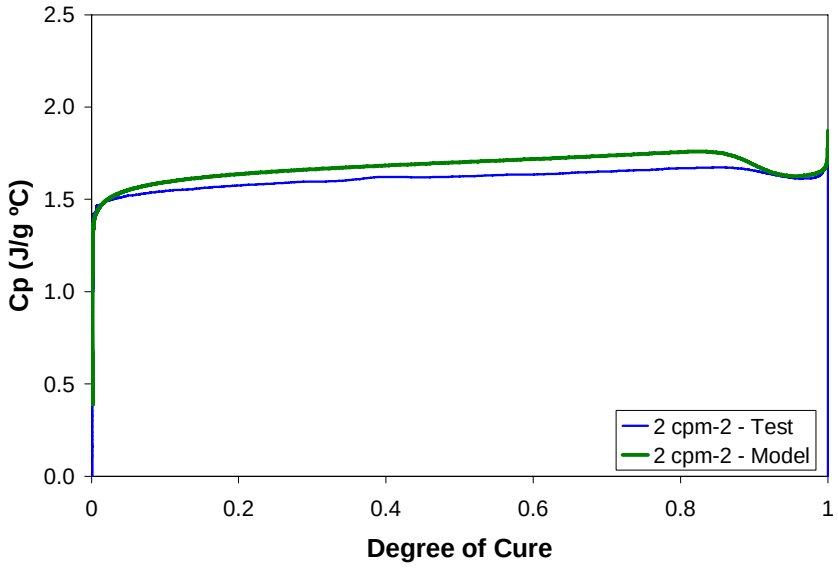

Figure 414. Heat capacity COMPRO model fit to the 2ºC/min (2) dynamic test.

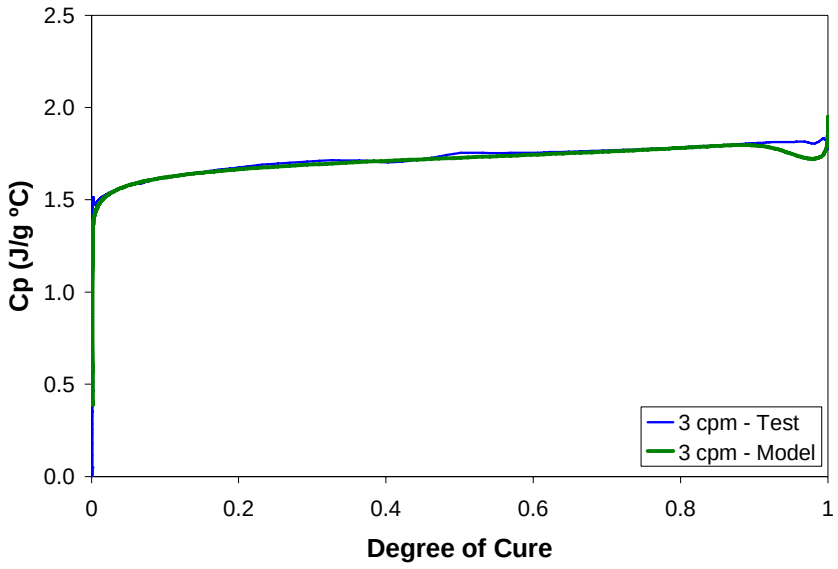

Figure 425. Heat capacity COMPRO model fit to the 3ºC/min dynamic test.

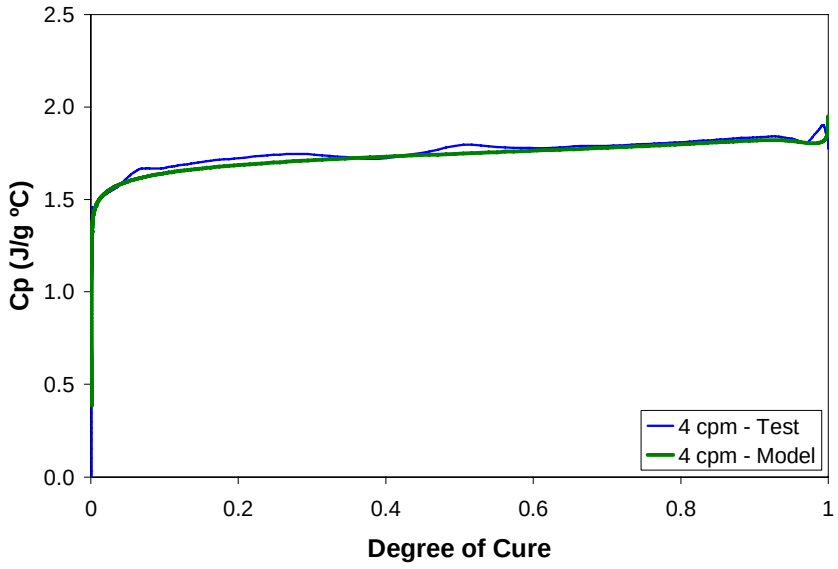

Figure 436. Heat capacity COMPRO model fit to the 4ºC/min dynamic test.

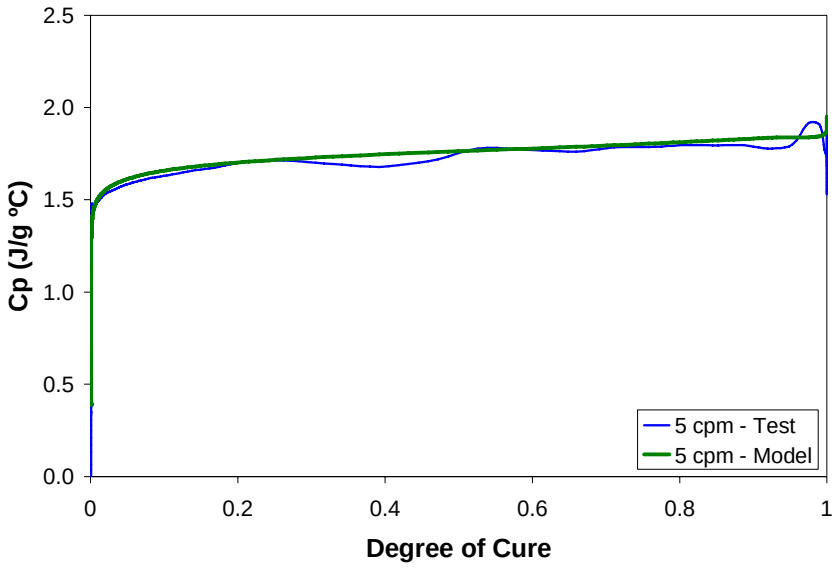

Figure 447. Heat capacity COMPRO model fit to the 5ºC/min dynamic test.

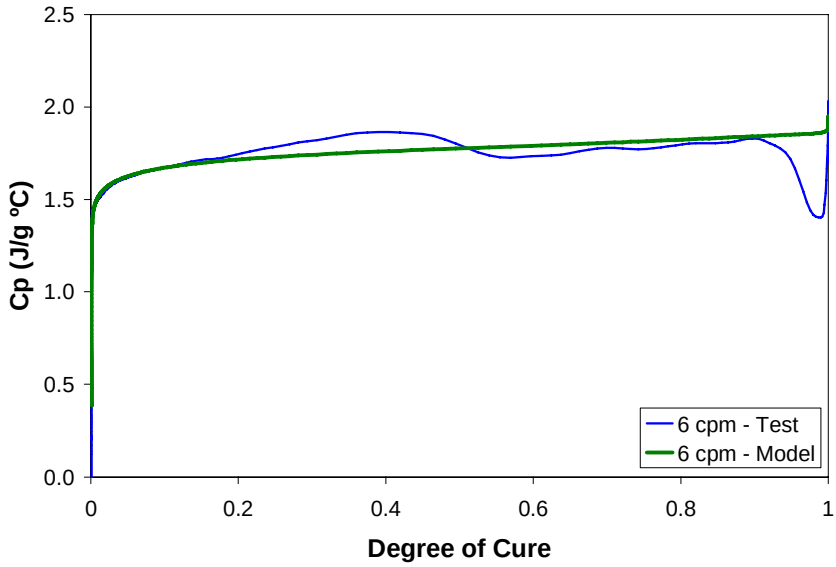

Figure 458. Heat capacity COMPRO model fit to the 6ºC/min dynamic test.

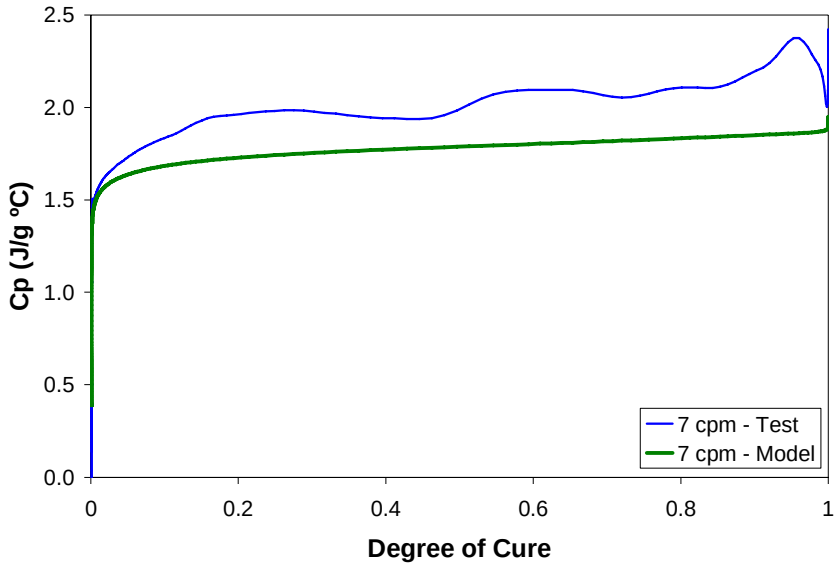

Figure 469. Heat capacity COMPRO model fit to the 7ºC/min dynamic test.

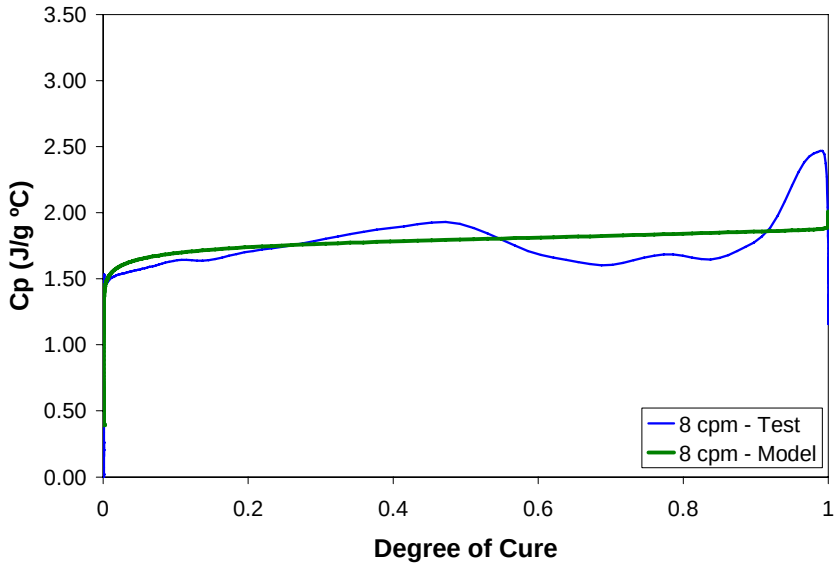

Figure 4730. Heat capacity COMPRO model fit to the 8ºC/min dynamic test.

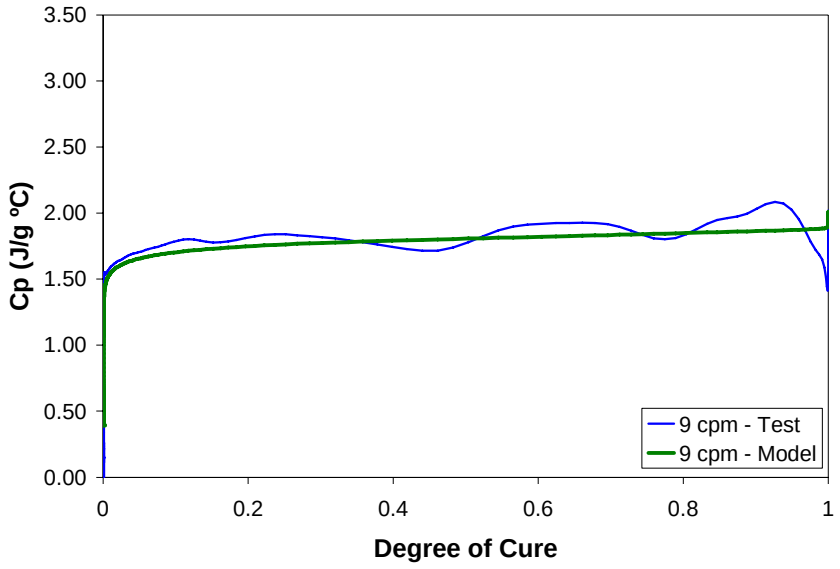

Figure 4831. Heat capacity COMPRO model fit to the 9ºC/min dynamic test.

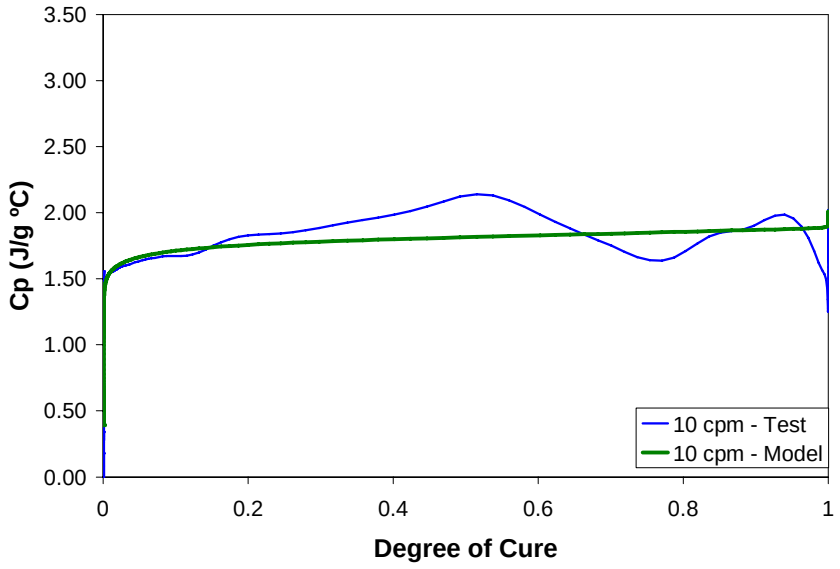

Figure 4932. Heat capacity COMPRO model fit to the 10ºC/min dynamic test.

Variation with time – Isothermal Tests

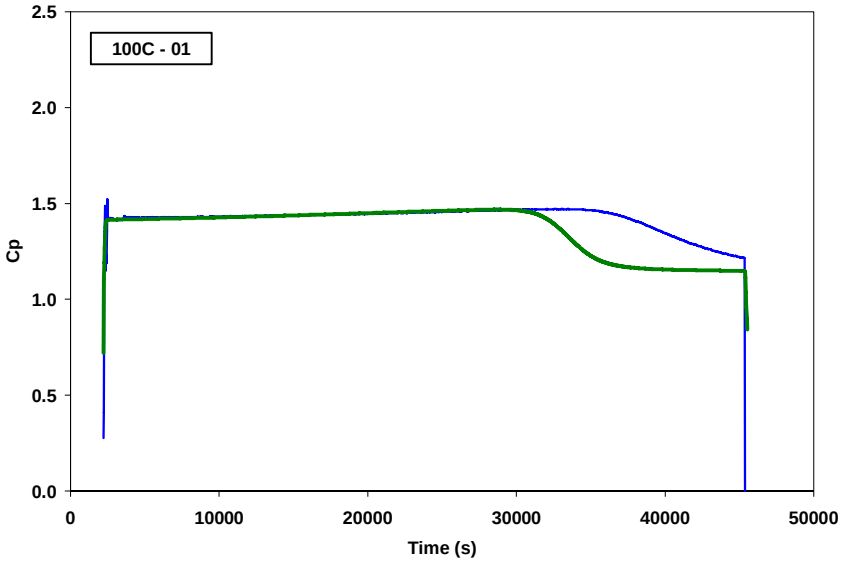

Figure 5033. Heat capacity COMPRO model fit to the 100ºC isothermal test.

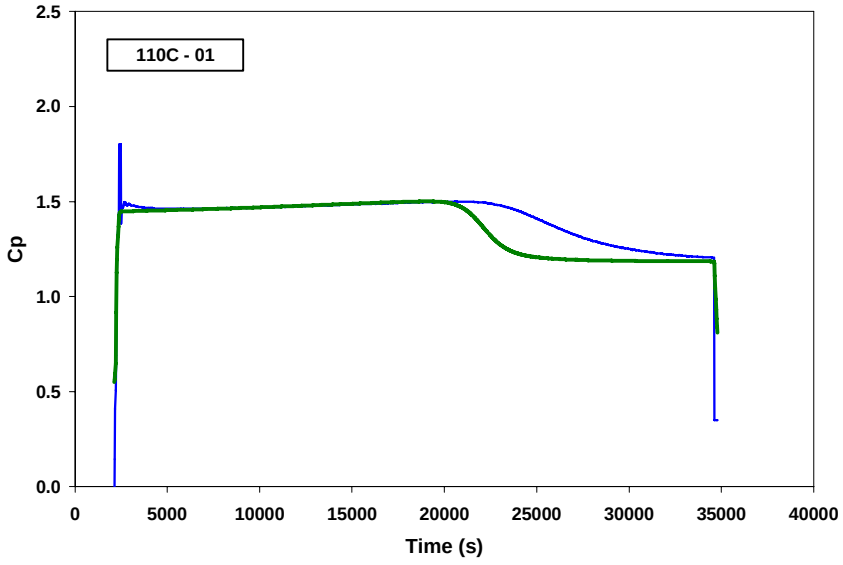

Figure 5134. Heat capacity COMPRO model fit to the 110ºC isothermal test.

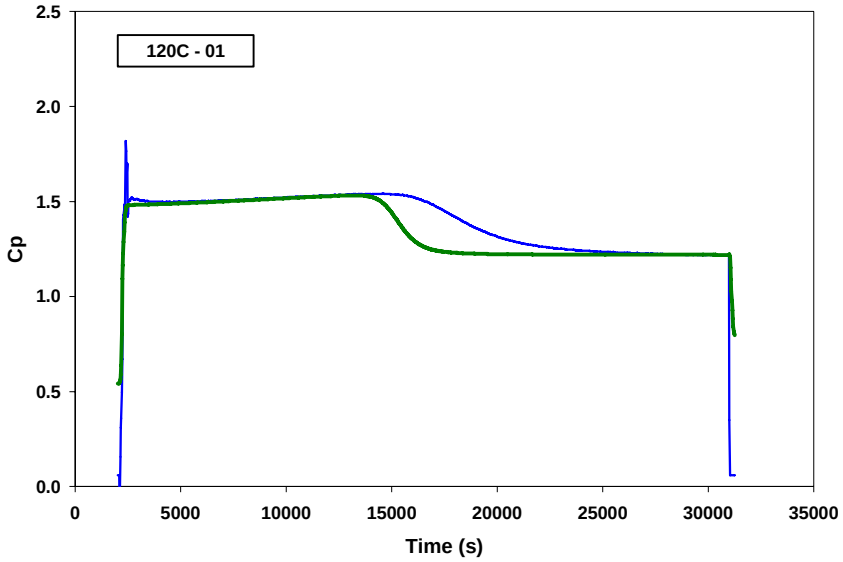

Figure 5235. Heat capacity COMPRO model fit to the 120ºC isothermal test.

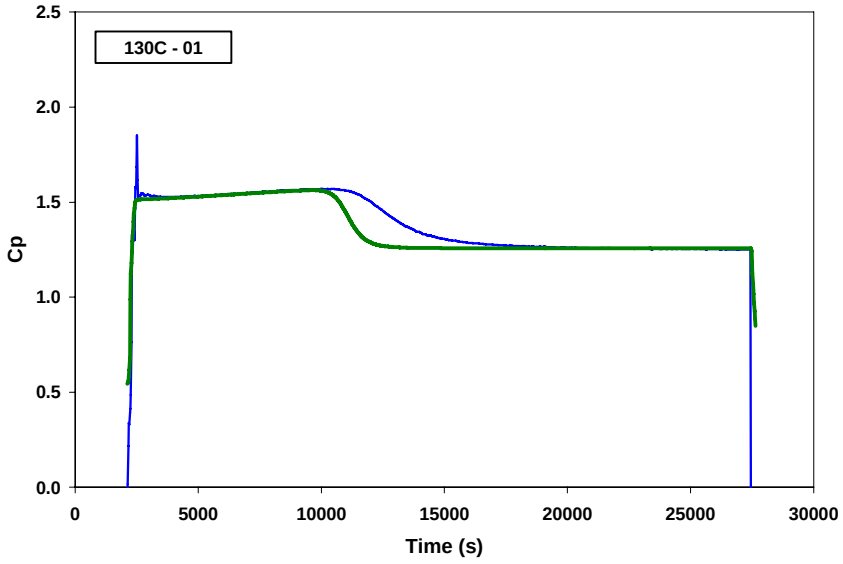

Figure 5336. Heat capacity COMPRO model fit to the 130ºC isothermal test.

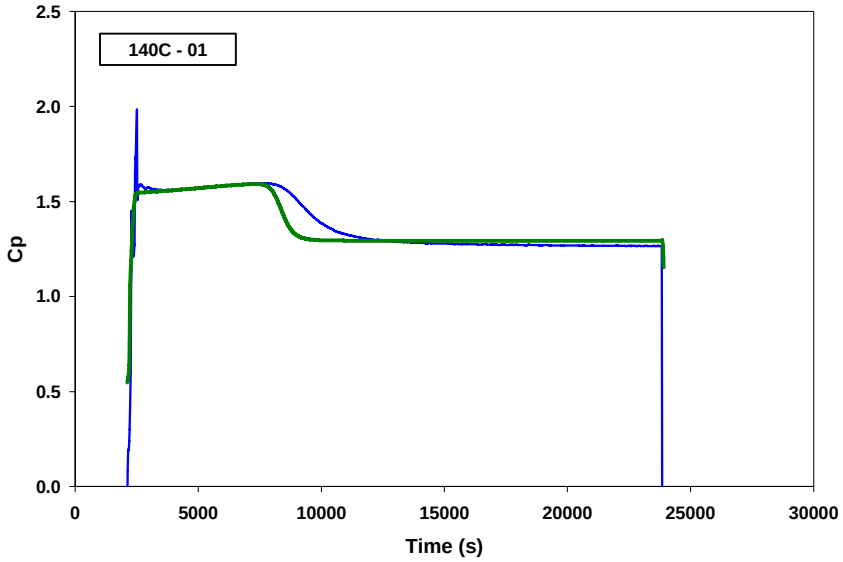

Figure 5437. Heat capacity COMPRO model fit to the 140ºC isothermal test.

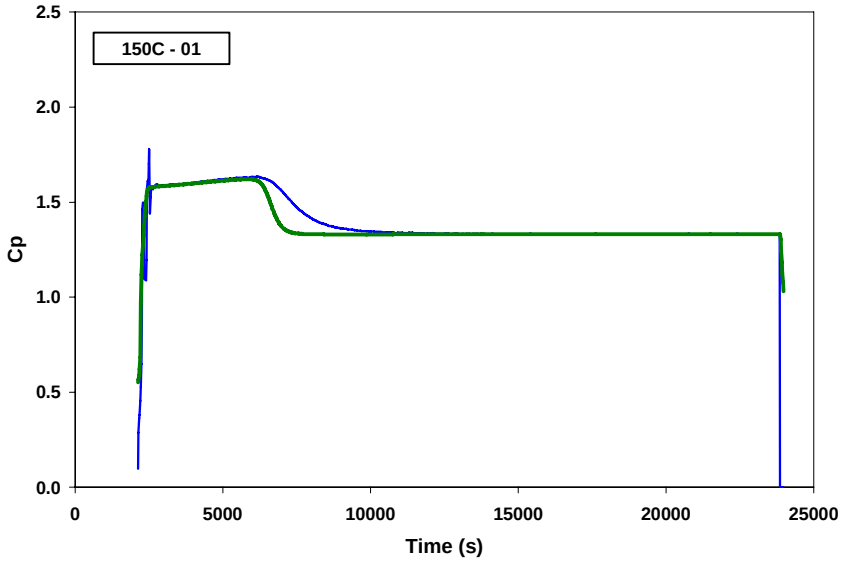

Figure 5538. Heat capacity COMPRO model fit to the 150ºC isothermal test.

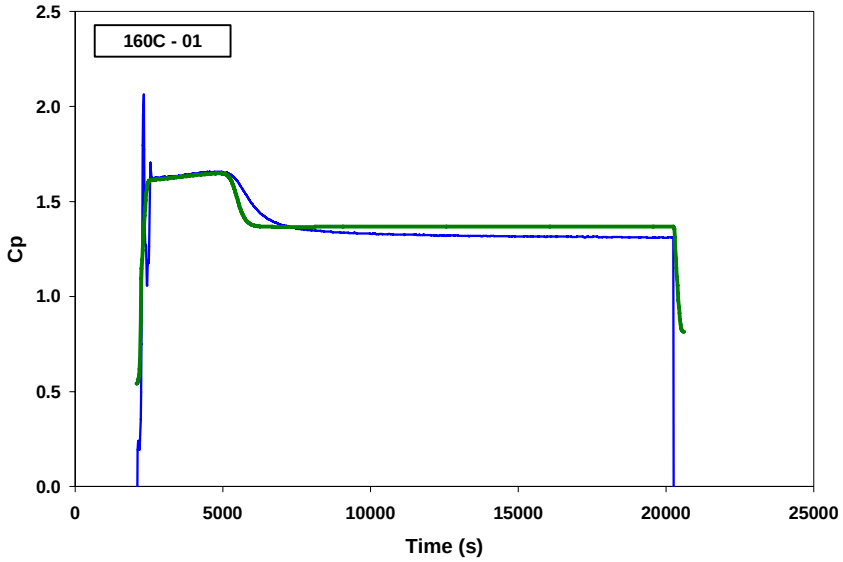

Figure 5639. Heat capacity COMPRO model fit to the 160ºC isothermal test.

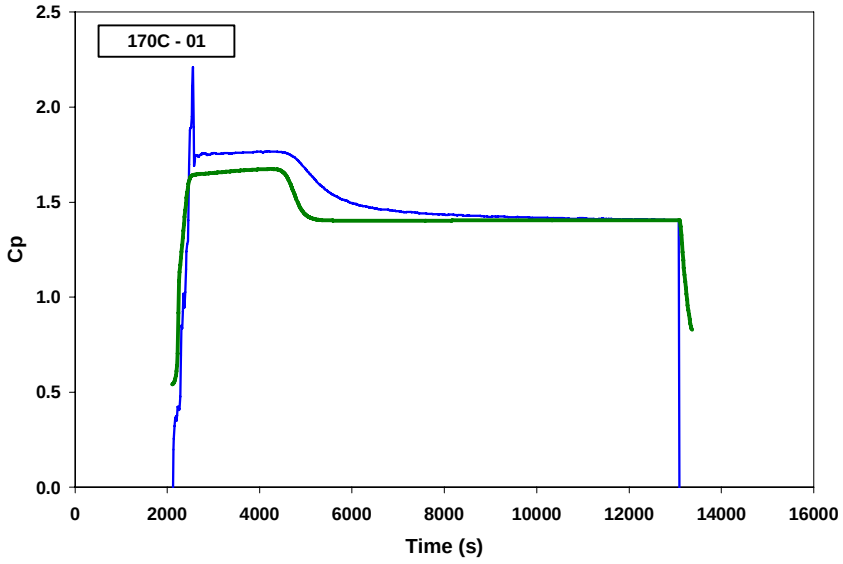

Figure 5740. Heat capacity COMPRO model fit to the 170ºC isothermal test.

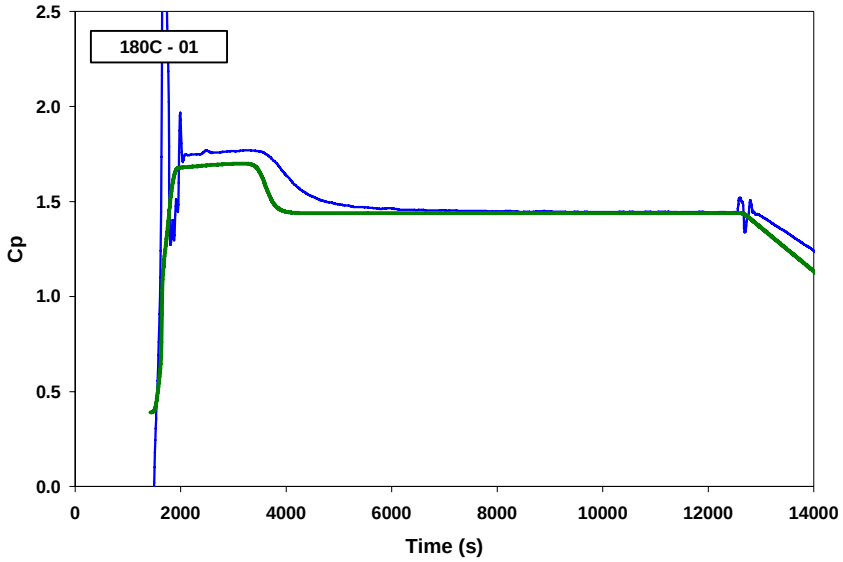

Figure 5841. Heat capacity COMPRO model fit to the 180ºC (1) isothermal test.

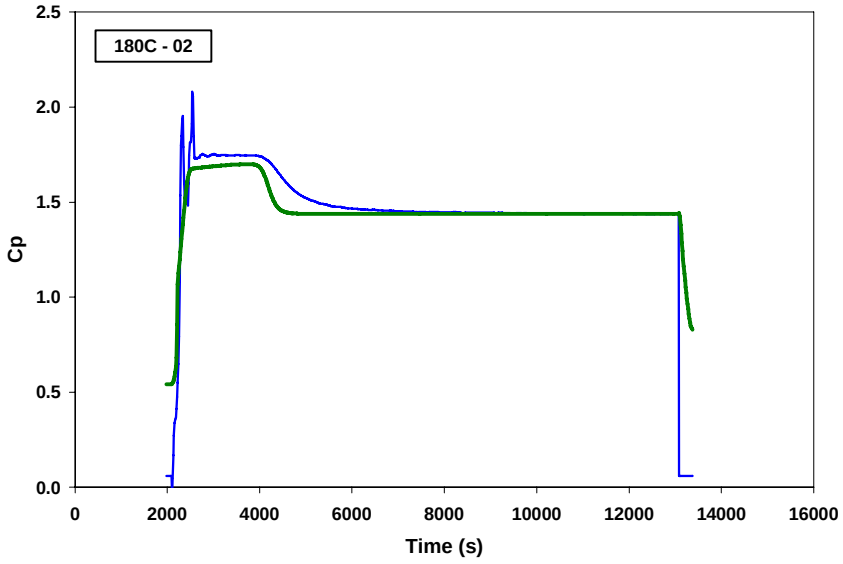

Figure 5942. Heat capacity COMPRO model fit to the 180ºC (2) isothermal test.

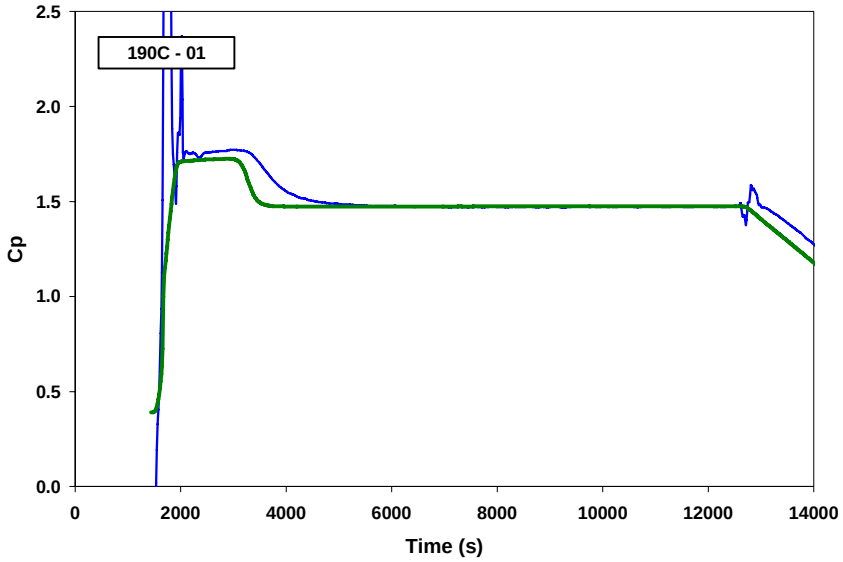

Figure 6043. Heat capacity COMPRO model fit to the 190ºC isothermal test.

Variation with degree of cure – Isothermal Tests

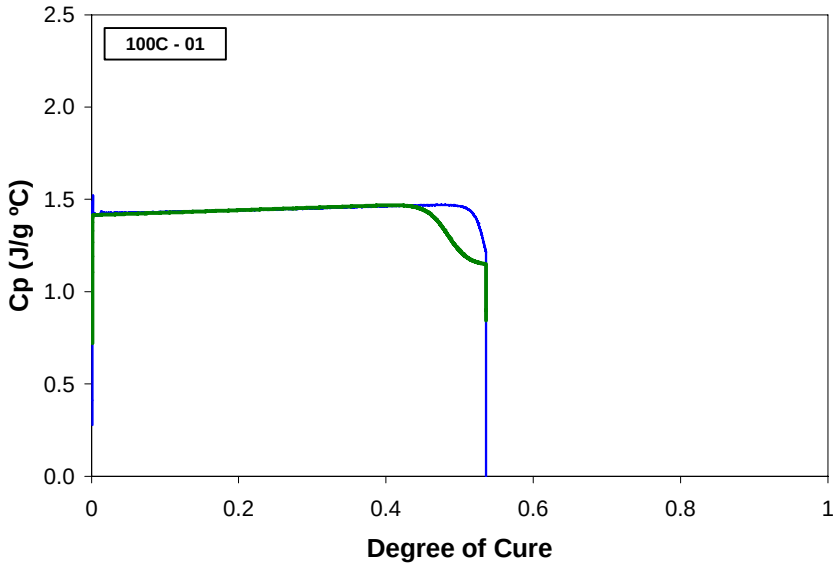

Figure 6144. Heat capacity COMPRO model fit to the 100ºC isothermal test.

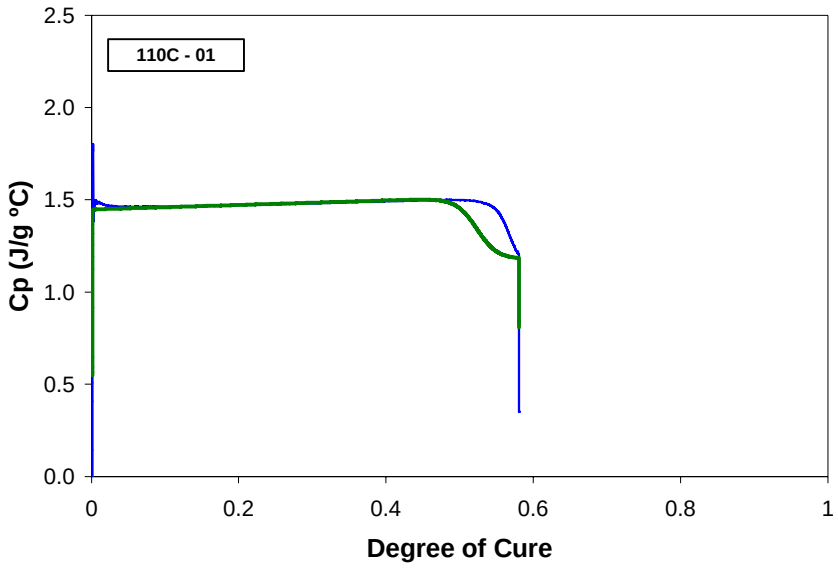

Figure 6245. Heat capacity COMPRO model fit to the 110ºC isothermal test.

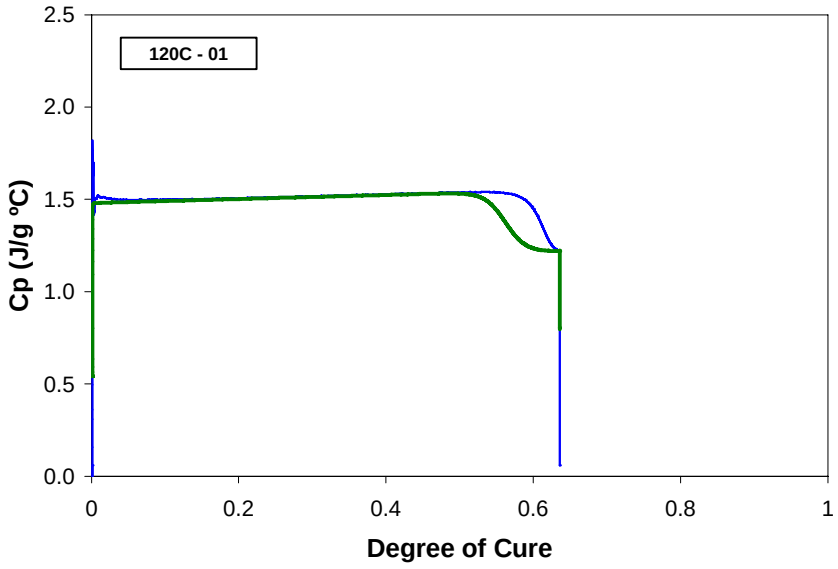

Figure 6346. Heat capacity COMPRO model fit to the 120ºC isothermal test.

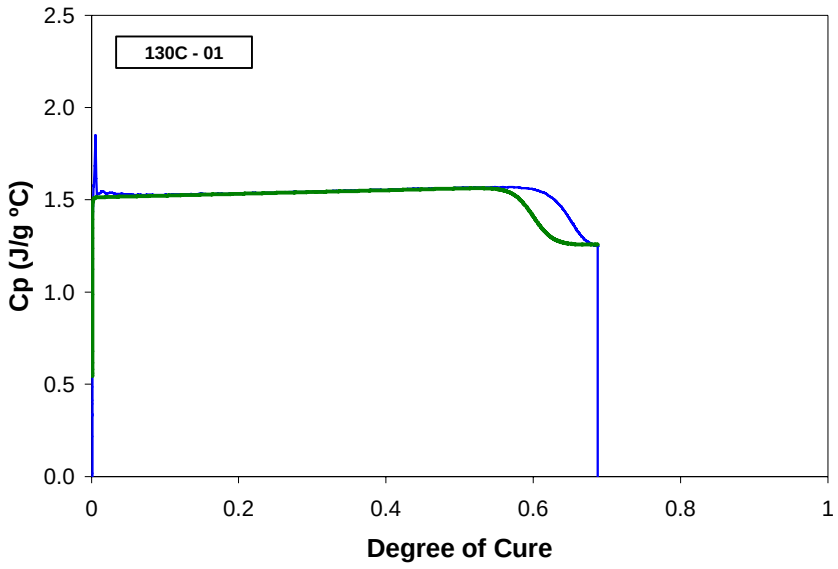

Figure 6447. Heat capacity COMPRO model fit to the 130ºC isothermal test.

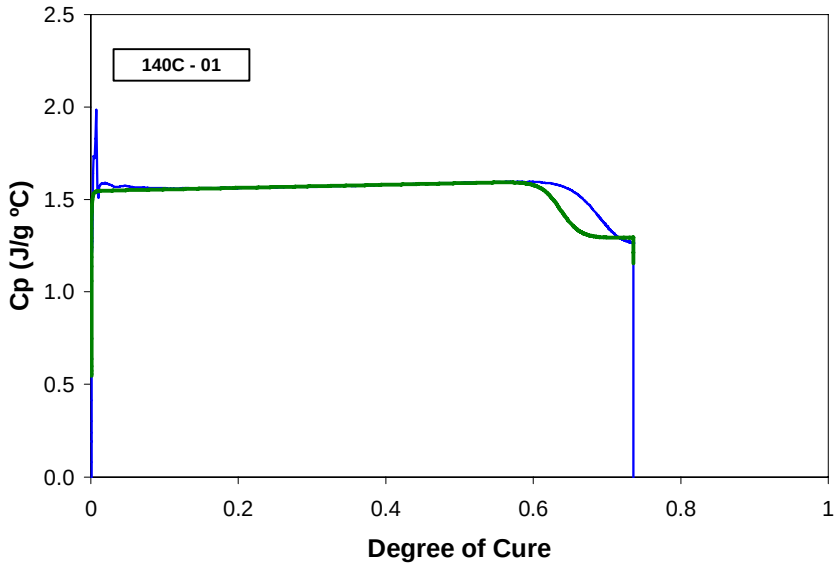

Figure 6548. Heat capacity COMPRO model fit to the 140ºC isothermal test.

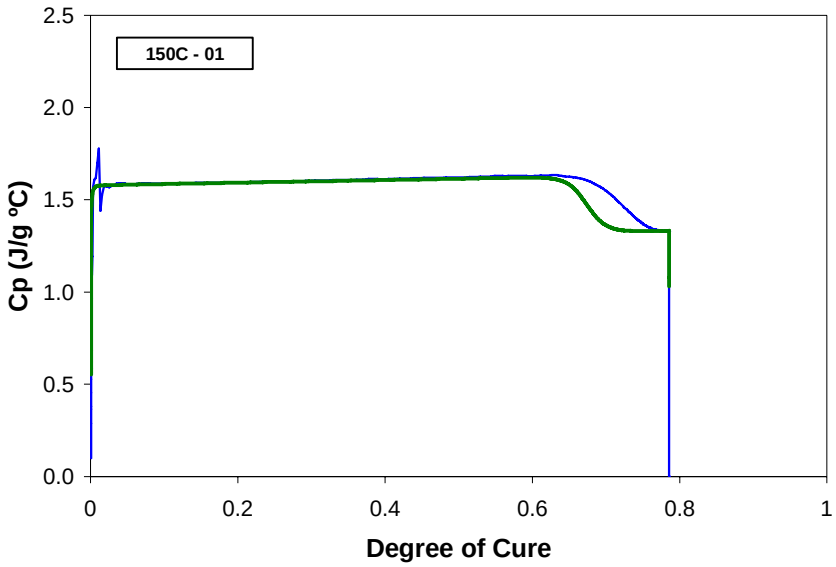

Figure 6649. Heat capacity COMPRO model fit to the 150ºC isothermal test.

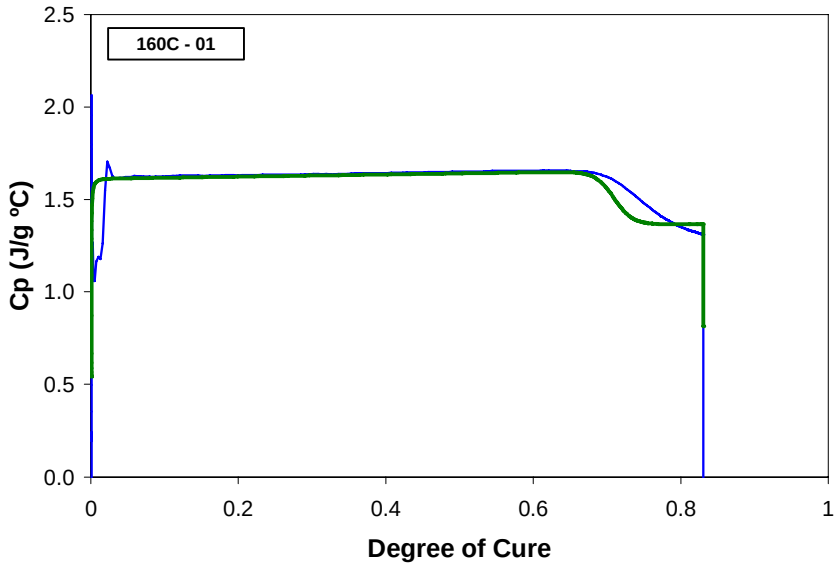

Figure 6750. Heat capacity COMPRO model fit to the 160ºC isothermal test.

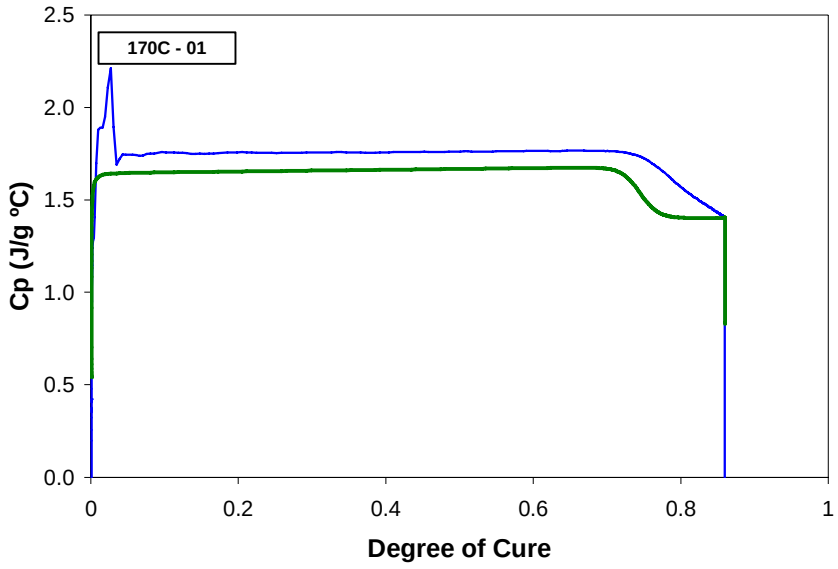

Figure 6851. Heat capacity COMPRO model fit to the 170ºC isothermal test.

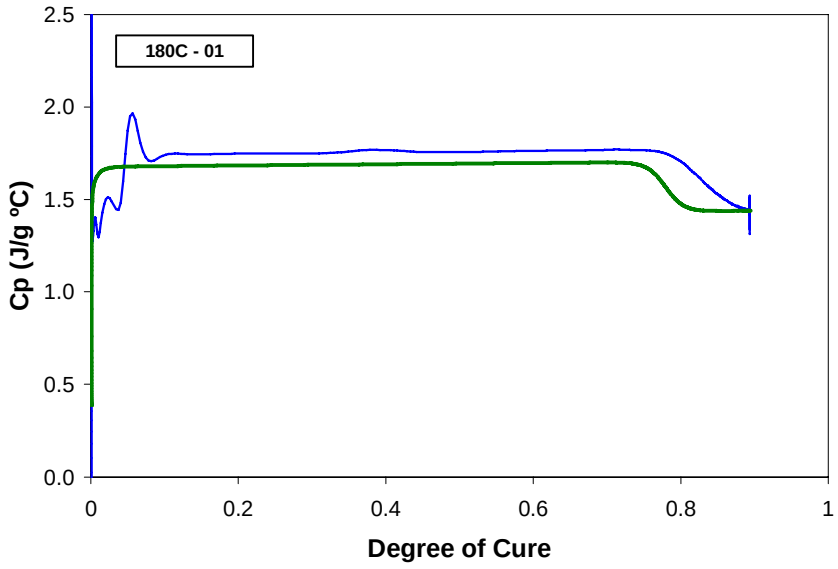

Figure 6952. Heat capacity COMPRO model fit to the 180ºC (1) isothermal test.

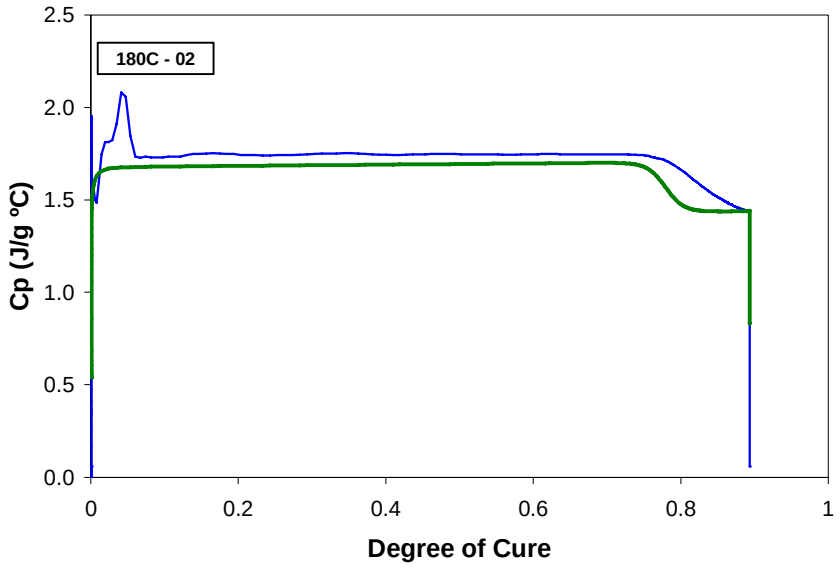

Figure 7053. Heat capacity COMPRO model fit to the 180ºC (2) isothermal test.

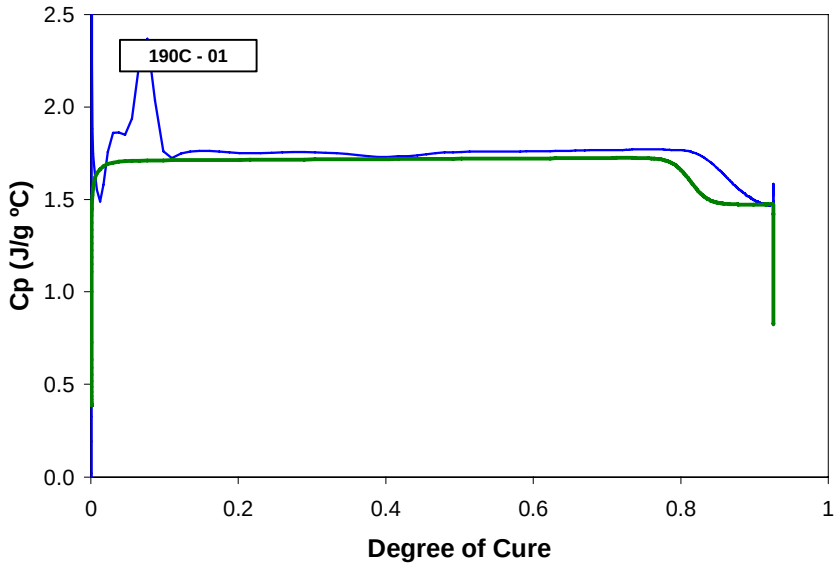

Figure 7154. Heat capacity COMPRO model fit to the 190ºC isothermal test.

Comments

The heat capacity model developed above is validated within the range of temperatures defined below:

Isothermal conditions	$20°C < Temperature < 190°C$
Dynamic conditions	$-70°C < Temperature < 275°C$

Thermal Conductivity

Introduction

COMPRO assumes orthotropic conductivity for all materials. Values for transverse conductivity (k_T), and longitudinal conductivity (k_L) of the composite must be specified for each material. The conductivities are calculated by COMPRO as linear functions of temperature and degree of cure for composite materials.

Theoretical

The thermal conductivity model equations are:

$$k_{Tc} = k_{Tc(0)} + a_{Tc}(T - T_0) + b_{Tc}(x - x_0)$$
$$k_{Lc} = k_{Lc(0)} + a_{Lc}(T - T_0) + b_{Lc}(x - x_0)$$

where c can be the fibre or the resin in the general case.

Raw Data

No measurements were available for thermal conductivity. A value of 0.148 W/m^{o}K (taken from Johnston[1]) was chosen for the conductivity of HexPly 8552.

Analysis

Not applicable.

Goodness of Fit

Not applicable.

Comments

Not applicable.

[1] A. Johnston, "An Integrated Model of the Development of Process-Induced Deformation in Autoclave Processing of Composite Structures", *Ph.D. Thesis,* The University of British Columbia, Vancouver, B.C., February 1997.

Flow Module

In this section, the following material properties are determined:

- Viscosity

All the relevant model equations and a summary table with all the determined flow COMPRO inputs are presented at the beginning of the section. A detailed description of how the inputs were determined follows.

MODEL EQUATIONS - FLOW MODULE

Viscosity

The viscosity model equation is:

$$\mu = \begin{cases} \mu_{01} e^{\frac{E_1}{RT}} + \mu_{02} e^{\frac{E_2}{RT}} \left(\frac{x_g}{x_g - x} \right)^{A+Bx+Cx^2} & \mu < \mu_{\max} \\ \mu_{\max} & \mu \geq \mu_{\max} \end{cases}$$

SUMMARY TABLE - COMPRO FLOW INPUTS

(IMPERIAL UNITS)

HexPly 8552

Viscosity

Constant	Value	Units
μ_{0_1}	7.4E-10	P
μ_{0_2}	4.81E-01	P
E_1	77.6338	BTU/mol
E_2	12.5377	BTU/mol
x_g	0.545	
A	2.466	
B	0.0	
C	0.0	
$\mu_{\max}$	1.0E+07	P

SUMMARY TABLE - COMPRO FLOW INPUTS

(SI UNITS)

HexPly 8552

Viscosity

Constant	Value	Units
μ_{0_1}	7.5E-11	Pa.s
μ_{0_2}	4.81E-02	Pa.s
E_1	81908	J/mol
E_2	13228	J/mol
x_g	0.545	
A	2.466	
B	0.0	
C	0.0	
$\mu_{\max}$	1.0E+06	Pa.s

COMPRO Data File for Flow Module (SI Units)

```
<viscosity model="5" number_of_parameters="10">
   <parameter name="A1" parameter_number="1" units="Pa s" value="7.5E-11" />
   <parameter name="E1" parameter_number="2" units="J/mol" value="81908." />
   <parameter name="A2" parameter_number="3" units="Pa s" value="4.81E-02" />
   <parameter name="E2" parameter_number="4" units="J/mol" value="13228." />
   <parameter name="R" parameter_number="5" units="J/(mol K)" value="8.314472" />
   <parameter name="aGel" parameter_number="6" units="none" value="0.545" />
   <parameter name="A" parameter_number="7" units="none" value="2.466" />
   <parameter name="B" parameter_number="8" units="none" value="0.0" />
   <parameter name="C" parameter_number="9" units="none" value="0.0" />
   <parameter name="Vimax" parameter_number="10" units="Pa s" value="1.E6" />
</viscosity>
```

Resin Viscosity

Introduction

A model for viscosity was developed. Viscosity tests were performed on the HexPly 8552 system and the data was used to fit the model.

Theoretical

COMPRO model 5 is used for calculating the viscosity of this resin system. The total viscosity is assumed to be a function of temperature and degree of cure. The viscosity model equation is:

$$\mu = \begin{cases} \mu_{01} e^{\frac{E_1}{RT}} + \mu_{02} e^{\frac{E_2}{RT}} \left(\frac{x_g}{x_g - x} \right)^{A+Bx+Cx^2} & \mu < \mu_{\max} \\ \mu_{\max} & \mu \geq \mu_{\max} \end{cases}$$

R is the universal gas constant.
T is the temperature.
x is the degree of cure.
μ_{01}, μ_{02}, E_1, E_2, x_g, A, B, C, and $\mu_{\max}$ are the model fit parameters.

Raw Data

Viscosity test data was obtained using a TA Instrument AR2000 rheometer. Parallel plate configuration (using 25mm disposable aluminium plates) was used to measure the change in the viscosity of the resin as it was heated up at predetermined rates. The gap between the plates was held constant at 1 mm in all cases and the tests were performed at a frequency of 1 Hz. The heating rates considered were 1, 2, 3, and 4 ºC/min and a total of eight tests were performed. At each rate, each test was performed twice. A summary of the tests performed is provided in Table 9.

Test	Temperature (ºC)	
	Start	End
1ºCpm-01	25.1	171.4
1ºCpm-02	24.9	171.8
2ºCpm-01	23.3	187.9
2ºCpm-02	25	188.1
3ºCpm-01	23.2	199.3
3ºCpm-02	23.4	201.1
4ºCpm-01	25	205.7
4ºCpm-02	24.5	207.3

Table 9: Summary of the viscosity tests performed on HexPly 8552.

The viscosity tests provide the response of the material to an applied oscillatory strain at the frequency of 1 Hz. The data obtained from the tests are the stress response to the excitation and the phase angle between the stress and strain. A complex viscosity is then calculated with the real and imaginary components representing the viscous and elastic properties of the material, respectively.

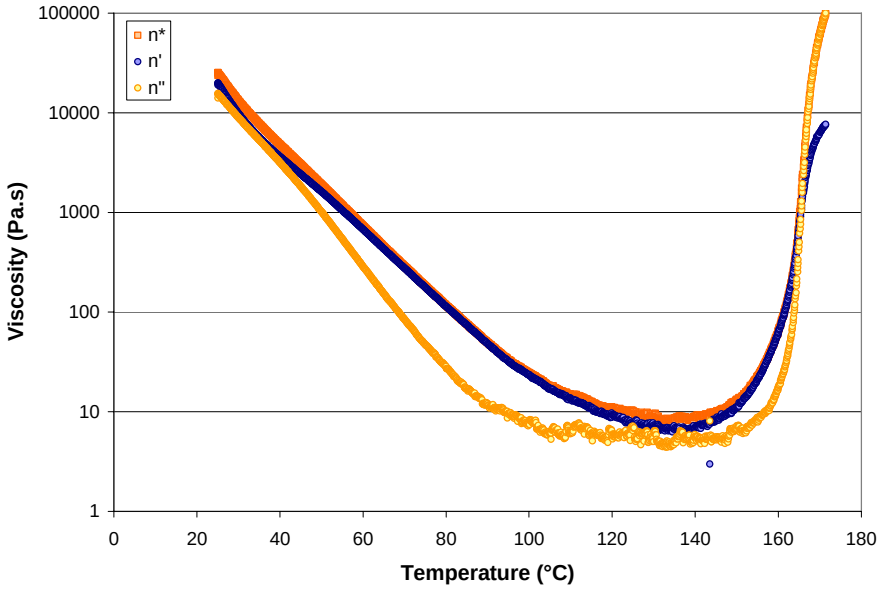

Figure 72. Real and imaginary components of the complex viscosity obtained from a 1ºC/min viscosity test.

The real part of the complex viscosity can be considered as the steady state fluid viscosity at low shear values, and is thus used for model fitting in this study. The raw data used in the model fitting is presented below:

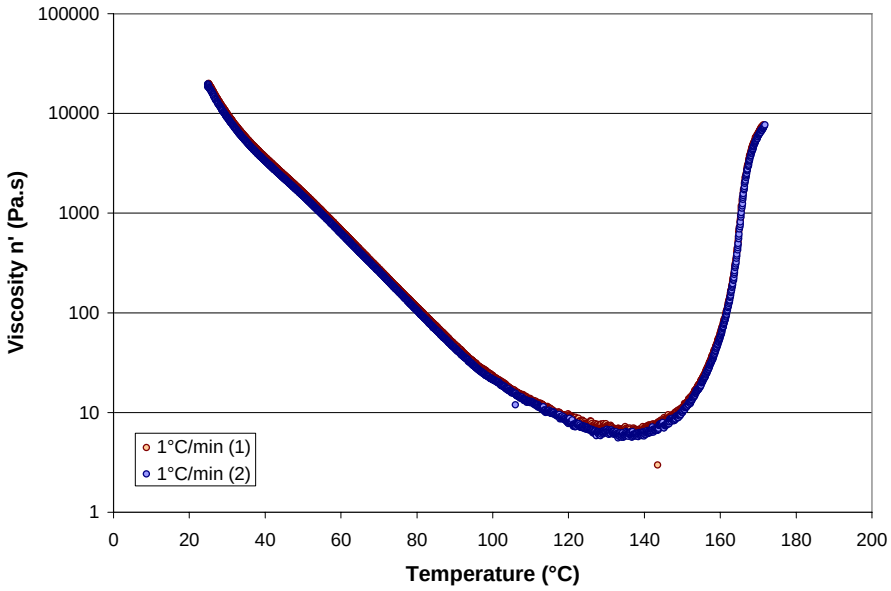

Figure 73. Viscosity test data measured at a temperature rate of 1ºC/min.

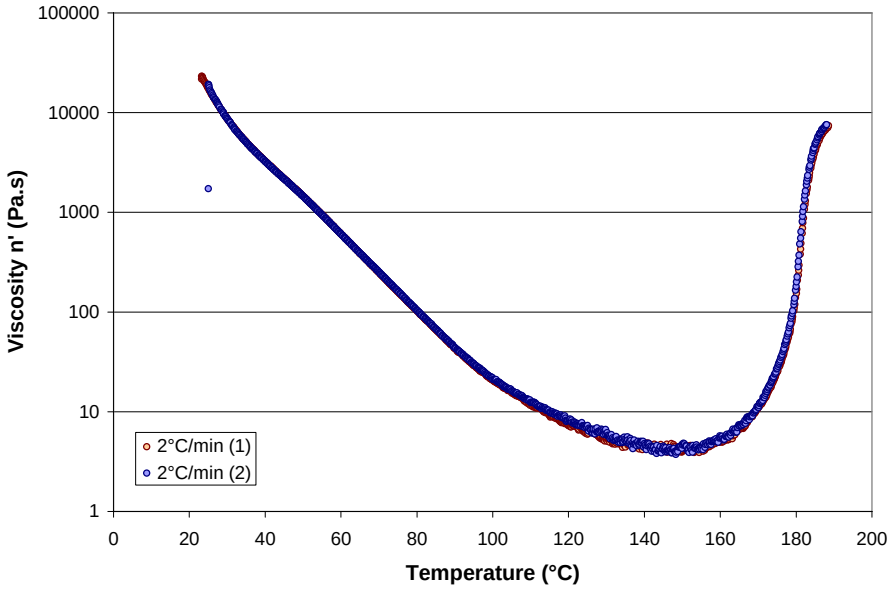

Figure 74. Viscosity test data measured at a temperature rate of 2ºC/min.

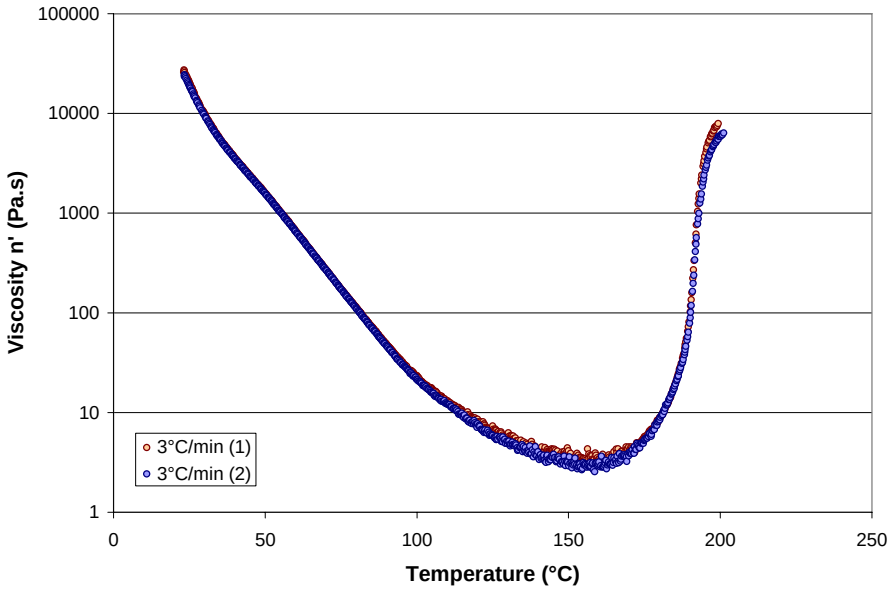

Figure 75. Viscosity test data measured at a temperature rate of 3ºC/min.

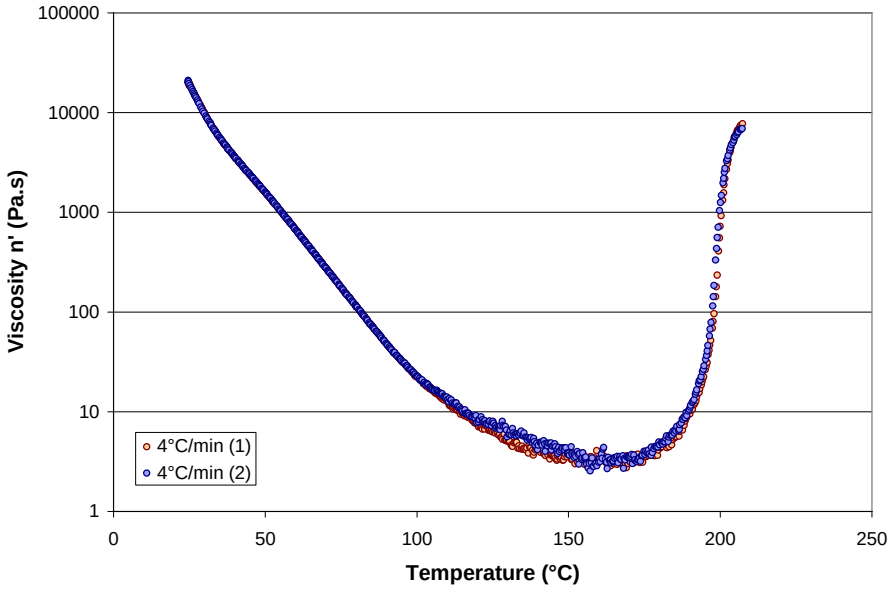

Figure 76. Viscosity test data measured at a temperature rate of 4ºC/min.

Analysis

The viscosity model fitted to the experimental data is a function of temperature and degree of cure. The thermal history of each sample was used to calculate the advancement of the degree of cure during the viscosity tests using the cure kinetics model developed earlier. Figure below shows the viscosity and degree of cure as a function of temperature for a 1ºC/min test.

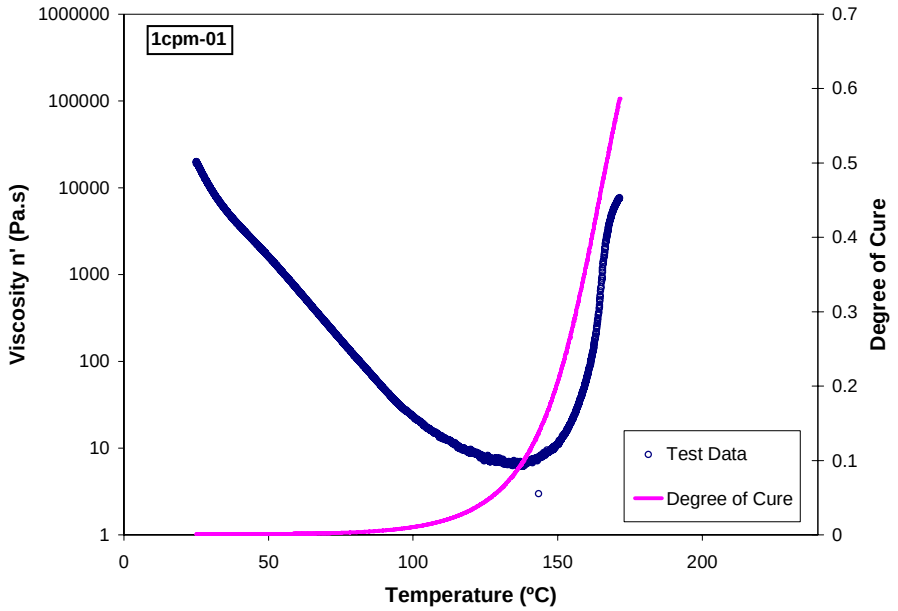

Figure 77. Viscosity measured and degree of cure calculated for a 1ºC/min test.

The viscosity model constants were determined by fitting the model to the experimental data.

Quality of Fit

The following figures show a comparison of the viscosity from the experimental data and as predicted by the model. A process map is also created and can be found in the Appendix.

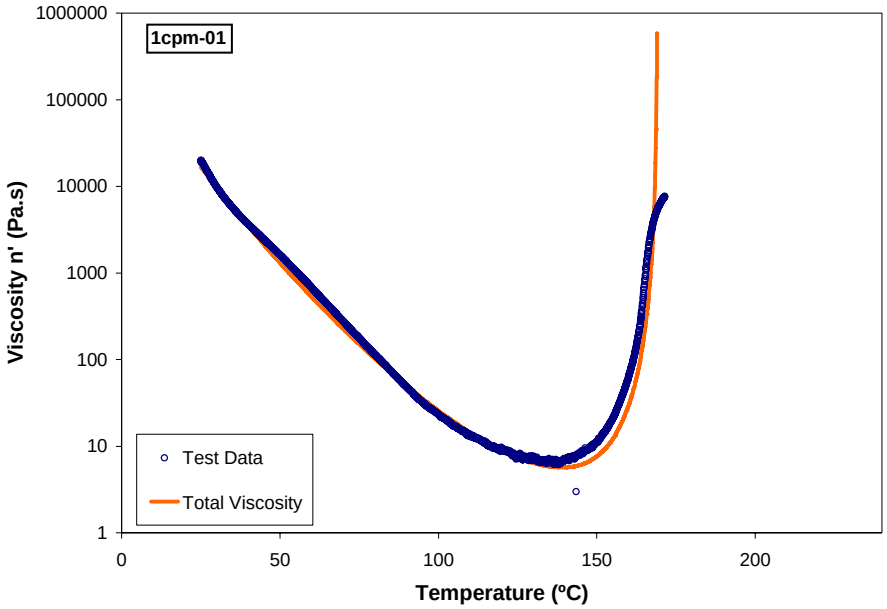

Figure 78. Viscosity data compared to the model predictions for the 1ºC/min (1) test.

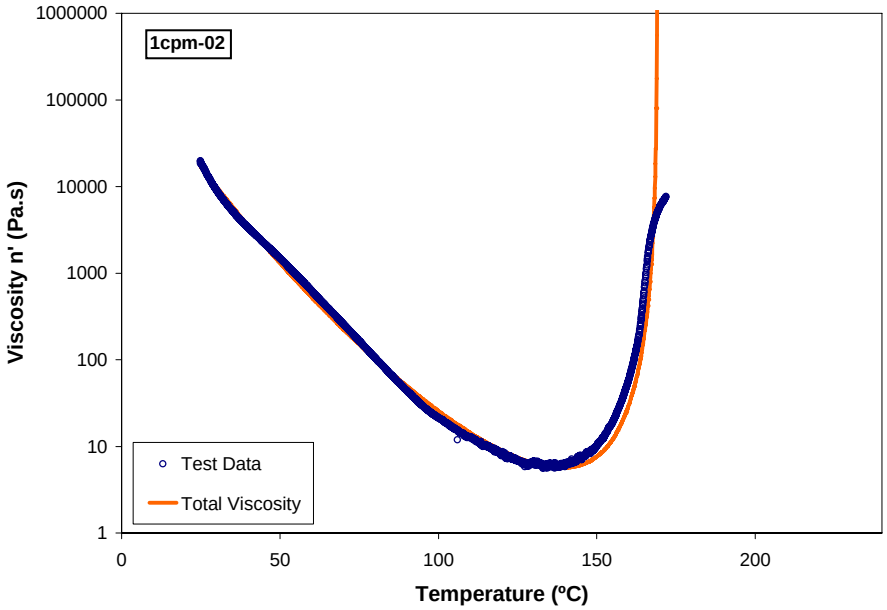

Figure 79. Viscosity data compared to the model predictions for the 1ºC/min (2) test.

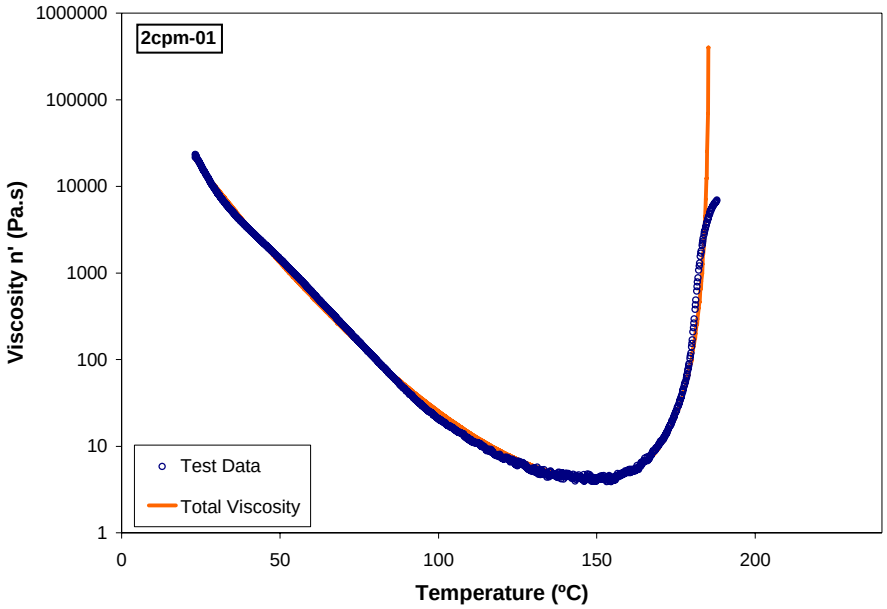

Figure 80. Viscosity data compared to the model predictions for the 2ºC/min (1) test.

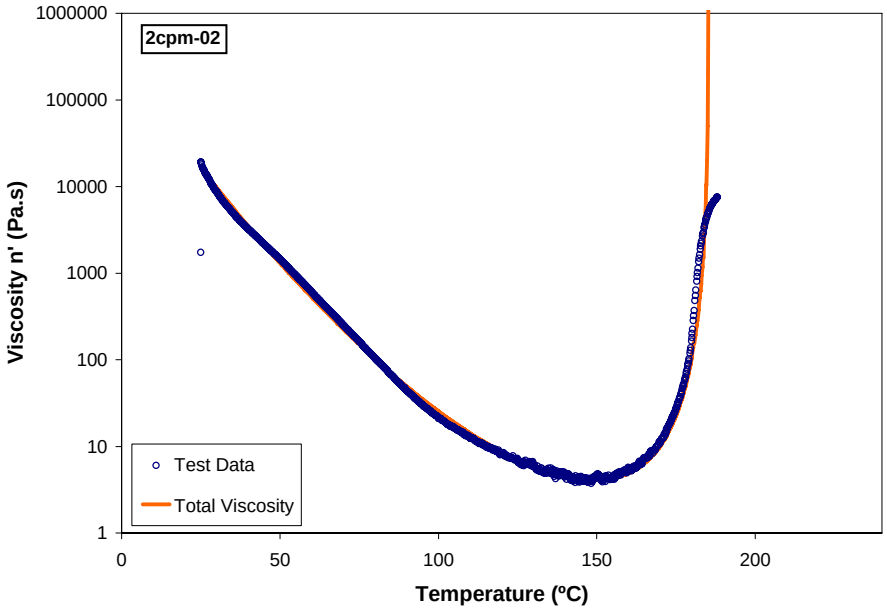

Figure 81. Viscosity data compared to the model predictions for the 2ºC/min (2) test.

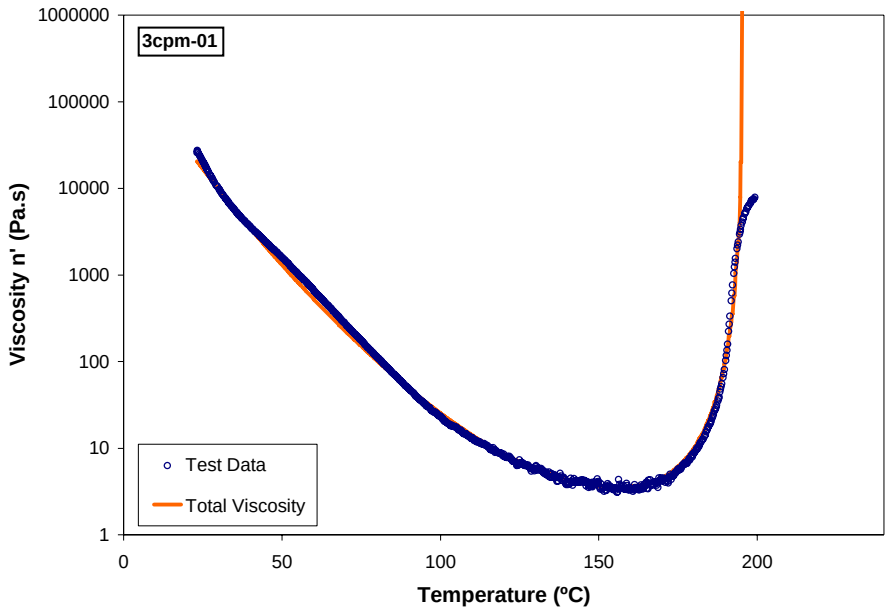

Figure 82. Viscosity data compared to the model predictions for the 3ºC/min (1) test.

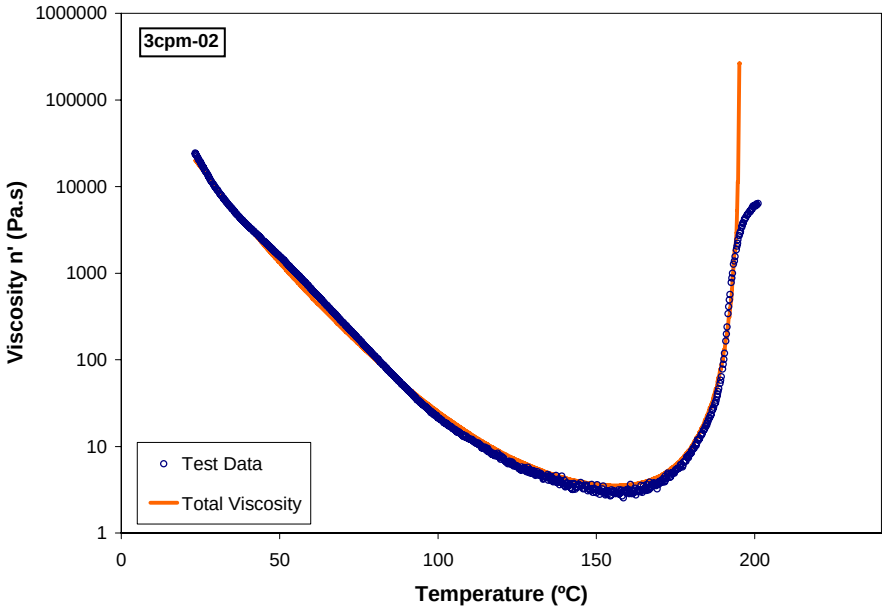

Figure 83. Viscosity data compared to the model predictions for the 3ºC/min (2) test.

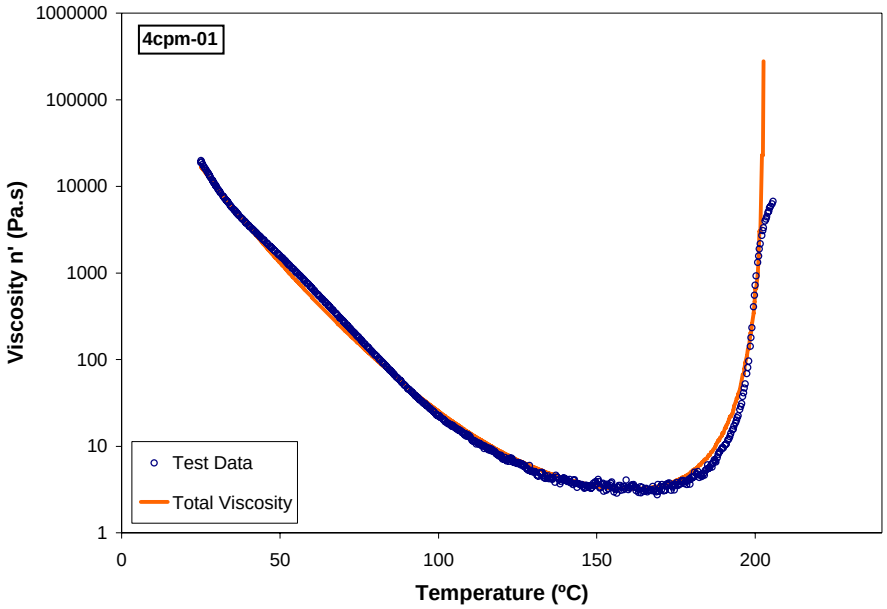

Figure 84. Viscosity data compared to the model predictions for the 4ºC/min (1) test.

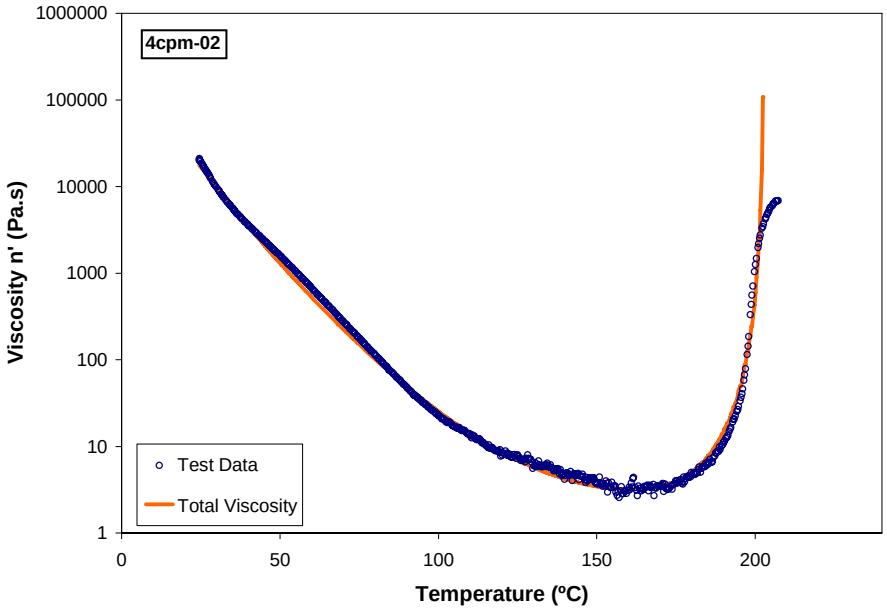

Figure 85. Viscosity data compared to the model predictions for the 4ºC/min (2) test.

Comments

The viscosity model developed above is based on the experimental data obtained at a frequency of 1Hz and is validated within the range of temperatures defined below:

$$25°C < Temperature < 250°C$$

$$0.1 < \mu < 10^6$$

$$\omega = 1.0Hz$$

Stress Module

In this section, the following material properties are determined:

- Resin Poisson's Ratio

All the relevant model equations and a summary table with all the determined stress COMPRO inputs are presented at the beginning of the section. A detailed description of how the inputs were determined follows.

MODEL EQUATIONS - STRESS MODULE

Resin Poisson's Ratio

COMPRO model 1 is used to model Poisson's Ratio Development:

$$\nu_r = \nu_{R_0} + A_{\nu_R}\left(T - \nu_{R_{T0}}\right) + B_{\nu_R}\left(\alpha - \nu_{R_{\alpha 1}}\right)$$

SUMMARY TABLE - COMPRO STRESS INPUTS

(IMPERIAL UNITS)

HexPly 8552

Resin Poisson's Ratio - COMPRO Model 1

Constant	Value	Units
ν_{R_0}	0.37	
A_{ν_R}	0.0	
$\nu_{R_{T0}}$	0.0	°F
B_{ν_R}	0.0	
$\nu_{R_{\alpha 1}}$	0.0	

The following pages show the same information with SI units.

SUMMARY TABLE - COMPRO STRESS INPUTS

(SI UNITS)

HexPly 8552

Resin Poisson's Ratio - COMPRO Model 1

Constant	Value	Units
ν_{R_0}	0.37	
A_{ν_R}	0.0	
$\nu_{R_{T0}}$	0.0	°C
B_{ν_R}	0.0	
$\nu_{R_{\alpha 1}}$	0.0	

The following page shows the corresponding COMPRO material data file, for these material inputs.

COMPRO Data File for Stress Module (SI Units)

```
<poissons_ratio model="pr1" number_of_parameters="5">
   <parameter name="NuR0" parameter_number="1" units="none" value="0.37" />
   <parameter name="ANuR" parameter_number="2" units="none" value="0.00" />
   <parameter name="NuRT0" parameter_number="3" units="C" value="0.00" />
   <parameter name="BNuR" parameter_number="4" units="none" value="0.00" />
   <parameter name="NuRA1" parameter_number="5" units="none" value="0.00" />
</poissons_ratio>
```

Resin Poisson's Ratio

Introduction

Resin Poisson's ratio was not modeled in this project. The input values provided are nominal and do not represent the material behaviour.

Theoretical

COMPRO model 1 is used to model Poisson's Ratio Development:

$$\nu_r = \nu_{R_0} + A_{\nu_R}\left(T - \nu_{R_{T0}}\right) + B_{\nu_R}\left(\alpha - \nu_{R_{\alpha 1}}\right)$$

where

ν_{R_0}	Poisson's ratio at DOC=0 and T=20°C
$\nu_{R_{T0}}$	reference temperature
$\nu_{R_{\alpha 1}}$	reference degree of cure
A_{ν_R} , B_{ν_R}	model fit parameters

Raw Data

No raw data was available for the resin Poisson's ratio for TORAY 2510. The value of ν_r = 0.37 at T_0 = 20 ^{o}C was assumed to be constant for the process.

Analysis

Not Applicable.

Quality of Fit

Not Applicable.

Comments

Not Applicable.

Appendix: Cure Kinetics and Viscosity Process Maps

The process maps presented in this section are prepared using the cure kinetics and viscosity models developed for HexPly 8552 in this project.

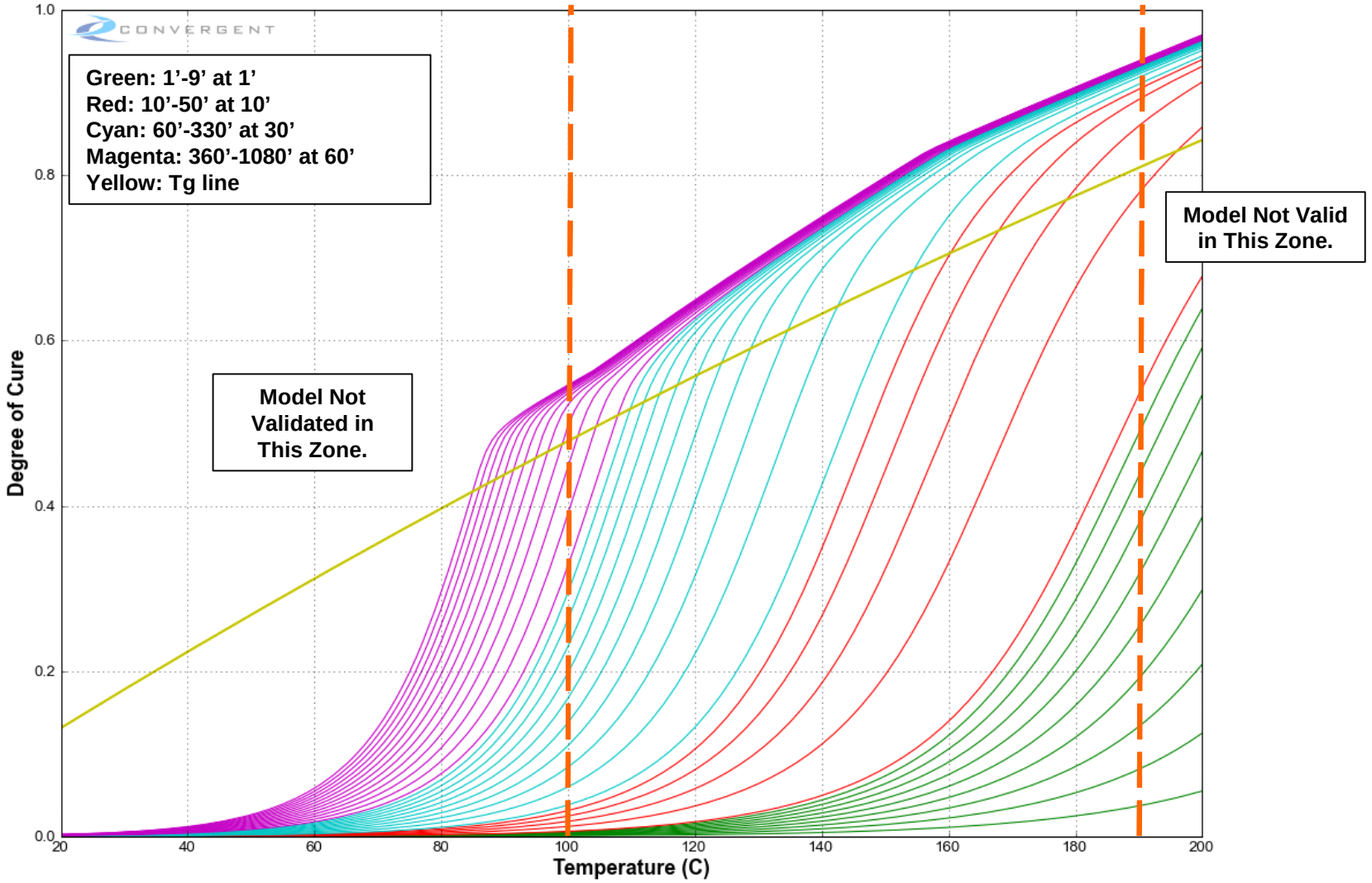

Figure 8656. Isothermal process map.

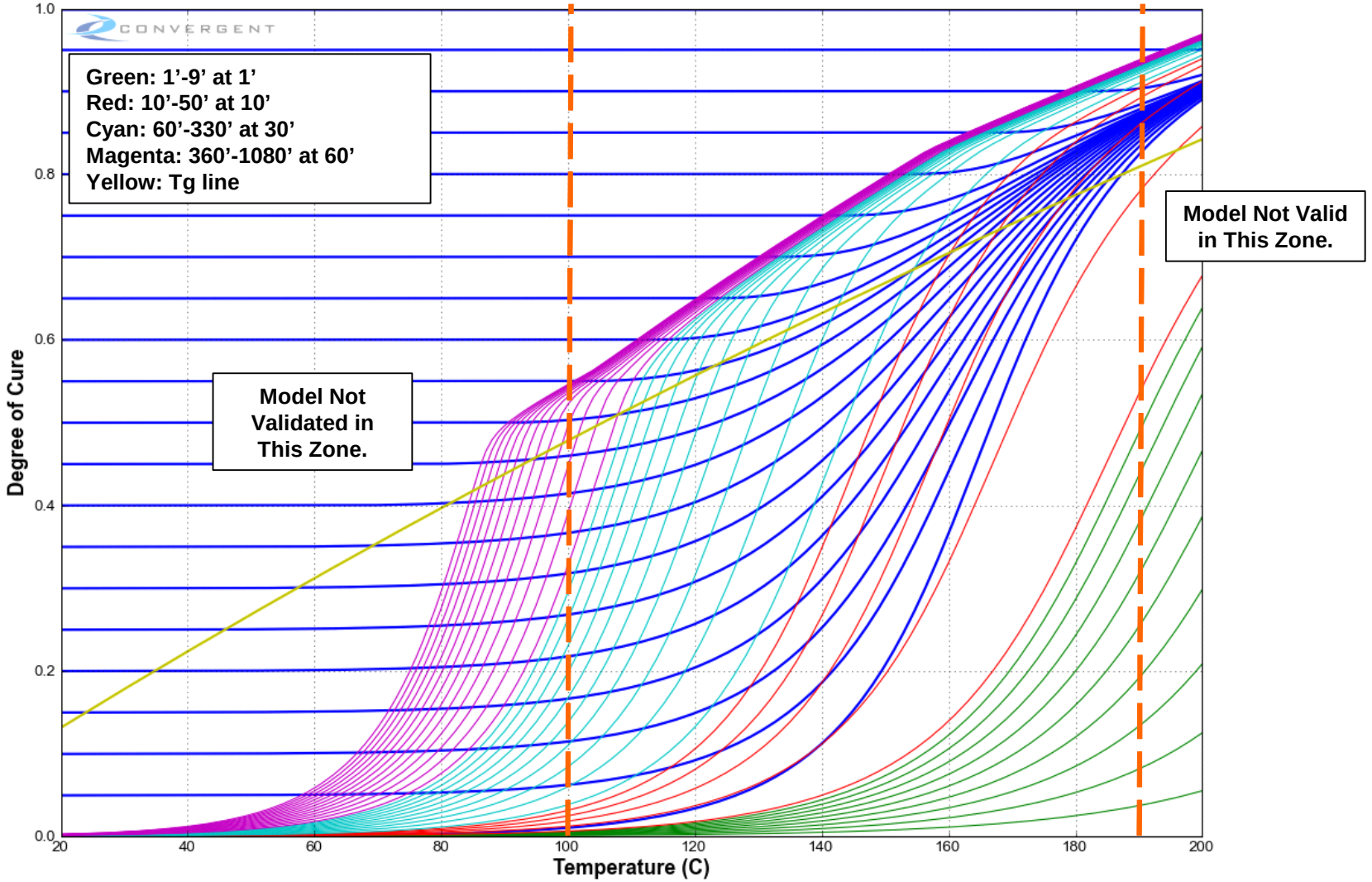

Figure 8757. Isothermal process map with 1°C/min dynamic overlay.

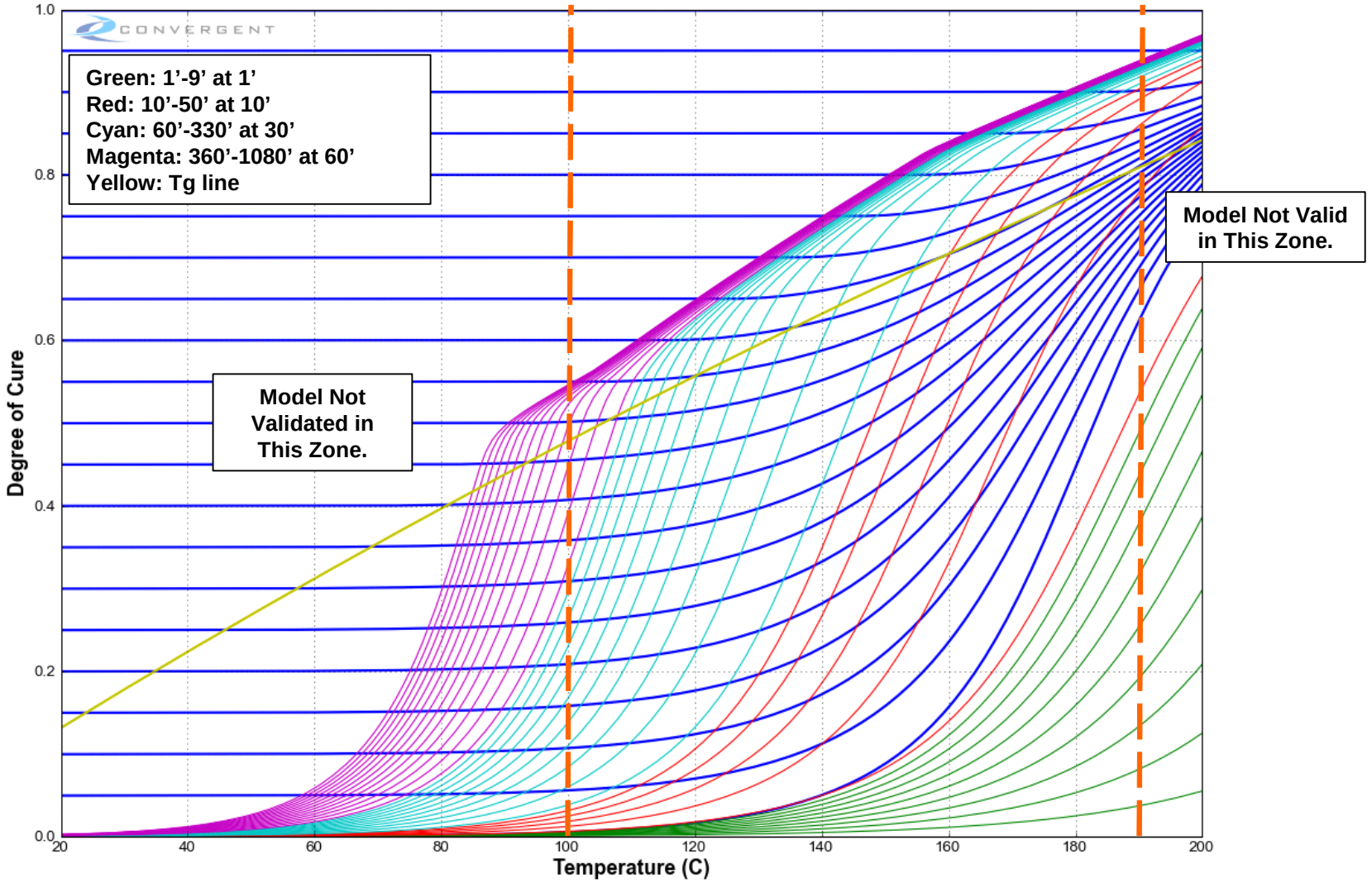

Figure 8858. Isothermal process map with 2°C/min dynamic overlay.

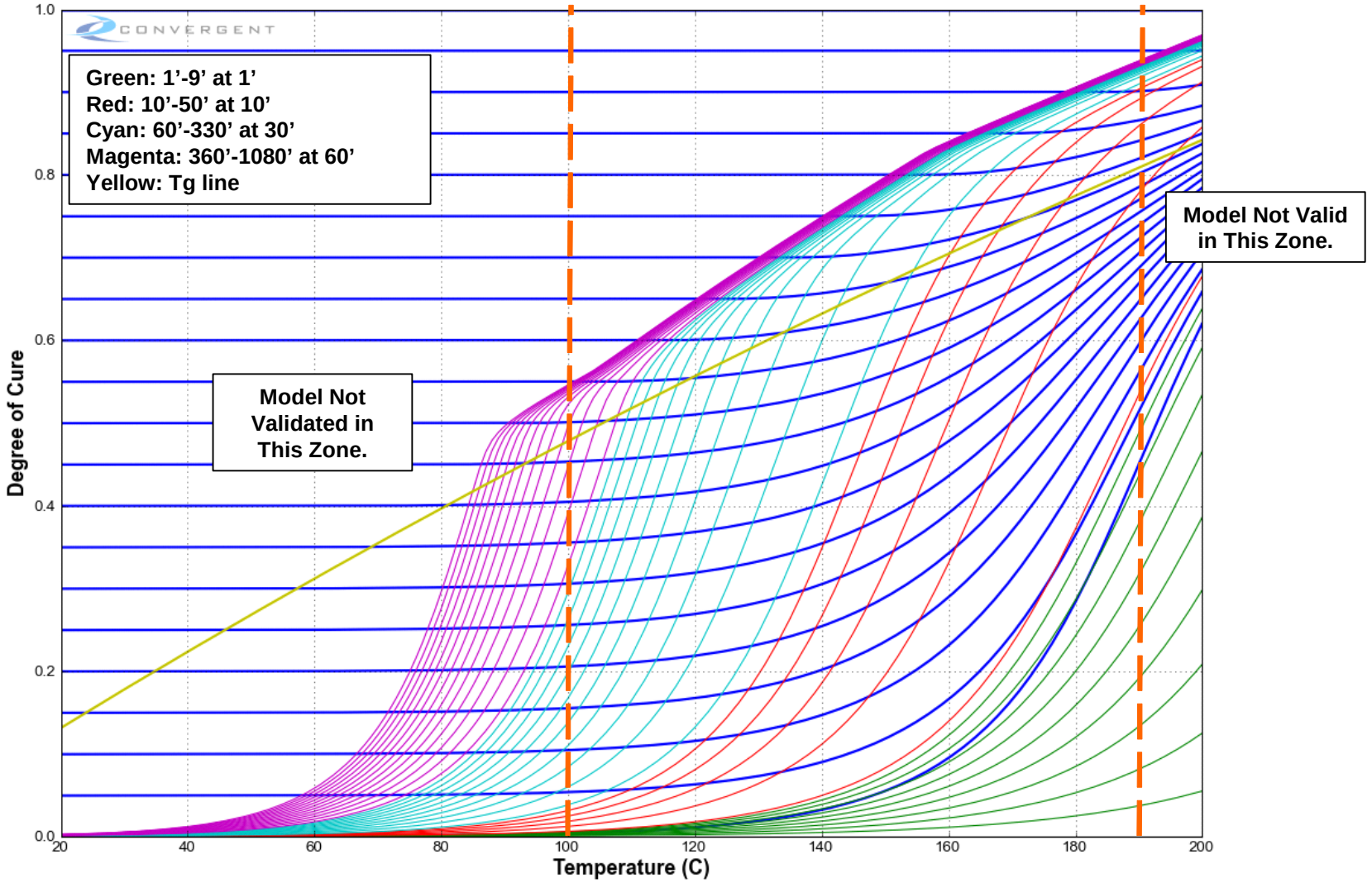

Figure 8959. Isothermal process map with 3°C/min dynamic overlay.

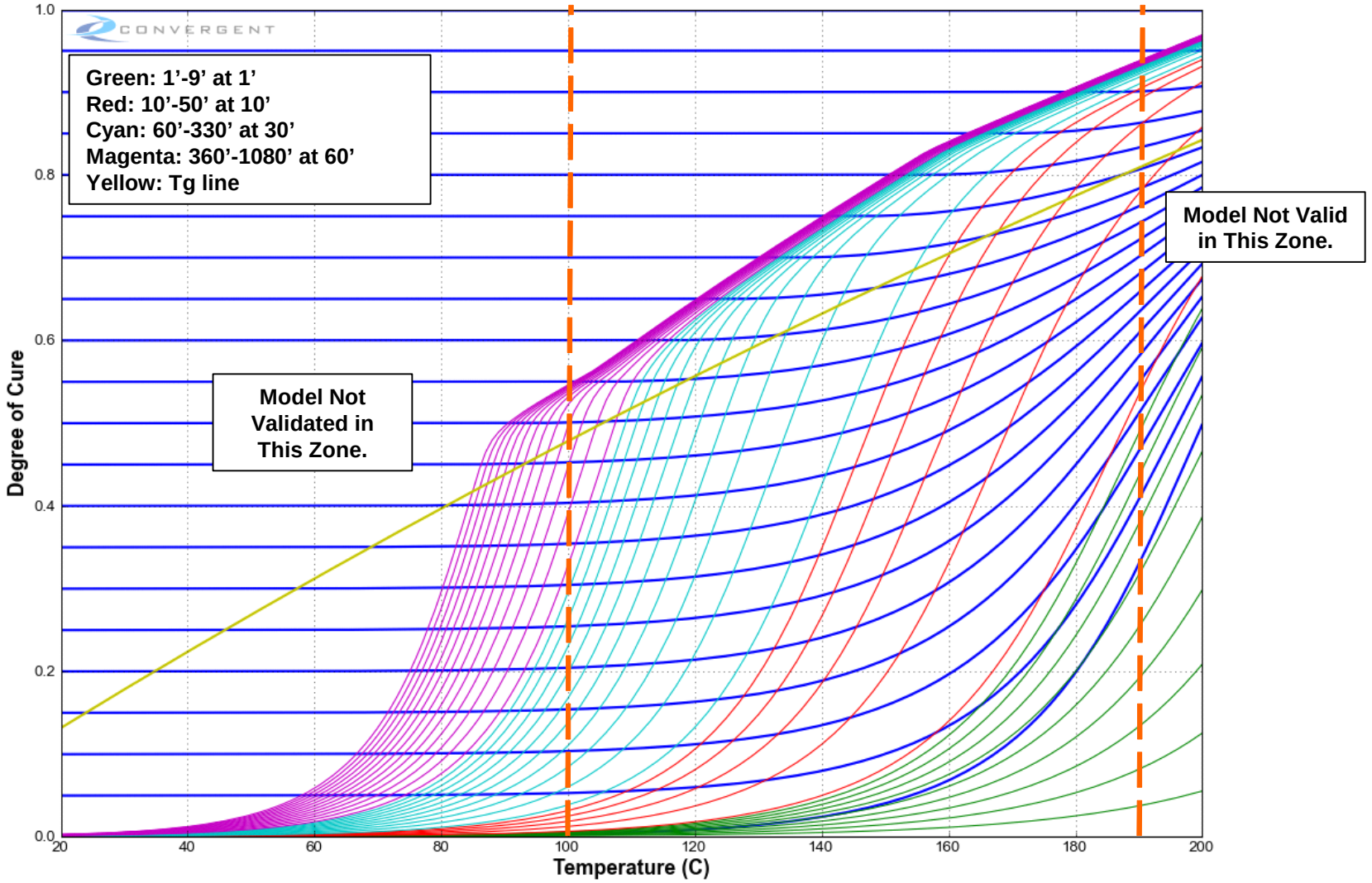

Figure 9060. Isothermal process map with 4°C/min dynamic overlay.

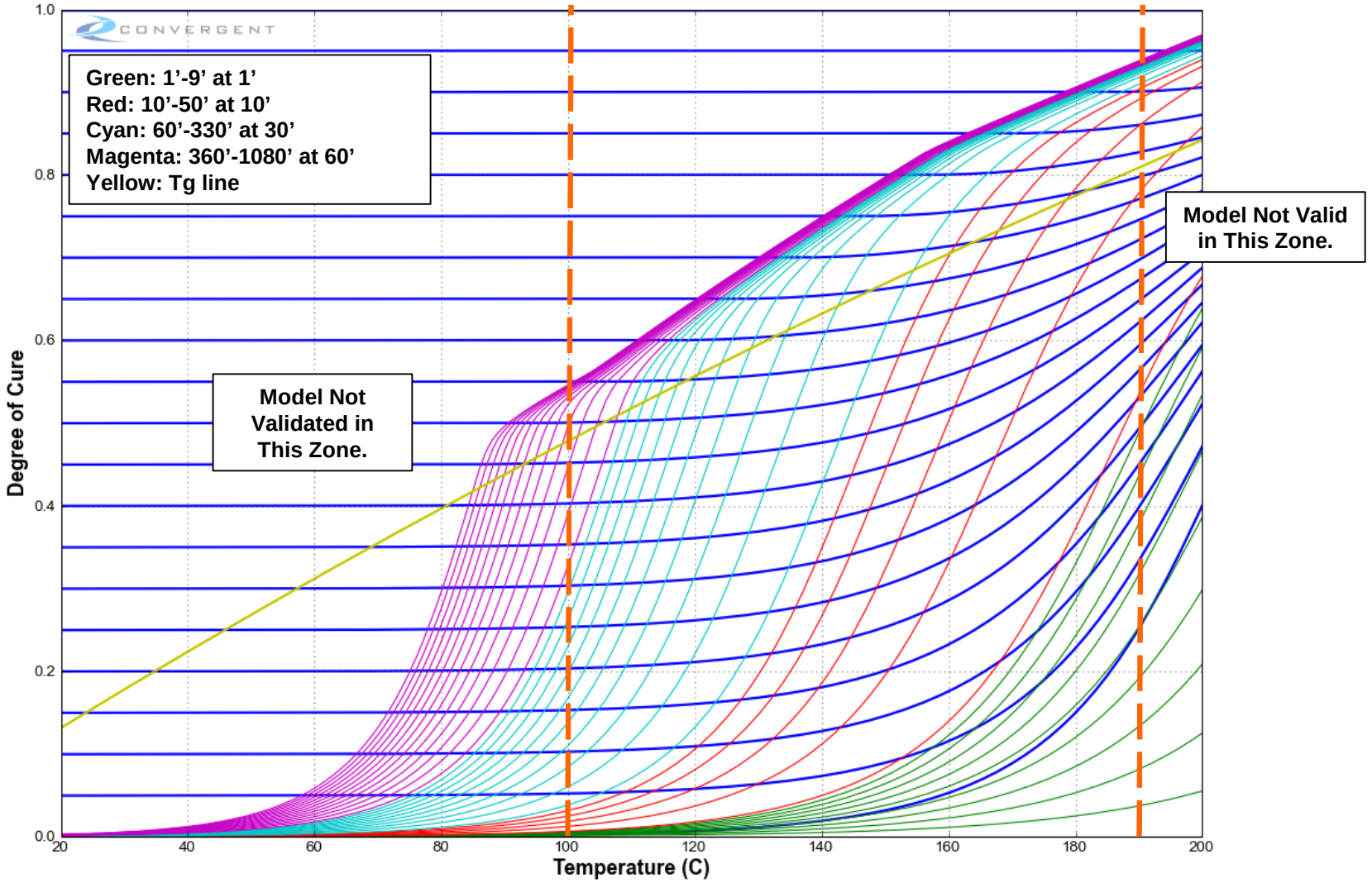

Figure 9161. Isothermal process map with 5°C/min dynamic overlay.

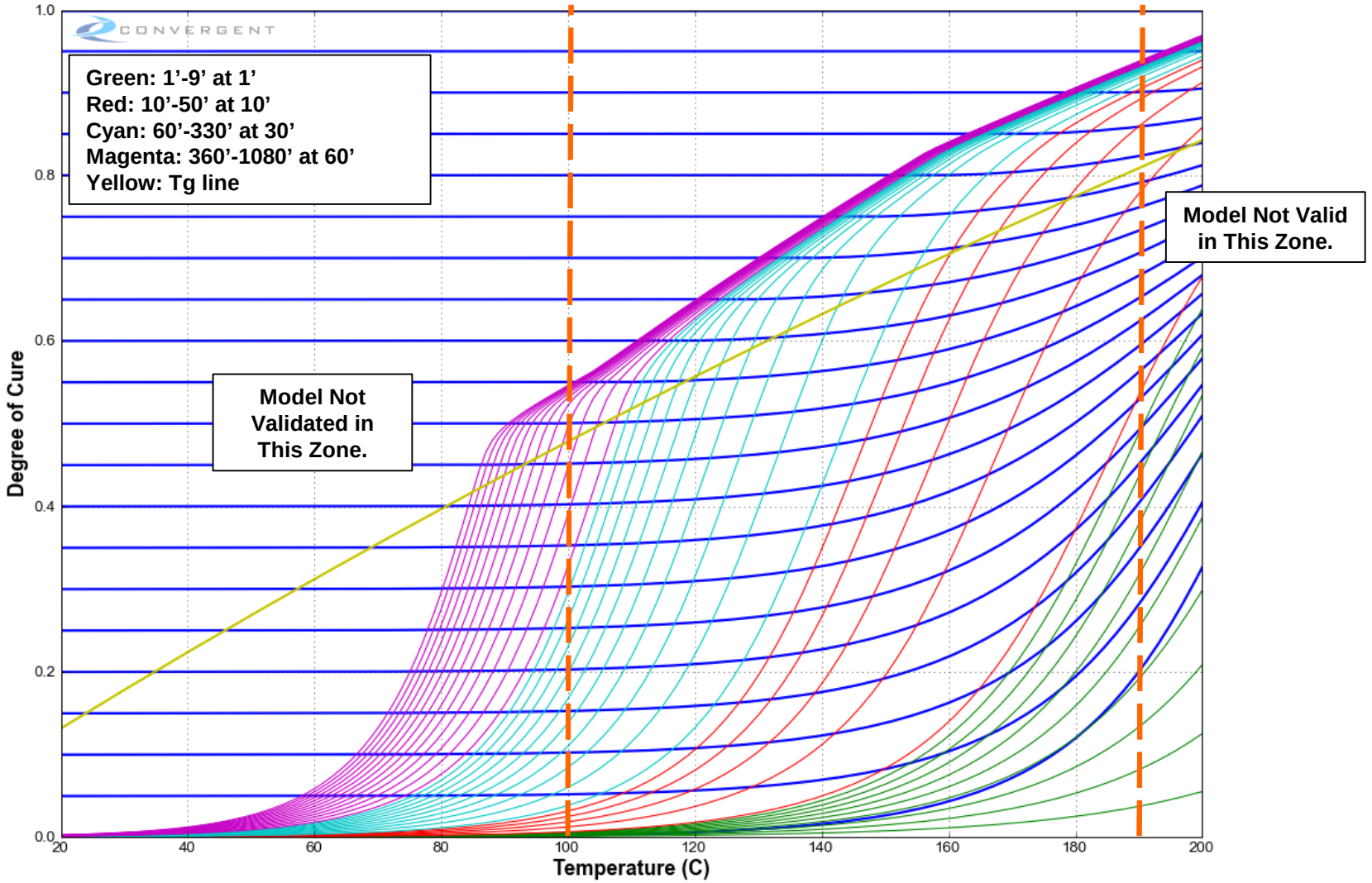

Figure 9262. Isothermal process map with 6°C/min dynamic overlay.

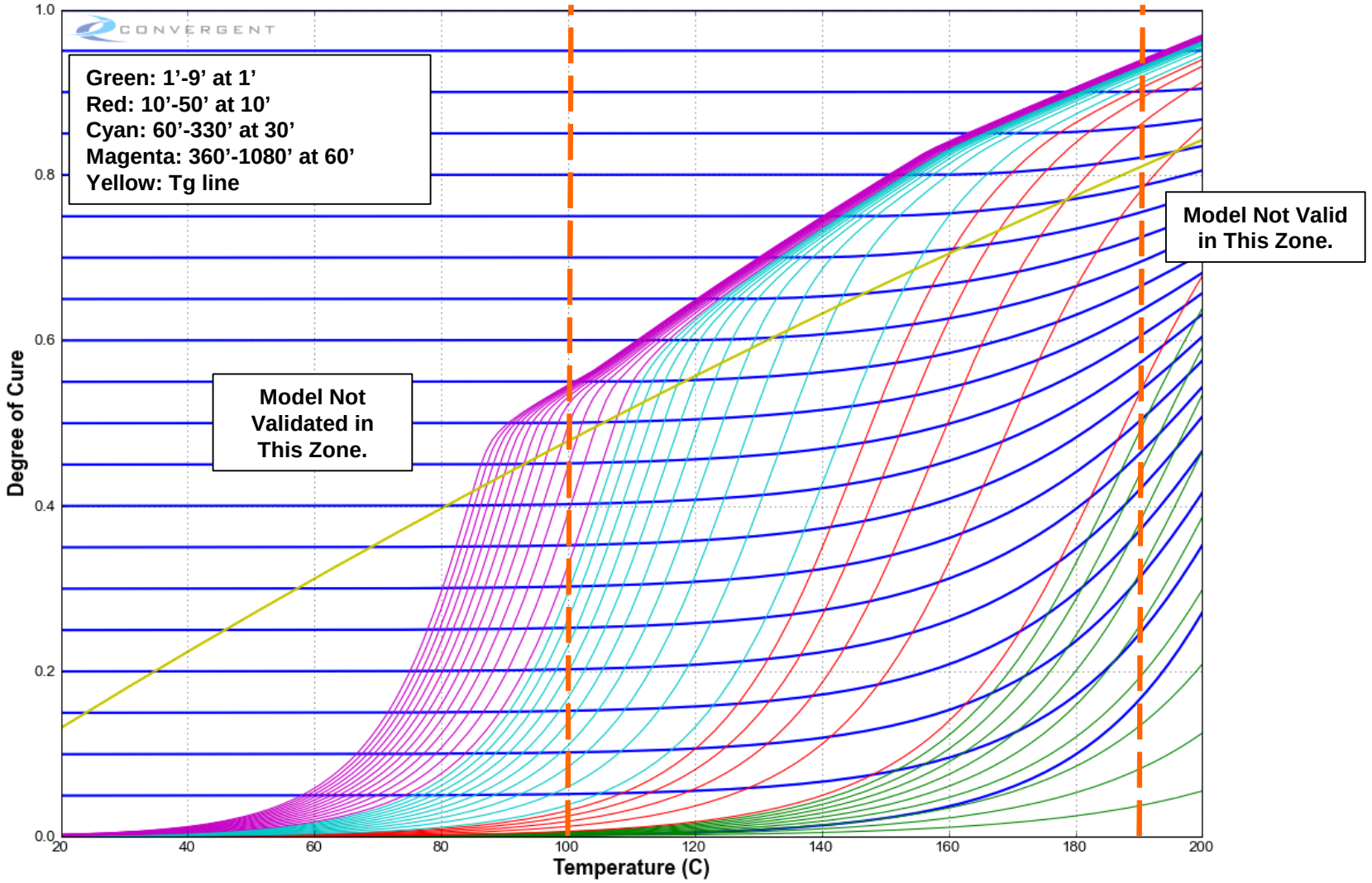

Figure 9363. Isothermal process map with 7°C/min dynamic overlay.

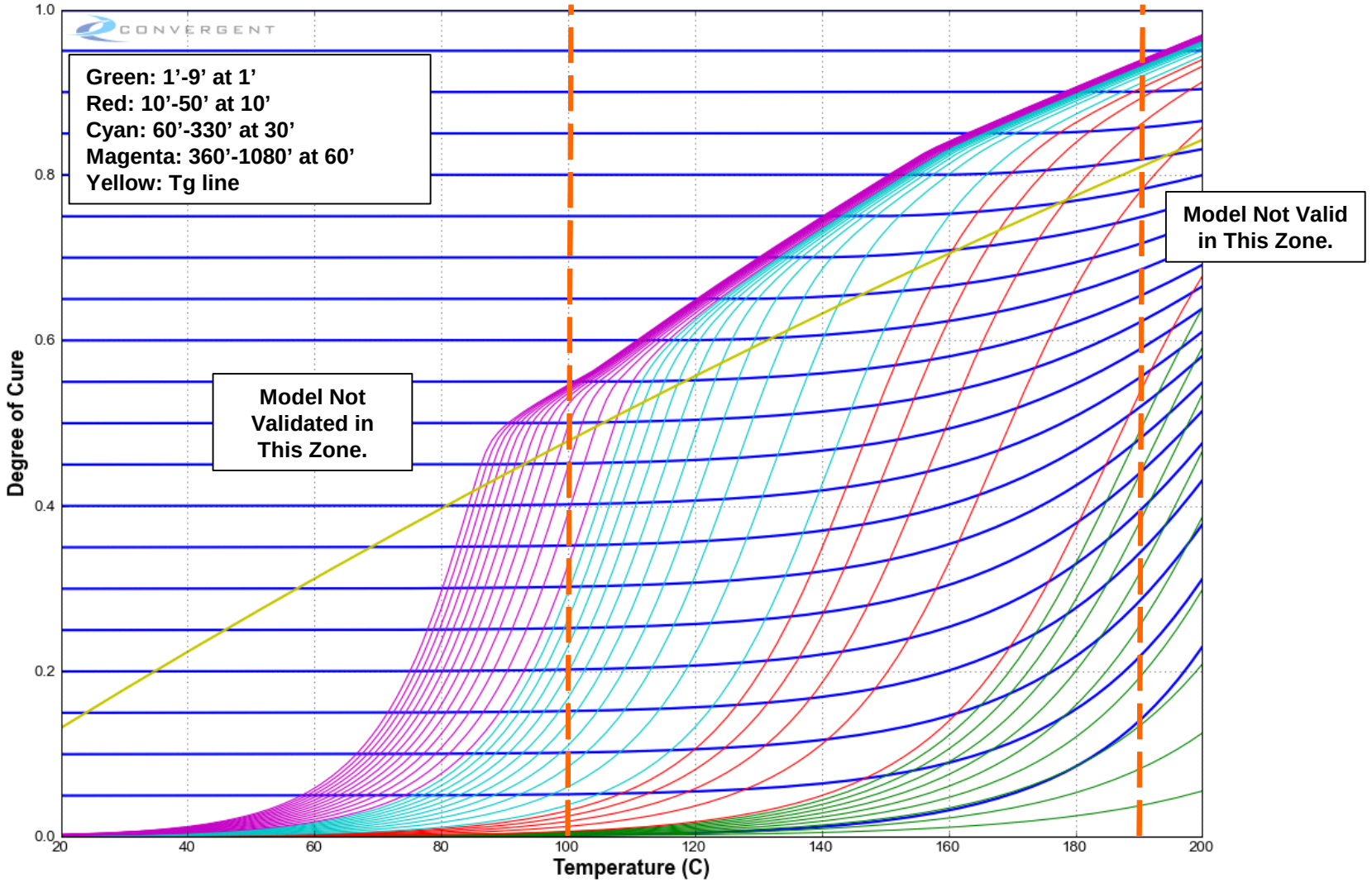

Figure 9464. Isothermal process map with 8°C/min dynamic overlay.

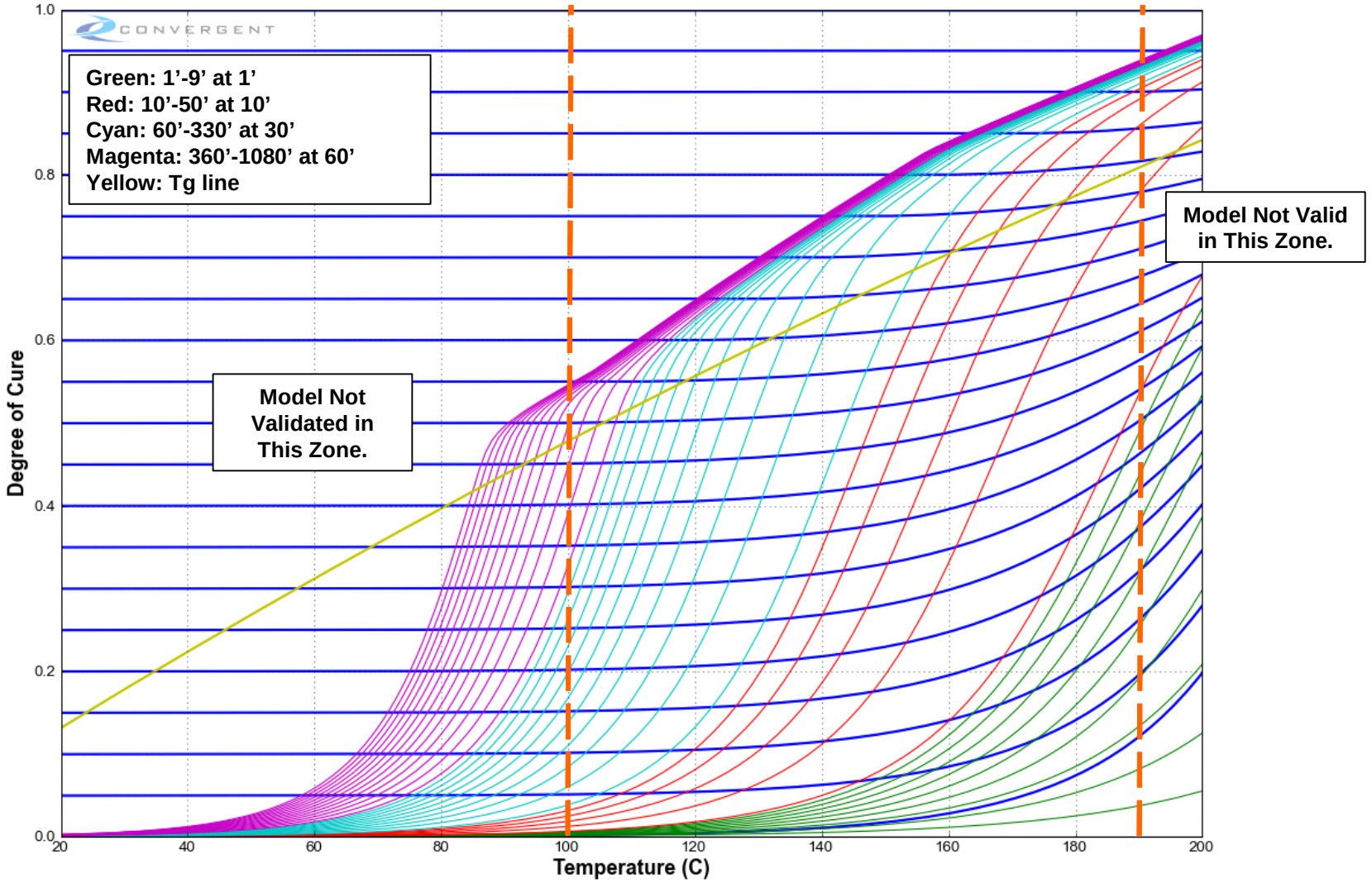

Figure 9565. Isothermal process map with 9°C/min dynamic overlay.

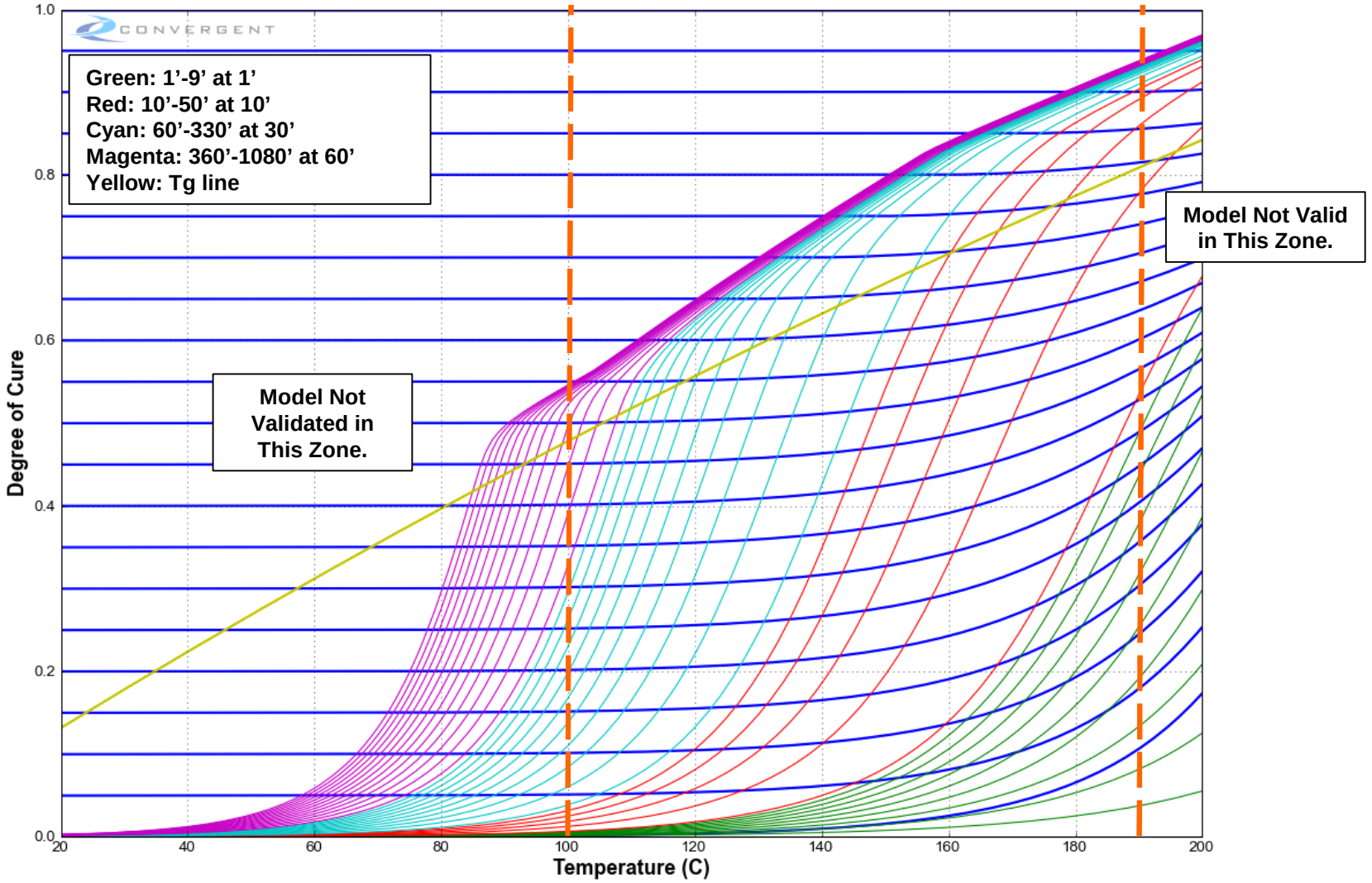

Figure 9666. Isothermal process map with 10°C/min dynamic overlay.

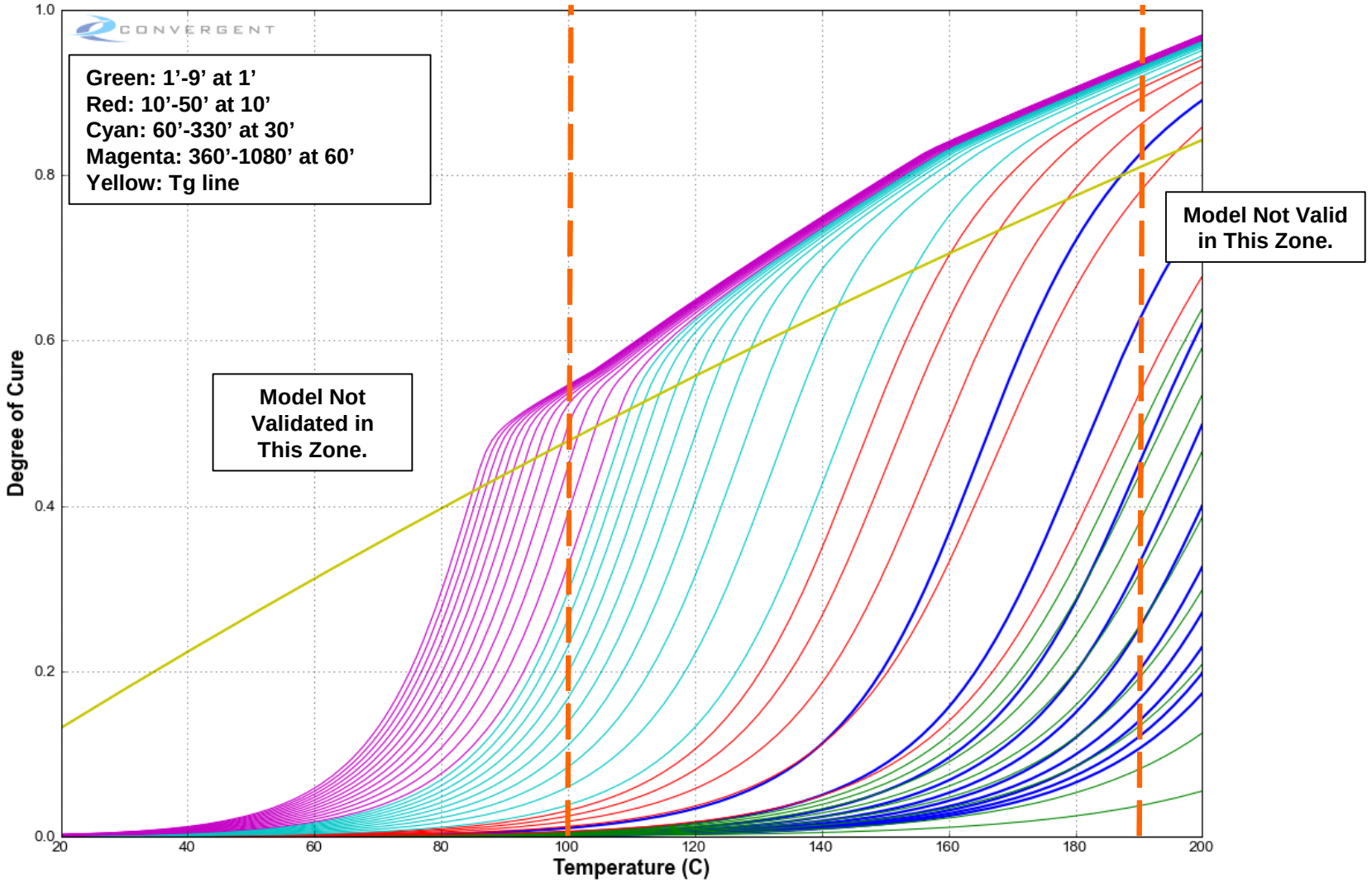

Figure 9767. Isothermal process map with 1-4°C/min uncured dynamic overlays.

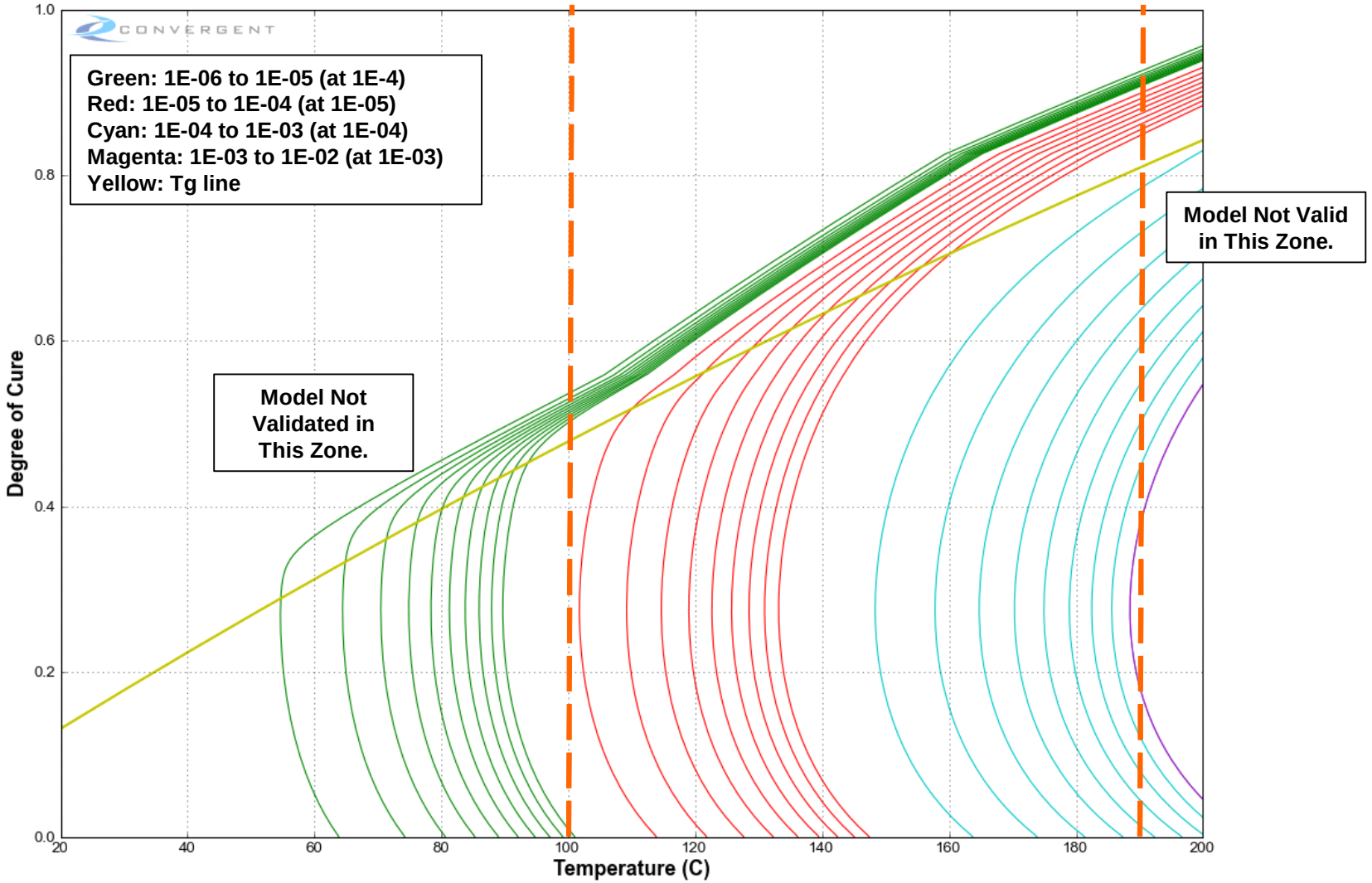

Figure 9868. Cure rate process map.

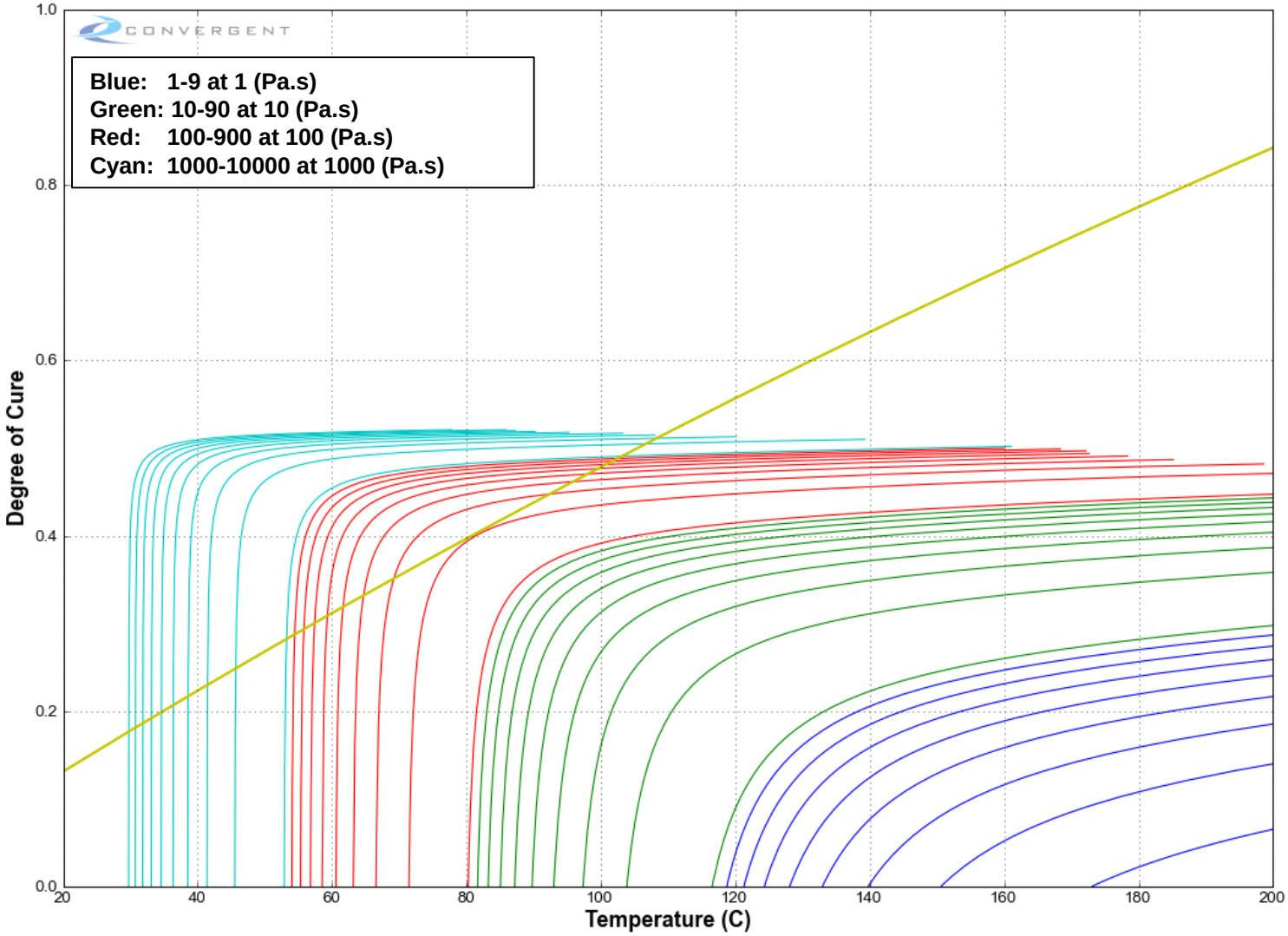

Figure 9969. Resin viscosity process map.